The Messenger

No. 168 – June 2017

ELT First Stone ceremony
1st and 2nd generation ESO Public Surveys
Cherenkov Telescope Array
Highlights of the VIPERS survey

DOI: 10.18727/0722-6691/5018

A Long Expected Party — The First Stone Ceremony for the Extremely Large Telescope

Tim de Zeeuw[1]
Fernando Comerón[1]
Roberto Tamai[1]

[1] ESO

The ceremony to seal the time capsule, signalling the beginning of construction of the dome and main telescope structure for the Extremely Large Telescope, took place at the Paranal Observatory on 26 May 2017, in the presence of the President of Chile, Michelle Bachelet and many international guests. Owing to high winds, the ceremony could not take place as planned on the levelled site on Cerro Armazones, but instead was held at the Paranal Residencia. A brief report of the event and its organisation is presented, and the welcome speech by the ESO Director General is included.

Late May is becoming a time for major highlights in the history of the Paranal Observatory. On 26 May 2017, over two hundred guests from Europe, Chile and the rest of the world gathered at the Paranal Residencia to celebrate the First Stone of the Extremely Large Telescope (ELT), as well as the connection of the Observatory to the Chilean power grid. This was exactly 19 years and one day after Antu, the first Unit Telescope of the VLT, saw first light, and one year and one day after the signature of the largest contract in the history of ground-based astronomy, for the construction of the dome and main structure of the ELT.

The date of the ceremony was carefully chosen to allow the presence of the President of Chile, Michelle Bachelet, who had expressed a strong personal interest in using this opportunity to pay her first visit to an ESO site. The support of the Chilean government to ESO's activities was made very visible by the attendance of the Ministers of Economy, Mining and Energy, and of many other Chilean authorities. The ambassadors of 12 of the 15 ESO Member States were present, as well as the Council President, Patrick Roche, members of the ESO governing bodies from the Netherlands, France, Spain and Italy, and higher officials from the governments of the latter two countries.


ePOD/J. P. Astorga

Figure 1. ELT Project Manager Roberto Tamai illustrates to President Bachelet the approximate real size of each of the nearly 800 segments that will comprise the ELT primary mirror, in front of a model reproduction of the telescope and enclosure, flanked by the Director of Operations, Andreas Kaufer (left), and the Director General, Tim de Zeeuw.

The significance of the event in the history of ESO was symbolised by the presence of the former Directors General Lodewijk Woltjer, Harry van der Laan and Catherine Cesarsky, as well as the Director General designate Xavier Barcons (see Figure 8). The leaders of major observatories and astronomy organisations including the Atacama Large Millimeter/submillimeter Array (ALMA), the Association of Universities for Research in Astronomy (AURA), the Carnegie Institution for Science, Gemini, the Giant Magellan Telescope (GMT), the Large Synoptic Survey Telescope (LSST), the National Radio Astronomy Observatory (NRAO), The University of Tokyo Atacama Observatory (TAO) and the International Astronomical Union (IAU) were also present. Managers of companies that are key to the ELT construction, most notably Astaldi and SAESA, were among the participants as well. Correspondents of numerous national and international media covered the ceremony, which was featured around the world.

The ceremony had been planned to take place at the top of Cerro Armazones, where the ELT will be located and where a large tent was being erected one week ahead of the event. However, in the days before the event exceptional conditions, with windspeeds much higher than usual, prevented the completion of the preparation works. Despite sustained efforts until the last possible minute, under nearly heroic conditions that involved crews staying at Armazones overnight waiting for the winds to abate, the day before the event it was decided to revert to a backup plan already prepared in cooperation with the Presidential team and to host the ceremony at the Paranal Residencia. This may well have been a blessing in disguise, as the comfortable environment of the Residencia made the ceremony much more interactive and protected the attendants from the hostile conditions on that day at Cerro Armazones, although at the cost of reducing the obvious symbolism of a ceremony on the summit where the ELT will rise.

Upon the arrival of President Bachelet and other senior dignitaries, an informal welcome reception took place at the Residencia which gave ample opportunity for interaction among the participants and with the President (Figures 1–3). This included, as planned, the leadership of the Paranal Union, who presented the President with a small vase containing soil from the five ESO sites in Chile (Vitacura, La Silla, APEX, Paranal and Armazones).

ePOD/J. P. Astorga

Figure 2. President Bachelet is shown posing for selfies with children from Taltal during the First Stone event in the Paranal Residencia.

ePOD/J. P. Astorga

Figure 3. Paranal Union leaders pose with President Bachelet after presenting her with a vase containing soil samples from the five ESO sites in Chile.

The formal ceremony started at 13:30 with the arrival of President Bachelet and the ESO Director General in the lower area of the Residencia, where the attendees were already waiting. A sequence of introductory videos was shown about the ELT (Figure 4) and the companies Astaldi, Cimolai, REOSC and Schott, which have so far signed large ELT contracts. Also included was a video prepared by SAESA, the company that has built the extension of the grid to Paranal and Armazones.

A welcome speech (presented on p. 5) was given by the Director General, in which a vision of a large telescope advanced a century and a half ago by Jules Verne was compared with the reality of the construction of the ELT. His speech was followed by one from Paolo Astaldi, President of the leading partner in the ACe Consortium that is building the dome and the main telescope structure. Next was a speech by the internationally renowned astronomer María Teresa Ruiz, currently President of the Chilean Academy of Sciences. The closing speech was given by President Michelle Bachelet, who stressed the importance of astronomy for the development of Chile and the great significance that the event had for the country. As President Bachelet noted in her speech, "With the symbolic start of this construction work, we are building more than a telescope here: it is one of the greatest expressions of scientific and technological capabilities and of the extraordinary potential of international cooperation".

The highlight of the ceremony came with the filling and sealing of a time capsule which had been manufactured in the Paranal workshop by Patricio Alarcón and his team. The Director General started by depositing a copy of the ELT Science Case as foreseen in 2011. President

ePOD/J. P. Astorga

Figure 4. (Left) Roberto Tamai, Project Manager of the ELT; Paolo Astaldi, President of the Astaldi construction group; Tim de Zeeuw, ESO Director General; Michelle Bachelet, President of the Republic of Chile; and María Teresa Ruiz, President of the Chilean Academy of Sciences, watch the opening video at the ELT First Stone ceremony.

Figure 5. (Right) The glass plate donated by President Michelle Bachelet to be included in the time capsule. The legend in Spanish reads: "Opening the sky of Chile to the questions of a whole planet".

ESO/F. Comerón

ESO/T. de Zeeuw

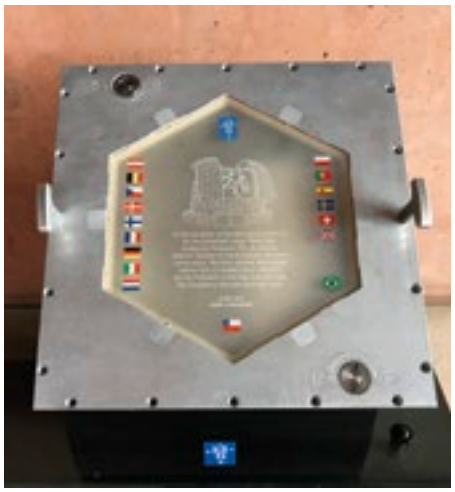

Figure 6. The time capsule that was filled during the ELT First Stone ceremony, manufactured at the Paranal mechanical workshop. The cover includes a 1:5 scale reproduction of a segment of the ELT primary mirror, made in Zerodur®.

ESO/M. Cayrel

Figure 7. The ESO ELT Team braving the wind on Cerro Armazones on the day after the official ceremony.

Bachelet followed by depositing a copy of the lavishly illustrated book, "Atacama", coauthored by ESO staff member Gerd Hüdepohl. Next, the Director General unrolled two posters with the pictures and names of staff working at ESO at the time, which were held up by the Director General and the President to be shown to the audience, then rolled up again and left inside the capsule. At that point, a group of six school children from the town of Taltal, in whose grounds Cerro Paranal is located, were called upon to join the President and the Director General to place in the time capsule their drawings describing what the observatory means for them. The Press Release[1] contains more details of the event, with photographs and videos.

Finally the President deposited a pen made of Chilean copper and the last item to be added to the time capsule was an elegant plate of glass, with the sentence "Opening the sky of Chile to the questions of a whole planet" written in Spanish, from President Bachelet (Figure 5). The time capsule was then closed with a cover that contains a 1:5 scale reproduction of a segment of the ELT primary mirror made in Zerodur®, the same material of which the actual segments will be made by Schott, with the flags of the ESO Member States and Chile engraved and a legend commemorating the ephemeris (Figure 6). The capsule is in storage at Paranal, until the time when progress on the construction of the dome allows it to be encased in one of the walls, where its cover will be left visible.

Following the ceremony many of the guests paid a visit to the VLT telescopes, which the President was unfortunately unable to join because of another commitment. In parallel, the extension of the Chilean electrical grid, constructed by SAESA with the support of the Chilean Government, was celebrated and the Armazones power station, that converts the voltage from 66kV to 23kV, was inaugurated.

The First Stone event was also the occasion to introduce the team of the ELT Project Managers to Paranal colleagues. The agenda of the four-day ELT Team visit included: the presentation of the ELT team and updated status to Paranal colleagues; exchanges of experience and lessons learned, and discussions on subjects of mutual interest; an extensive visit to the telescopes and technical facilities; and a visit to Armazones (Figure 7). This contact will facilitate the assembly, integration and verification of the ELT and its smooth integration into the operations of the Paranal Observatory.

Figure 8. Past, present and future Directors General of ESO at the Paranal Residence. From left to right: Lodewijk Woltjer (1974–1987); Harry van der Laan (1988–1992); Catherine Cesarsky (1999–2007); Tim de Zeeuw (2007–2017); and Xavier Barcons (2017–). Regrettably, Riccardo Giacconi (1993–1999) could not attend the ceremony.

Figure 9. President Bachelet accompanied by most of the Paranal logistics team who played a major role in organising the ceremony.

The symbolic laying of the ELT First Stone coincided with the signature of the Armazones site handover to the ACe Consortium, following resolution of a number of technical and legal matters. From now on, access to Armazones will have to be approved by ACe. In the next few months, the on-site construction activities will begin giving shape to the gigantic telescope and change the physiognomy of Armazones forever. All the hard work will eventually lead to another, even bigger, celebration; the First Light of the ELT in 2024.

Acknowledgements

The success of the event and all the concurrent activities in the same week at the Paranal Observatory owes much more than can be described in this article to the Paranal logistics team led by Christine Desbordes (pictured in Figure 9); to the Education and Public Outreach Department led by Lars Christensen and by Laura Ventura in Chile; to the many colleagues working at Paranal who agreed to leave the comfort of their rooms at Paranal for a couple of nights stay in Antofagasta, thus making it possible for many important guests to stay at the Observatory on the nights before or after the First Stone event; to the executive assistants of the Cabinet and the Representation in Chile, Isolde Kreutle, Jane Wallace, Priya Hein and María Adriana Arrau, for handling and coordinating the invitations, confirmations and transport schedules of many of the guests; and to the production company, Macoffice, which took care of the hardware for the ceremony, including the tent at Armazones whose installation was ultimately prevented by the wind. ESO is also indebted to the Presidential Avanzada team for their invaluable assistance and advice with the preparation of the ceremony.

Links

[1] Press Release on ELT First Stone: http://www.eso.org/public/news/eso1716

Text of Speech

Welcome

Tim de Zeeuw, ESO

President Bachelet, Ambassadors, Ministers Céspedes, Rebolledo and Williams, Members of the Congress, Senator Giannini, State Secretaries, Council President, Council delegates, Mr. Astaldi, Messrs Sammartano, Marchiori, Diaz and Alliende, former Directors General Woltjer, van der Laan and Cesarsky, Director General designate Barcons, other distinguished guests, colleagues and friends, it is a pleasure to welcome you on this historic occasion.

It is unfortunate that the unusually inclement weather prevents access to the platform on Cerro Armazones, so we gather here in the Paranal Residence instead.

Let me start by taking you back about 150 years. In 1865, Jules Verne published a famous book entitled “The Journey to the Moon”. It turned out to be uncannily prophetic, describing an Apollo-sized capsule with three persons on board, launched by a monster cannon located near Tampa in Florida, very close to Cape Canaveral. All at the initiative of an American gun club, with a key role for, yes, a French scientist.

It is probably less well known that the story also describes the construction of a giant telescope at 4300 metres altitude on Longs Peak in Colorado, in order to be able to see the capsule orbiting the Moon. Verne calculated that this needed a telescope with a main mirror of 4.8 metres diameter, which was fully two and a half times larger than that of the largest telescope at the time, Lord Rosse’s Leviathan of Parsonstown, Ireland. A bold step! Verne mentions that the telescope tube was 84 metres long and that the entire system was built in a single year. The site had of course to be in the United States for reasons of national pride.

It took a century before Borman, Lovell and Anders orbited the Moon in Apollo 8 in December 1968. It took another eighty years before Verne’s giant telescope was built, not in Colorado but instead on Mount Palomar in California, and with an improved design. This

is the world-famous 200-inch telescope, often referred to as the Big Eye, and inaugurated in 1948.

Only 40 years later, technology had already advanced sufficiently to gain another factor of two in mirror diameter, and today a dozen fully steerable 8–10-metre-class optical telescopes are in operation, including the world-leading Very Large Telescope (VLT) here on Paranal. It is a distinct pleasure to recognise Lo Woltjer, who initiated the VLT project and got it funded and approved, Harry van der Laan who selected Paranal as the site, placed all the major contracts and designed the successful collaborative model for instrumentation development, and Catherine Cesarsky who brought the VLT to full operation. Riccardo Giacconi had a key role during construction and first light, but could unfortunately not be here today.

Nearly twenty years have passed since first light of the Very Large Telescope. ALMA has meanwhile been constructed on Chajnantor in Chile by an international partnership and is operational, and telescope technology has advanced again. Today we officially start construction of the Extremely Large Telescope (ELT). Its dome will have a diameter of 85 metres and a height of approximately 80 metres, so that Verne's telescope tube would fit. However, the ELT has a segmented main mirror with a diameter of an astounding 39 metres. This is a jump of a factor four to five over any existing telescope! The collecting area of the ELT primary mirror is nearly 1000 square metres, which is larger than that of all 8–10-metre-class telescopes in the world combined. Jules Verne would have liked it!

A revolutionary telescope needs an excellent site, and the choice of Cerro Armazones was the result of a world-wide site selection process, chaired by Rene Rutten, who is here today. The Chilean government generously extended the land donated to ESO in 1995 towards the east, so that it now contains both Paranal and Armazones, and ESO can operate the ELT as part of the Paranal Observatory. The first discussions on this topic were with President Bachelet during her previous term. The process was completed under President Piñera, with key preparatory work done by Ambassador Rodriguez of the Ministry of Foreign Affairs and by ESO's previous representative Massimo Tarenghi. Since then ICAFAL, also represented here, have prepared the giant platform and a new access road, so that today we take the next step, again with President Bachelet. I am sure that the location of the ELT in Chile is a justified source of national pride, just as in Verne's story.

The Chilean government carefully protects the quality of the night skies and realises that the international observatories provide training and employment for many Chileans: telescope operators, technicians, engineers, astronomers and administrative staff. Chilean universities have developed internationally competitive astronomy programmes, and some have started engineering programmes for astrotechnology, creating capabilities and know-how that will benefit Chilean society more generally. ESO is proud to be associated with this impressive growth of capabilities, which is also reflected in the fact that the President of the Chilean Academy of Sciences, María Teresa Ruiz, who will also speak today, is an internationally acclaimed astronomer.

Almost exactly a year ago, ESO signed the largest ever contract in ground-based astronomy with the ACe consortium, consisting of Astaldi, Cimolai and the nominated subcontractor EIE Group, for the construction of the giant dome and the 3000-tonne telescope structure. Today's event marks the official start of the construction of the telescope structure and dome of the ELT.

Today also marks the connection of Paranal and Armazones to the Chilean electrical grid. The Chilean Government has helped ESO to find a solution for the supply of power to the Observatory, through the Comisión Nacional de Energía, la Superintendencia de Electricidad y Combustibles, and the Ministries of National Assets and Foreign Affairs and our consultants from MegaRed. The connection to the central grid in Paposo is managed by Grupo SAESA, and I am very pleased that it is represented here today. The grid connection will reduce costs, provide greater reliability and stability, and will also reduce the Observatory's carbon footprint.

It has taken 18 years to get to this point, thanks to the efforts of many people all over the world, including former Italian delegate Nanni Bignami who unfortunately passed away very suddenly two days ago. Roberto Gilmozzi initiated the precursor 100-metre-diameter OWL project, Riccardo Giacconi promoted it, Catherine Cesarsky oversaw the careful process that resulted in the start of a full design study in early 2007 for what was, by then, a single European project, and Jason Spyromilio led the extended design effort, carried out with industry in the Member States.

In the years that followed it was possible to convince the 15 ESO Member States to commit significant additional funding for the ELT Programme despite the financial crisis. I am very grateful for this support, which was provided because of the enormous scientific return and ESO's track record in delivering quality. The key authorisation for construction was granted in 2014 under Council President Barcons, who is now the Director General designate.

Two other giant telescopes are planned, the Giant Magellan Telescope (GMT) on Las Campanas here in Chile, and the Thirty Meter Telescope (TMT) in the northern hemisphere. Together with the ELT, these telescopes will open a new era of discovery whose implications may well go beyond astronomy. The cooperation between these three projects to address technological challenges is yet another example of international collaboration for the sake of science. I am pleased to acknowledge our colleagues from GMT and TMT present here for this joint endeavour, as well as for providing the framework of a stimulating and healthy competition from which we all benefit.

The size of the primary mirror of the ELT, and the revolutionary telescope design which includes built-in adaptive optics to correct for the turbulence in the atmosphere, will make the ELT the world's biggest and sharpest eye on the sky for the foreseeable future. This giant leap in capability is as large as that experienced by Galileo when he first turned his telescope to the heavens!

The goal for its use is not that of Verne, to see details on the Moon, or the developments in the Moon Village proposed by the European Space Agency, or to watch all of Middle Earth, but instead to study the deep Universe, to resolve the light of nearby galaxies into that of its constituent stars, and above all to image and characterise the rocky planets that we now know orbit most stars. It is in fact possible that the ELT will find evidence for life on other worlds. It is ironic that this would be done from the magnificent desolation of the Atacama Desert.

The ELT construction effort is carried out by a large team with staff from across ESO, led by Roberto Tamai who works closely with ESO's top management. Many team members are here. Roberto will make sure that the construction will stay on schedule, so that what was once a dream becomes reality.

The ELT will no doubt produce discoveries that we simply cannot imagine today, and it will surely inspire numerous people around the world to think about science, technology and our place in the Universe. This will bring great benefit to the ESO Member States, to Chile, and the rest of the world. For this reason we seal the ELT time capsule today for all mankind.

ESO/E. Vernet

The Deformable Secondary Mirror being hoisted into its hub, already mounted on the top end of Unit Telescope 4.

DOI: 10.18727/0722-6691/5019

The Adaptive Optics Facility: Commissioning Progress and Results

Robin Arsenault[1]
Pierre-Yves Madec[1]
Elise Vernet[1]
Wolfgang Hackenberg[1]
Paolo La Penna[1]
Jérome Paufique[1]
Harald Kuntschner[1]
Jean-François Pirard[1]
Johann Kolb[1]
Norbert Hubin[1]

[1] ESO

All the Adaptive Optics Facility (AOF) subsystems are now in Paranal and the project team is working on commissioning activities on Unit Telescope 4 (UT4) of the Very Large Telescope. Excellent progress has been made; the new secondary mirror unit, the Deformable Secondary Mirror (DSM), was installed in October 2016 and UT4 is now operating routinely with the DSM in non-adaptive optics mode. The other modules of the AOF, the Ground Atmospheric Layer Adaptive optiCs for Spectroscopic Imaging (GALACSI), the 4 Laser Guide Star Facility (4LGSF) and the GRound-layer Adaptive optics Assisted by Lasers (GRAAL), have been installed and are being qualified. The coupling with the High Acuity Wide field *K*-band Imager (HAWK-I) and the Multi Unit Spectroscopic Explorer (MUSE) has been tested and all elements are functional and ready to proceed with their full commissioning. The goal for the AOF is to complete GALACSI wide-field mode technical commissioning by the end of summer 2017 and the GRAAL ground-layer adaptive optics mode by the end of the year.

ESO Project Team:

D. Bonaccini Calia, P. Duhoux, J.-L. Lizon, S. Guisard, P. Lilley, L. Petazzi, P. Hammersley, I. Guidolin, L. Kern, T. Pfrommer, C. Dupuy, R. Guzman, J. Quentin, M. Quattri, R. Hozlöhner, D. Popovic, M. Comin, S. McClay, S. Lewis, F. Gago, M. Sarazin, P. Haguenauer, A. Jost, J. Argomedo, S. Tordo, R. Donaldson, R. Conzelmann, M. Lelouarn, R. Siebenmorgen, M. Downing, J. Reyes, M. Suarez Valles, S. Stroebele, S. Oberti, P. Gutierrez Cheetam, M. Kiekebusch, C. Soenke, E. Aller-Carpentier, P. Jolley, J. Vernet, A. Manescau-Hernandez, L. Mehrgan, G. Calderone, A. van Kesteren, G. Chiozzi, H. Sommers, D. Dorigo, T. Bierwirth, J.-P. Kirchbauer, S. Huber, G. Fischer, A. Haimerl, S. Leveque, P. Amico, G. Hubert, S. Brillant, P. Baksai, J.C. Palacio, I. Munoz, E. Fuenteseca, P. Bourget, P. Hibon, F. Selman, G. Hau, S. Egner, T. Szeifert, J.C. Guerra.

Introduction

Towards the end of 2016, the only missing pieces of the Adaptive Optics Facility (AOF) complex (see Arsenault et al., 2010, 2014a and 2016 for previous progress updates) were the new secondary mirror (M2) unit — the Deformable Secondary Mirror (DSM) — and the Ground Atmospheric Layer Adaptive optiCs for Spectroscopic Imaging (GALACSI) adaptive optics (AO) module. The new M2 unit was installed in October 2016 during a shutdown of Unit Telescope 4 (UT4 — Yepun) and the whole telescope was recommissioned with the new M2 unit by December 2016. Since then, UT4 has returned to operations and the Paranal telescope and instrument operators (TIOs) and science support staff have been trained to use the telescope with this new secondary mirror in non-adaptive optics mode. The AOF team remains in close contact with Paranal staff and closely monitors any errors and issues to provide support and solutions.

At the end of 2016, the GALACSI instrument was dismounted from the Adaptive Secondary Simulator and InStrument Testbed (ASSIST) in the Garching integration hall and packed for transport to Chile. After reintegration in Paranal, all functionalities were recovered. In late March 2017, GALACSI was installed on UT4 and was then ready to enter the commissioning phase.

The project is now fully involved in commissioning activities and these will continue during 2017 and into part of 2018. Commissioning runs are scheduled almost every month during bright time. Some of them may be returned to science operations if commissioning progress is rapid and if there are no technical problems or bad weather. The intention is to complete the commissioning of the Multi Unit Spectroscopic Explorer (MUSE) with the GALACSI Wide Field Mode (WFM) at the end of the summer 2017, with Science Verification planned for August 2017. Commissioning of the High Acuity Wide field *K*-band Imager (HAWK-I) and the GRound-layer Adaptive optics Assisted by Lasers (GRAAL) in ground layer adaptive optics (GLAO) mode is planned by the end of 2017. Then only MUSE with GALACSI in Narrow Field Mode (NFM) will remain to be commissioned in 2018.

Installation of new M2 unit on UT4

In September 2016, the 14 crates containing the DSM system (Arsenault et al., 2013a; Manetti et al., 2014; Briguglio et al., 2014), totalling 9 tonnes and 50 cubic metres, were unpacked in the New Integration Hall (NIH) in Paranal. The system was re-assembled in the NIH and functionalities tested. It was an opportunity to cross-train our Paranal colleagues and demonstrate several handling operations, including the critical thin-shell mirror handling.

Before proceeding with the removal of the old Dornier M2 unit, a laser tracker was installed on the telescope centrepiece and used to record reference positions of markers on the telescope structure and the M2 hub and spiders. Additionally, reference measurements were taken to characterise the telescope optical behaviour and performance, some of them using the GRAAL Maintenance and Commissioning Mode (MCM) wavefront sensor. Close-out measurements were also taken for the instruments available at UT4 (the Spectrograph for INtegral Field Observations in the Near Infrared [SINFONI], HAWK-I, MUSE and the VLT Interferometer [VLTI]) with the support of Science Operation. These would later be used to verify that telescope and instrument performance had not been degraded after the installation of the new M2 unit.

On 14 October 2016, the first transport took place to UT4 and the DSM hub was brought to the telescope. The next day the DSM followed the same route. Extreme care was taken during the transport and the load was accompanied on foot all the way to monitor the smoothness of the ride. The replacement began with the removal of the Beryllium M2 mirror. Then within one day the Dornier hub was removed and the new M2 hub, with its DSM dummy weight, installed instead. Three days later the DSM was installed in

Figure 1. A jubilant team after the installation of the DSM on UT4.

its hub (see p. 7). Using the laser tracker, it was possible to verify that the DSM hub ended up, after its installation on the telescope, within 1 mm of the Dornier hub's position, while its longitudinal axis was colinear within 1 arcminute. Calibrated mechanical spacers and alignment tools allowed this feat, as well as the expertise of the optical engineers in Garching and Paranal. The whole operation was led by the Paranal mechanical team under the close supervision of the contractor Microgate and the Garching DSM team.

It is amazing to think that, after such an intrusive and major operation on the telescope, the first pointing on sky was successful, with pointing errors of the same magnitude as usual, and the active loop was closed successfully after the first iteration! Figure 1 illustrates the effect of this achievement on the whole team.

Telescope re-commissioning

During the first nights after installation, basic tests were carried out to verify the behaviour of the DSM hexapod. The focusing motion was as expected and the three focal planes could be accommodated within the DSM focusing range. The impact of M2 centring on the telescope coma was measured using the GRAAL MCM wavefront sensor. Excellent agreement between the centring of the old Dornier and the new M2 was achieved, and the GRAAL MCM mode proved extremely useful during all the telescope recommissioning phases. It also shows that mechanical flexure introduced by the new M2 unit is fully comparable to that experienced with the old Dornier.

The new magnitude zero points for HAWK-I were found to be identical, within 3 %, to the former values and the emissivity was measured as 25 % for the Dornier and 24 % for the new M2 unit. The plate scale change was measured at 1.00047 ± 0.0005 on the Nasmyth B guide probe, which compares to 1.00067 when measured directly on HAWK-I; these results mean that, for all practical purposes, the plate scale change is negligible.

A series of 10-second *J*-band images were taken of the globular cluster M30 using the new M2 unit. Figure 2 (left) shows one of the best images obtained with the DSM, with a full width at half maximum (FWHM) of the star images of 0.37 arcseconds (visual band seeing was 0.5 arcseconds at the time of the exposure); see Figure 2, right. This measurement demonstrates that the optical quality of the DSM in non-adaptive optics mode allows seeing-limited observation even under excellent seeing conditions.

The next step consisted of assessing the changes in the operation of the active optics. The strategy was to record the active optics aberration measurements of the telescope after application of the so-called "OneCal", the look-up table for the primary mirror (M1) modes versus altitude. Comparisons were made between the Dornier and the DSM. The values are very similar between both, and the active optics functionality and operational aspects are preserved with the DSM as well. The secondary chopping was also tested and behaved as expected. Only two points remained to be examined — the flexure of the DSM reference body and the DSM flattening vector.

The trefoil and astigmatism terms evolve with altitude as can be seen in Figure 3. Only the terms along the altitude axis show a variation. This does not come as a surprise as it was known that the reference body of the DSM is subjected to this sort of deformation. At the zenith, the reference body is deformed in a threefold sag shape (trefoil) because of the system of three supporting points. At the horizon this deformation evolves toward an astigmatism. The left plot in Figure 3 shows that this variation is seen by the active optics of the telescope and corrected by M1. However, the level is quite acceptable and, since the end of the commissioning,

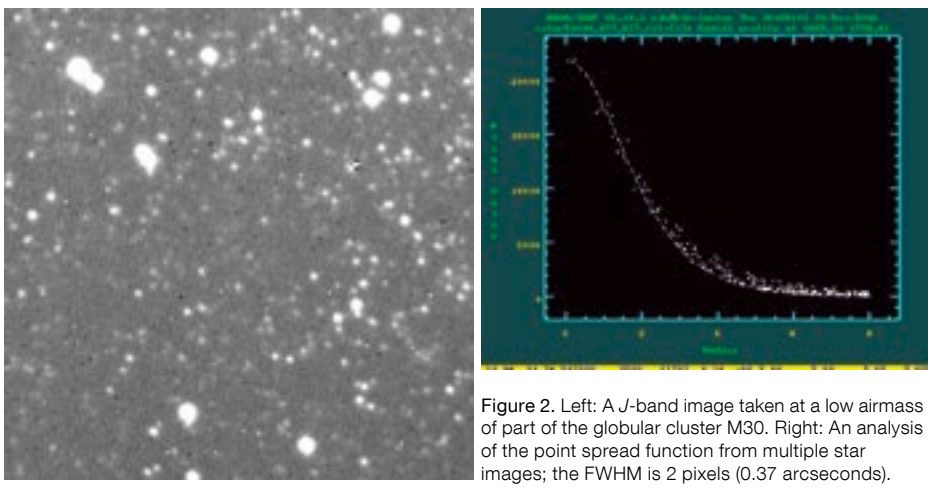

Figure 2. Left: A *J*-band image taken at a low airmass of part of the globular cluster M30. Right: An analysis of the point spread function from multiple star images; the FWHM is 2 pixels (0.37 arcseconds).

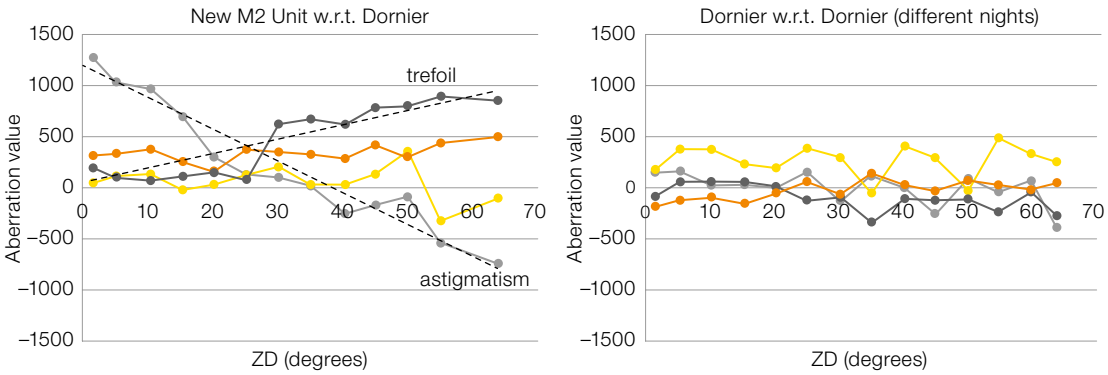

Figure 3. Left: The difference in OneCal residual aberrations between the DSM and the old Dornier M2 unit as a function of zenith distance (ZD). Zernike pairs of orthogonal modes for trefoil and astigmatism are shown. Right: Same as left figure but for two different sets of measurements of the Dornier M2 unit on different nights, showing the typical noise level. The DSM shows clear trends of the astigmatism and trefoil aberrations with altitude (zenith distance).

the active optics has managed this change without issue. Note that the corresponding mode amplitude applied in the DSM flattening vector has been modified to ensure that the horizontal axis crossover occurs at a typical operation airmass.

The same type of analysis reflected a slightly higher scatter in the higher M1 mode amplitudes. We believe that this is due to some high-order aberrations in the DSM flattening vector. After these measurements a calibration was carried out to optimise the DSM flattening vector and reduce its content in high-order aberrations.

Finally, a detailed analysis of the field stabilisation performance took place. Many small issues were encountered, resulting from the telescope environment and the somewhat different control parameters required by the DSM, but all were progressively resolved. The final performance is certainly adequate. The only remaining issue is poorer performance when the telescope is facing into a strong wind. More data need to be recorded to fully understand the root cause of this problem before it can be fixed.

An analysis of the field stabilisation closed-loop rejection transfer function was performed. For a control frequency of 32 Hz, integration time of 0.01 s and control parameters of K_p = 0.7, K_i = 1.5 and $K_{offload}$ = 0.02 and a 3 Hz cutoff frequency, a 6 dB overshoot (> 45° phase margin) was observed.

HD 49798	Before	After
K	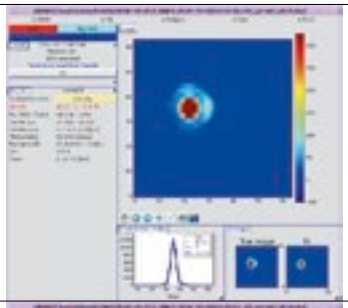	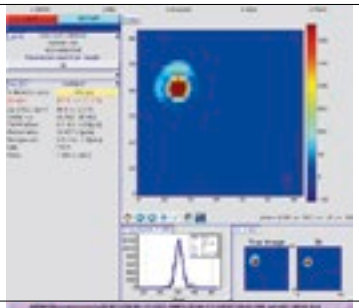
H+K	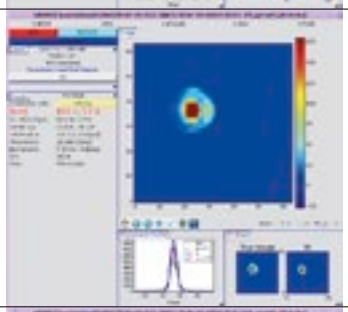	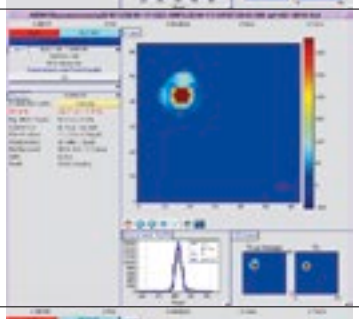
H	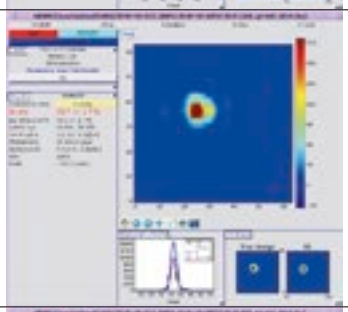	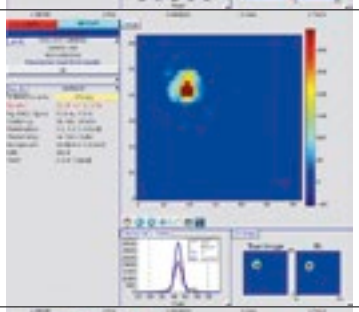
J	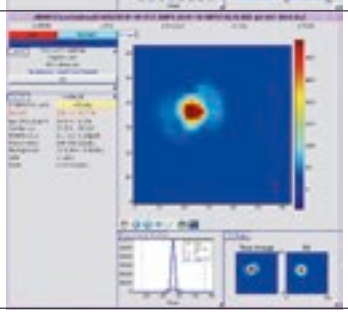	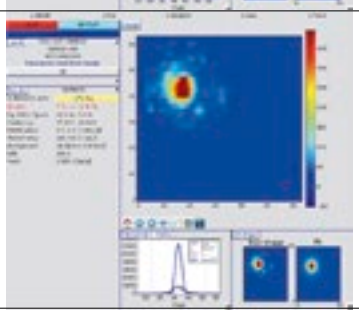

Figure 4. PSF samples for the star HD 49798. The "Before" and "After" columns refer to images obtained with the Dornier M2 unit and the new DSM M2 unit, respectively. The external seeing values were similar in both cases.

UT4 instrument recommissioning

To complete the recommissioning process, the instrument scientists of HAWK-I, MUSE, SINFONI and the VLTI performed a dedicated set of tests to assess the behaviour of these instruments after the new M2 installation. These tests addressed several aspects of the instruments' performance; we show here only a few excerpts from the recommissioning reports. Figure 4 shows a sample of SINFONI PSFs and corresponding Strehl ratios in different bands for the star HD 49798. The results are essentially identical, except in the *J*-band where high spatial frequency residuals can be noticed (static speckles around the diffraction limited core); these residuals are due to the high spatial frequency aberrations of the DSM optical surface. The situation was later improved by calibrating and updating the reference vector position of the DSM when in non-AO mode.

The HAWK-I recommissioning report also thoroughly reviewed several performance criteria for the instrument. The Two Micron All Sky Survey (2MASS) Touchstone Fields were observed and reduced using the new Cambridge Astronomy Survey Unit (CASU) pipeline. The variation of the FWHM across the whole field of view was compared and appeared as expected (see Figure 5). The ellipticity of the star images was also examined in the different fields. The report concluded that the installation of the new M2 unit has had no impact on the overall performance of HAWK-I.

The reports on MUSE and VLTI also concluded that the behaviour remained similar before and after the installation of the new M2 unit. Small differences were observed in behaviour, enough to realise that the M2 has been exchanged, but there was certainly no loss in performance with respect to the Dornier M2 unit.

DSM commissioning with the GRAAL Maintenance and Commissioning Mode

The last step of the new M2 commissioning was the verification of the performance of the DSM in AO mode. The GRAAL MCM mode (Arsenault et al., 2014b; Paufique et al., 2012) was developed for this purpose; it is based on single conjugate AO, making use of a 1 kHz – 40 × 40 subaperture wavefront sensor (WFS) looking at a bright natural guide star on-axis, therefore fully exploiting the 1172 actuators of the DSM. The tests were carried out during a run in February 2017. Unfortunately, many nights were lost to high humidity and only slightly more than half of the ten nights could be used for on-sky tests. The result is that less time was available to optimise the performance. In particular, not enough time was available to characterise the non-common path aberrations and apply an accurate offset for them on the DSM. Nevertheless, excellent images and performance could be obtained and all the servo-loops and offloads could be validated in this technical mode (this is, however, not a science observing mode; see Figure 6).

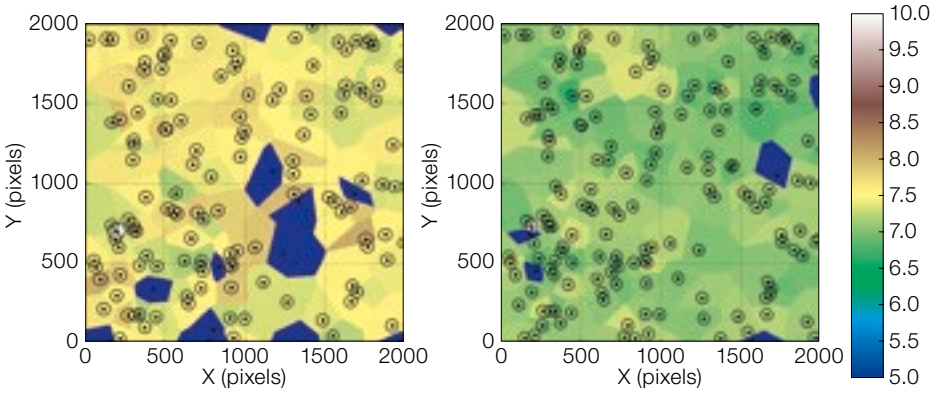

Figure 5. Images of the behaviour of the FWHM across HAWK-I images in *Y*-band at airmass 1.0. Left: with the Dornier M2 unit; Right: with the DSM. The scale shows the FWHM in pixels (pixel scale is 0.106 arcseconds) and annuli around the star positions indicate measured ellipticity.

First commissioning of the GALACSI Wide Field Mode

On 12 March 2017, following re-integration and verification in the NIH, the GALACSI module (La Penna et al., 2014; Arsenault et al., 2013b; Stuik et al., 2012) was transported to UT4 and installed on the Nasmyth platform (Figure 7). Precautions were taken to protect the MUSE hardware during installation (a special protective fence was designed and manufactured). First light was obtained on 20 March on GALACSI, despite an emergency telescope shutdown which delayed the GALACSI installation by one week.

In April 2017, there was another on-sky commissioning run during which many technical tests were conducted to reliably enable the full adaptive optics correction performance of the GALACSI WFM, making use of the DSM and the 4LGSF (Hackenberg et al., 2014; Bonaccini Calia et al., 2014; Holzlöhner et al., 2008; Holzlöhner et al., 2010; Holzlöhner et al., 2012; Amico et al., 2015). The complete automatic acquisition sequence was run on numerous occasions and timed. The acquisition involves presetting the telescope to the target, acquiring the 4 Laser Guide Stars within the 5 arcsecond field

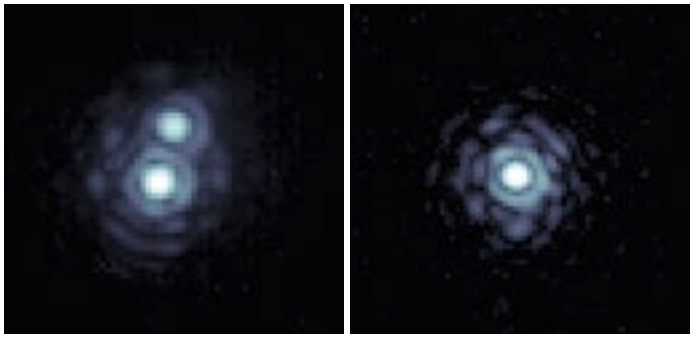

Figure 6. Left: *K*-band narrow filter image of a double star with 0.2 arcsecond separation, obtained with GRAAL MCM. Right: A bright star image exhibiting 80 % Strehl ratio (also with *K*-band narrow filter). The seeing was 0.55 arcseconds at the time.

Figure 7. Left: GALACSI being hoisted through the azimuth hatch after transport from the Paranal New Integration Hall to UT4. Right: The very tight margin to manoeuver this sensitive module between the Nasmyth acquisition and image rotator unit and the MUSE fore-optics can be seen.

of view of the four GALACSI wavefront sensors, performing the detection and centering of the tip-tilt natural guide star, and then closing all the loops. The final results are impressive; after a few nights spent on improving the automatisation of this process, the overhead for the AOF acquisition after the telescope is ready (two active optics cycles) was measured to be less than one minute (50 seconds). It should be remembered that the specification for the overhead was 5 minutes and the goal 2 minutes.

Amongst many performance tests conducted, one of them consisted of evaluating the stability of the registration between the actuator pattern of the DSM and the WFS sub-aperture pattern. Shifts with respect to one another are due to mechanical flexure in the large distance between them and could lead to a degradation of the optical quality of the images delivered by GALACSI to MUSE. Figure 8 shows that, thanks to a rigid design and good optical alignment, the stability of the pupil shift is pretty good from zenith down to 35° altitude, meaning that a compensation strategy for this misalignment may not be needed, thus simplifying the GALACSI operations.

Rejection transfer functions have been measured for both the high-order correction loop and the tip-tilt loop. Both look good and can be fitted nicely by the model of the dynamic system with respectively 1.3 ms and 4.3 ms of pure delay.

System performance has been finally characterised. A gain of 1.5–2 in FWHM at 750 nm was observed between open loop (with telescope field stabilisation) and full closed loop. The seeing matched the atmospheric specification (~1.1 arcseconds) and the target was low in the sky (zenith distance 50°). This is a very good first sign that the GALACSI WFM performs as specified. The ratio of turbulence in the first 500 metres above the telescope to the total turbulence given by the SLOpe Detection And Ranging (SLODAR) measurement and the internal estimation was ~90 % — i.e., quite high — a situation which is best suited to ground-layer AO correction (Kuntschner et al., 2012). Figure 9 illustrates this correction but much better results were obtained later.

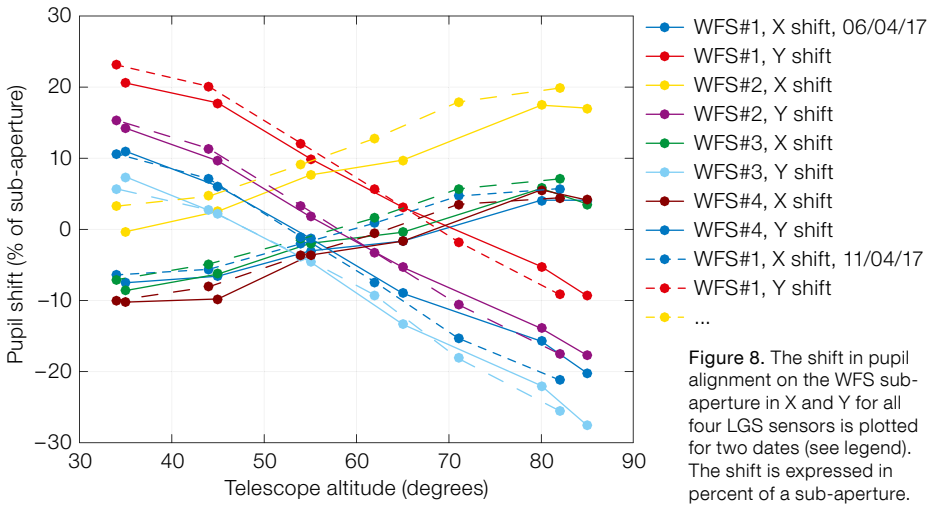

Figure 8. The shift in pupil alignment on the WFS sub-aperture in X and Y for all four LGS sensors is plotted for two dates (see legend). The shift is expressed in percent of a sub-aperture.

The results obtained during later nights improved somewhat, and the statistics showed much better performance. The gain between GLAO and non-GLAO depends strongly on the fraction of turbulence in the lower atmospheric layers. If a large fraction is concentrated below 500 metres, GALACSI will substantially improve the ensquared energy (a gain of four has been obtained). Conversely, if this fraction falls below ~20 %, the gain will be lower and the observer must decide whether seeing-limited observations must be conducted (with shorter acquisition time and without lasers) or simply another mode (MUSE NFM) or instrument. This information is provided from Multi-Aperture Scintillation Sensor (MASS) and Differential Image Motion Monitor (DIMM) data at the Observatory. Figures 10 and 11 demonstrate the ensquared energy performance with open and closed loop, allowing a first assessment of gains, but with limited statistics. From Figure 11, one can determine that

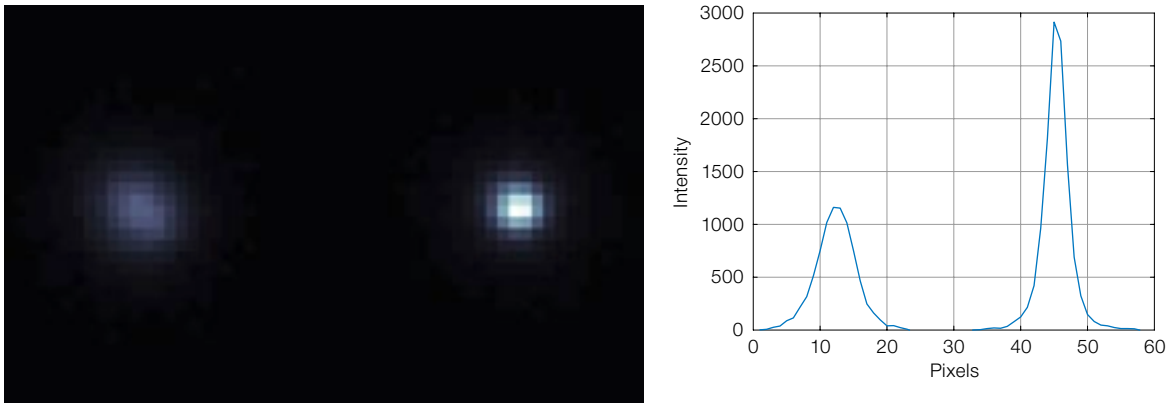

Figure 9. The quality of the image enhancement by GLAO correction is illustrated by before and after images (left) and profiles through the image centres (right). See text for full description.

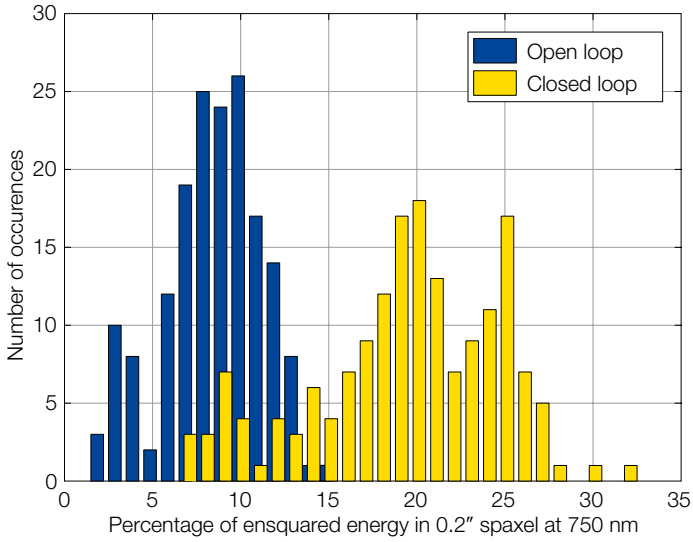

Figure 10. The distribution of values of ensquared energy per 0.2 arcsecond spaxel with GLAO loop is shown for closed loop (yellow) and open loop (blue; only with field stabilisation).

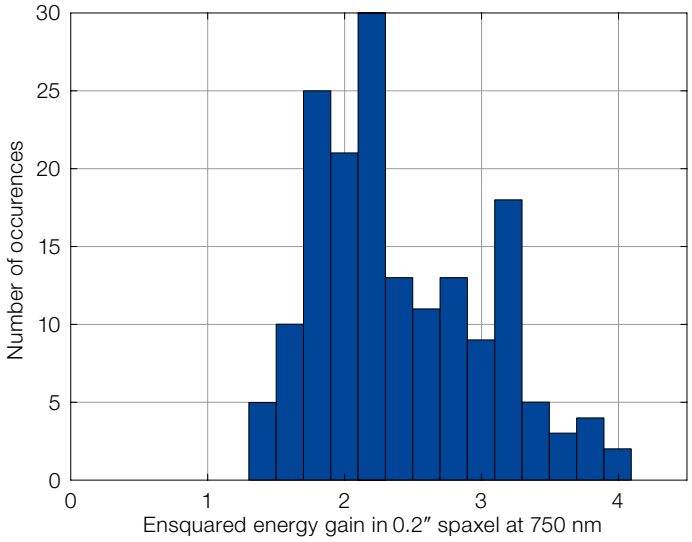

Figure 11. The distribution of gain in ensquared energy per 0.2 arcsecond spaxel with GLAO loop correction is plotted.

a gain of 2.0 can be obtained about 69 % of the time, a gain of 1.9 76 % of the time and a gain of 1.8 83 % of the time. We will closely follow up how these histograms evolve as more statistics are collected with successive commissioning runs.

During one of the commissioning nights, the patch of sky where we pointed happened to have a nice target in the middle, so we couldn't resist taking images at 850 nm with the commissioning camera (Figure 12). The left-hand image of Saturn was taken with field stabilisation; the right hand image with full GLAO. The seeing was fair (0.8 arcseconds) and the pointing was almost at zenith for these observations.

Finally, we could verify that the sensitivity of GALACSI was consistent with that measured on ASSIST in Garching. The tests were performed on an 18.6 magnitude star, the loop was closed and was stable, and the performance was within specification (the specified limiting magnitude of GALACSI is 17.5). Figure 13 shows the raw image on which the loop is closed (left), and the resulting images from averages of 50 frames (centre) and 12 000 frames (right). The 50-frames average will be shown in the GALACSI display panel, so that the user can be confident that the loop is locked on a star.

Conclusions: AOF is on-sky!

Since March 2017, the AOF has been fully installed on UT4. The 4LGSF was the first AOF component to be bolted onto the telescope and it is fully commissioned on-sky (first light was in April 2016). Then the new M2 unit (DSM) was installed and replaced the old Dornier M2 unit in October; since then, the new M2 unit is routinely being used by the TIOs to make science observations with the suite of UT4 instruments. GRAAL was attached to the telescope in late 2016, but will not be fully commissioned until the end of 2017. Last but not least, GALACSI is now also available at Paranal. GALACSI WFM commissioning has begun and the

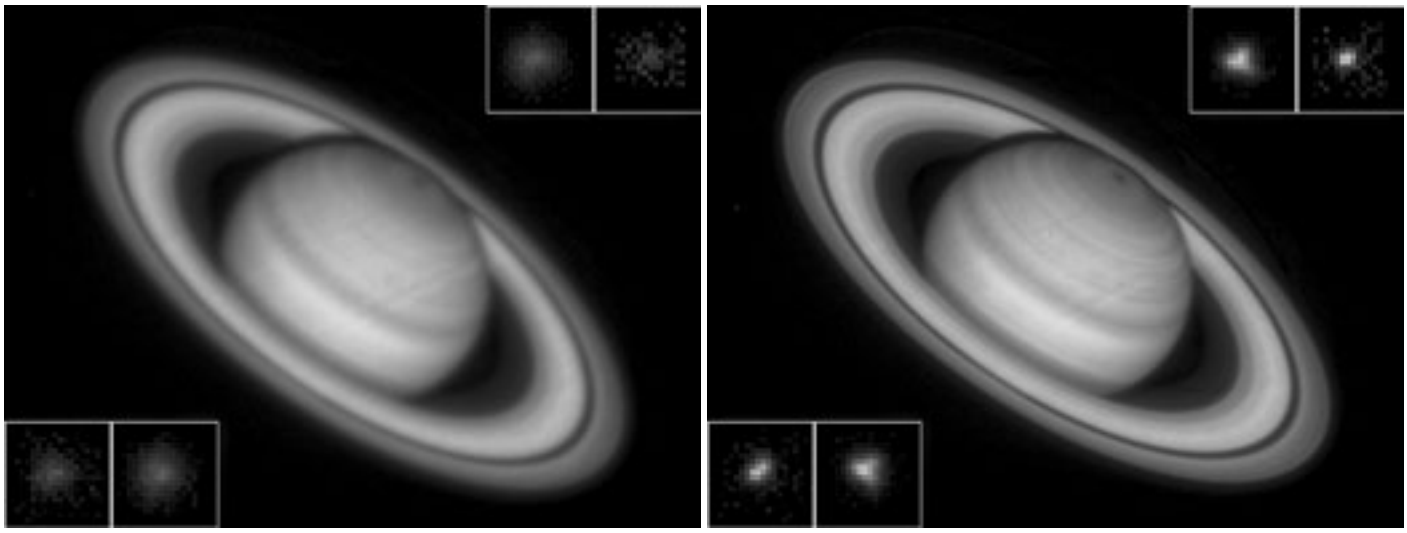

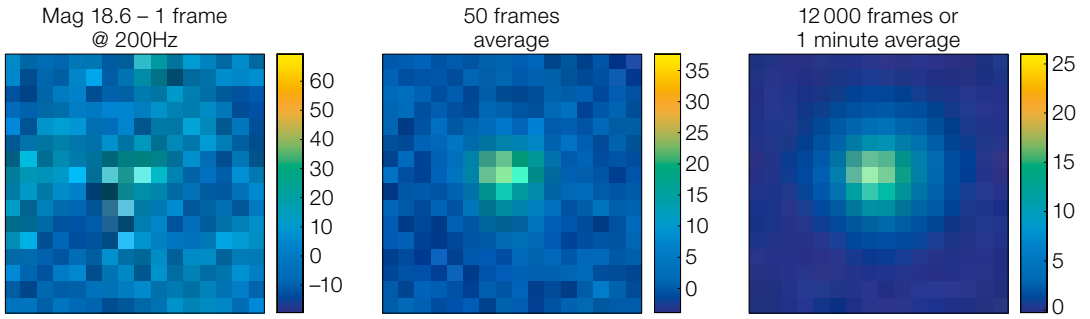

Figure 12. (Above) Saturn observed without (left) and with (right) GLAO. The insets show the effect of the correction on some stellar images.

Figure 13. Individual 200 Hz frame showing the tip-tilt star signal (left), with 50 (centre) and 12 000 (right) frames averaged. The star magnitude is 18.6 and the spaxel size is 0.2 arcseconds.

performance is found to be extremely promising so far.

As an anecdote, the AOF team took the picture shown in Figure 14, illustrating better than a long speech and without ambiguity that the AOF is now on sky (for readers interested in the technical details, each character is created using one laser guide star by controlling its associated 1 kHz jitter mirror; the image was recorded during a 4 s exposure of the Laser Pointing Camera installed on the telescope top ring).

Figure 14. The writing is on … the sky!

References

Amico, P. et al. 2015, The Messenger, 162, 19
Arsenault, R. et al. 2010, The Messenger, 142, 12
Arsenault, R. et al. 2013a, The Messenger, 151, 14
Arsenault, R. et al. 2013b, Third AO4ELT Conference, Florence, Italy
Arsenault, R. et al. 2014a, Proc. SPIE, 9148, 914802
Arsenault, R. et al. 2014b, The Messenger, 156, 2
Arsenault, R. et al. 2016, The Messenger, 164, 2
Bonaccini Calia, D. et al. 2014, Proc. SPIE, 9148, 91483P
Briguglio, R. et al. 2014, Proc. SPIE, 9148, 914845
Hackenberg, W. et al. 2014, Proc. SPIE, 9148, 91483O
Holzlöhner, R. et al. 2008, Proc. SPIE, 7015, 701521
Holzlöhner, R. et al. 2010, A&A, 510, A20
Holzlöhner, R. et al. 2012, Proc. SPIE, 8447, 84470H
Kuntschner, H. et al. 2012, Proc. SPIE, 8448, 844808
La Penna, P. et al. 2014, Proc. SPIE, 9148, 91482V
Manetti, M. et al. 2014, Proc. SPIE, 9148, 91484G
Paufique, J. et al. 2012, Proc. SPIE, 8447, 944738
Stuik, R. et al. 2012, Proc. SPIE, 8447, 84473L

DOI: 10.18727/0722-6691/5020

ESO Public Surveys at VISTA: Lessons learned from Cycle 1 Surveys and the start of Cycle 2

Magda Arnaboldi[1]
Nausicaa Delmotte[1]
Dimitri Gadotti[1]
Michael Hilker[1]
Gaitee Hussain[1]
Laura Mascetti[2]
Alberto Micol[1]
Monika Petr-Gotzens[1]
Marina Rejkuba[1]
Jörg Retzlaff[1]
Robert Ivison[1]
Bruno Leibundgut[1]
Martino Romaniello[1]

[1] ESO
[2] TERMA GmbH, Europahaus, Darmstadt, Germany

The ESO Public Surveys on VISTA serve the science goals of the survey teams while increasing the legacy value of ESO programmes, thanks to their homogeneity and the breadth of their sky coverage in multiple bands. These projects address a variety of research areas: from the detection of planets via microlensing, to stars, the Milky Way and Local Group galaxies, to extragalactic astronomy, galaxy evolution, the high-redshift Universe and cosmology. In 2015, as the first generation of imaging surveys was nearing completion, a second call for Public Surveys was opened to define a coherent scientific programme for VISTA until the commissioning of the wide-field multi-fibre spectrograph, 4MOST, in 2020. This article presents the status of the Cycle 1 surveys as well as an overview of the seven new programmes in Cycle 2, including their science goals, coverage on the sky and observing strategies. We conclude with a forward look at the Cycle 2 data releases and the timelines for their release.

Introduction

ESO has operated two telescopes that are mostly dedicated to Public Surveys since 2010: namely, the 4-metre Visible and Infrared Survey Telescope for Astronomy (VISTA; Sutherland et al., 2015) and the 2.6-metre VLT Survey telescope (VST; Arnaboldi et al., 1998; Capaccioli & Schipani, 2011). These provide coverage from the ultraviolet (0.33 micron) through to the *Ks*-band (2.15 microns). In 2012, Public Spectroscopic Surveys also started using the spectrographs Ultraviolet and Visual Echelle Spectrograph, UVES, GIRAFFE and the ESO Faint Object Spectrograph and Camera, EFOSC2. The spectroscopic surveys were further expanded in 2014 with the addition of two new surveys on Unit Telescope 3 (UT3) using the VIsible MultiObject Spectrograph (VIMOS).

As the first cycle of ESO Public Surveys with VISTA approached its sixth year of successful telescope operations in 2015, ESO opened the call for submission of letters of intent for a second cycle of Public Surveys to run until the end of 2020, the expected date for the decommissioning of the VISTA InfraRed CAMera (VIRCAM). Thirteen letters of intent were submitted by the community by the deadline of October 2015; these involved more than thirteen Principal Investigators (PIs) and 517 co-investigators, with an oversubscription factor of over twice the total available observing time. The joint VISTA/VST Public Survey Panel (PSP) was asked to review these letters to identify a well-balanced scientific programme for VISTA. An important consideration for the VISTA Cycle 2 Public Surveys was the exploration of scientific and observing parameter space that had not been covered by the previous surveys. These recommendations were passed to the Observing Programmes Committee (OPC) and the ESO Director General.

In this article, we provide an overview of the status of the VISTA imaging surveys that started in 2010 and their impact in terms of data releases and refereed publications. We then describe the selection process of the new surveys and provide a summary of their science goals, observing strategies, and the content and timelines of their planned data releases.

Looking further ahead, the construction and deployment of two wide-field spectrographs is foreseen: the Multi Object Optical and Near Infrared Spectrograph (MOONS; Cirasuolo et al., 2011) and the 4-metre Multi Object Spectroscopic Telescope (4MOST; de Jong, 2011) on the VLT and VISTA respectively. They have large multiplexing wide field capabilities and extended wavelength coverage. These spectrographs will be used for follow-up studies of interesting candidates identified via their colours and/or morphological properties from the Public Surveys and/or space missions (for example, the ESA satellite, Gaia, and eROSITA). In the current ESO instrument plan, the 4MOST spectrograph will replace the wide field near-infrared camera, VIRCAM, on VISTA, with commissioning being planned for the end of 2020.

VISTA Cycle 1 surveys: time allocation and current status

The first cycle of approved VISTA Public Surveys includes six imaging projects[1] that began observations in April 2010. Figure 1 shows the completion fractions of the requested time in their observing plans with respect to time. An overview of each of the Cycle 1 surveys is given in Table 1 along with their full titles and acronyms; a more complete description of each of these surveys is presented in *The Messenger* 154 (2013).

The overall time allocations for these surveys are between 1500 and 2200 hours, except for the VHS, which requires 4710 hours for completion. The VHS takes up 28 % of the allocated telescope time to date, while about 12 % goes to each one of the other surveys; additionally Chilean regular and other open-time programmes have been allocated 3 % and 4 % of time respectively. Figure 2 shows a pie chart summarising the time committed to the VISTA surveys between Periods 85 and 99, as a percentage of the total allocated telescope time.

Based on statistics gathered over three years (from October 2012 to September 2015), the total execution time of successfully observed OBs from the VISTA Cycle 1 surveys is 2340 hours per year. The time for open and Chilean time amounts to about 6 % of the total time in that period. Thus, 2490 hours/year are available for successful observations with VISTA. In 2015, the projected observations for the VISTA Cycle 1 surveys showed that observing time would become available in certain right ascension (RA) ranges; hence the need to release a call for VISTA Cycle 2 Public Surveys.

Survey ID, title & homepage	Science topic	Area (square degrees)	Filters	Magnitude limits	Observing time to 1 April 2017 (hours)
UltraVISTA http://home.strw.leidenuniv.nl/~ultravista/	Deep high-*z*	1.7 Deep	*Y J H Ks*	25.7 25.5 25.1 24.5	1780
		0.73 Ultra deep	*Y J H Ks*	26.7 26.6 26.1 25.6	
			NB118	26.0	
VHS — VISTA Hemisphere Survey http://www.ast.cam.ac.uk/~rgm/vhs/	All sky	17800	*Y J H Ks*	21.2 21.1 20.6 20.0	4490
VIDEO — VISTA Deep Extragalactic Observations Survey http://www-astro.physics.ox.ac.uk/~video	Deep high-*z*	12	*Z Y J H Ks*	25.7 24.6 24.5 24.0 23.5	1799
VVV — VISTA Variables in the Via Lactea http://vvvsurvey.org/	Milky Way	560	*Z Y J H Ks*	21.9 21.1 20.2 18.2 18.1	2157/Completed
VIKING — VISTA Kilo-Degree Infrared Galaxy Survey http://www.astro-wise.org/projects/VIKING/	Extragalactic	1500	*Z Y J H Ks*	23.1 22.3 22.1 21.5 21.2	2384
VMC — VISTA Magellanic Clouds Survey http://star.herts.ac.uk/~mcioni/vmc/	Resolved SFH	180	*Y J Ks*	21.9 21.4 20.3	1759

Table 1. General observational parameters for the Cycle 1 VISTA Public Surveys[1]. The columns illustrate the Public Survey programme acronym (column 1), a broad classification of the scientific goal (column 2), the targeted total area (column 3), the filters (column 4), the magnitude limits (10σ AB for VMC; otherwise 5σ AB) in the different filters (column 5) and the observing hours completed up to 1 April 2017 (column 6).

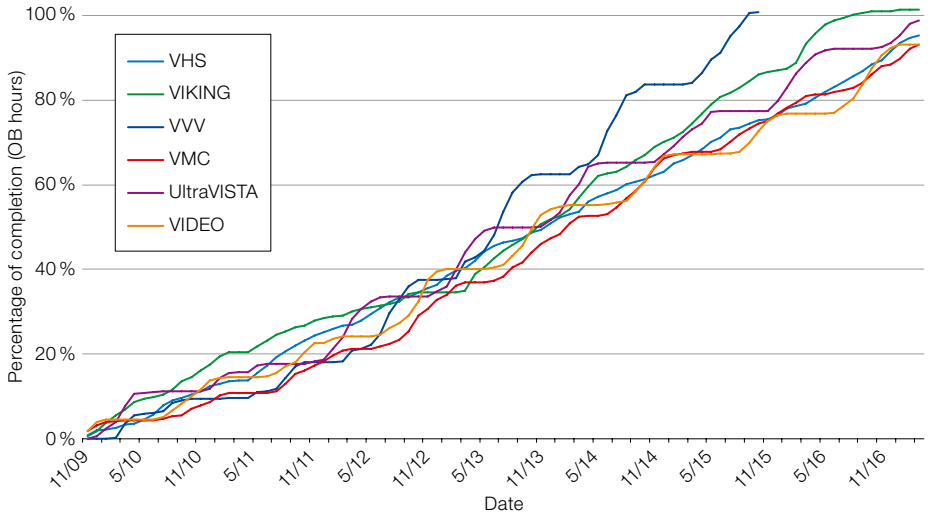

Figure 1. The percentage completion for the Cycle 1 VISTA Public Surveys with respect to the allocated time. Note that completion fractions include the observations taken during dry runs in 2009. The VVV completed its observations in October 2015. VIKING completed observations by the end of 2016, but requires the re-observation of a few tiles that were found to be out of the specified constraints. UltraVISTA, VHS, VMC and VIDEO all had completion fractions larger than 90 % by April 2017.

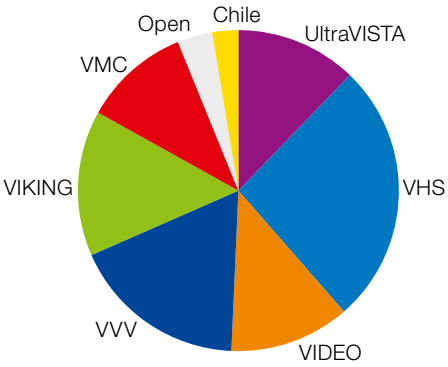

Figure 2. Pie chart showing VISTA time allocation to the Cycle 1 and 2 surveys, as well as Chilean and open time programmes, since Period 85.

The scientific impact of the VISTA surveys and legacy value of the data products

The VISTA surveys produce large, coherent data sets. The constant monitoring of the system stability and the observations of standard stars in combination with the extensive data reductions carried out by the data centres[2, 3, 4] provide for uniform data with many astrophysical applications. The VISTA survey data are listed on the Phase 3 data release manager page[5] and can be searched using the ESO Science Archive Facility[6] (SAF, see Arnaboldi et al., 2014; Retzlaff et al., 2016).

Current active releases provide more than 40 TB of science data products from the VISTA Cycle 1 surveys which have been delivered by the teams. These products, including calibrated images, source lists, photometric catalogues and light curves for multi-epoch observations, are available to the community for their independent scientific research. There are also approximately 12 TB of additional science data products for VISTA, which have been superseded by newer products but remain available on demand by archive users, for example, for verification purposes.

Astronomers have access to images, covering 11 × 10^3 square degrees area in *Y*-, *J*- and *Ks*-bands from VHS, and deep images plus catalogues from the UltraVISTA, VIDEO and VIKING surveys. For example, they can extract measurements from the billion-source catalogue for stars in the Milky Way bulge from the VVV survey, or from the light curves of Cepheid stars in the Magellanic Clouds in VMC. Community use can be quantified by means of the downloaded volume of the VISTA Cycle 1 survey data, and the

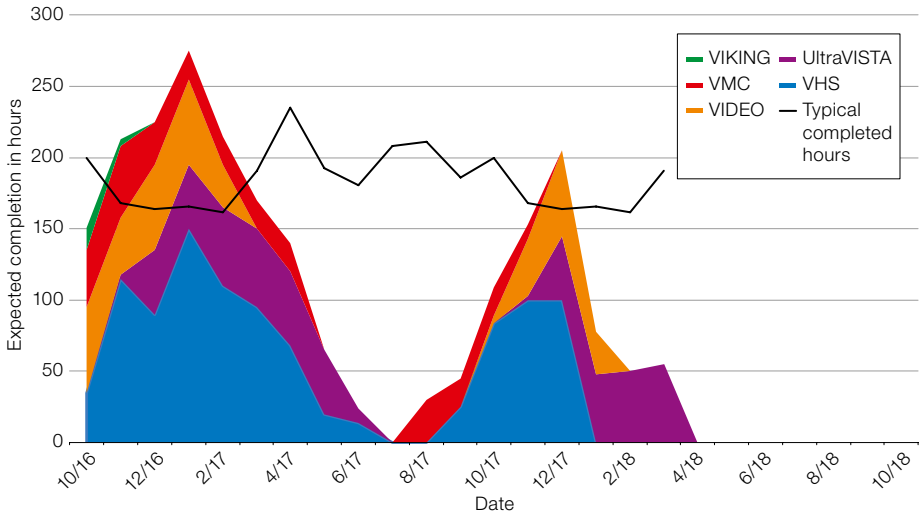

Figure 3. (Left) A histogram of the expected hours of observations for the Cycle 1 VISTA surveys in the period October 2016 to April 2018. The areas are colour coded according to the Cycle 1 survey acronyms. The full line indicates the typical completed hours per month based on VISTA operations over the previous 4.5 years. The available time between the colored areas and the black line was assigned to the new projects selected during the second VISTA call. Some Cycle 2 surveys began observations before April 2017, to exploit time freed up over certain RA ranges by the completion of some Cycle 1 surveys).

Figure 4. (Lower) Cumulative curves describing the volume download (Gb) by archive users of the Cycle 1 VISTA science products (left) and the number of queries (centre) and distinct users (right) accessing the ESO catalogue query interface (see Romaniello et al. [2016] for more information).

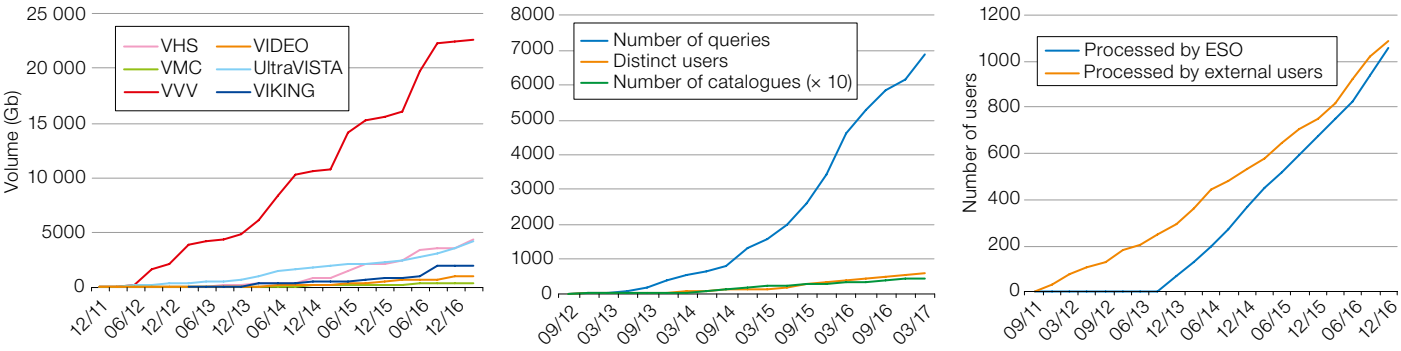

number of distinct queries of the catalogues that have been published through the query interface (see Figure 4).

A robust legacy from the Cycle 1 surveys is also demonstrated by the sizeable contribution to the total number of refereed publications based on VISTA data. Among the merit parameters that quantify the scientific impact of the first cycle of VISTA Public Surveys, there are the number of refereed publications by the survey teams and archive users. By April 2017, there were more than 300 refereed publications based on the data generated by the Cycle 1 surveys, according to the ESO Telescope Bibliography[7]. The numbers of refereed publications are as follows: VHS 45; UltraVISTA 82; VVV 129; VIDEO 25; VIKING 32; and VMC 34. A total of 86 refereed publications (~ 25 % of the total) are based on VISTA archival data (raw or reduced) and come from authors who were not co-investigators in the Public Survey proposals.

VISTA Cycle 2 surveys: science goals and observing strategies

In this section we provide an overview of the selection process of the Cycle 2 surveys and a summary of their science goals, observing strategies and relevant milestones. As noted earlier, the process of selecting and defining the second cycle of VISTA surveys started in October 2015 with the submission of 13 letters of intent from the community. The PSP met in January 2016 and recommended seven projects that were subsequently invited to submit formal proposals for the May 2016 OPC meeting. Following their review and endorsement by the PSP, the OPC and the Director General, the teams prepared Survey Management Plans (SMPs), which were in turn reviewed by the ESO survey team. This process was completed in January 2017, with the publication of the approved SMPs on the ESO Public Surveys web pages[1] and their announcement in the ESO Science Newsletter[8]. The seven new projects formally began observations on 1 April 2017. The full titles and acronyms of each of these surveys are given in Table 2 along with a brief summary of their observing parameters; in Figure 5 and 6 we show the footprints of the approved surveys and the requested hours in each RA bin per year, together with an illustration of the available hours per year.

The majority of the new surveys explore the time domain. When the VVVX reaches completion in 2020, its multi-epoch observations will have a baseline of over ten years (when combined with the Cycle 1 VVV survey). The science quality and the constant monitoring of the stability of the VISTA/VIRCAM system support the requirements of these surveys to measure accurate and consistent stellar positions and fluxes in several bands, over this timeframe. VINROUGE exploits the stability of VISTA in combination with the efficiency of the Target of Opportunity (TOO) mode to trigger the quick follow-up and monitoring of transient events.

Survey Acronym	Survey title & homepage	PI	Area (square degrees)	Filters	Total hrs	Multi-epoch observations
VINROUGE	Kilonova counterparts to Gravitational wave sources http://www.star.le.ac.uk/nrt3/VINROUGE/	N. Tanvir	~300 (10 triggers)	*Y J Ks*	420	yes
Cont. UltraVISTA	Completing the legacy of UltraVISTA http://home.strw.leidenuniv.nl/~ultravista/	J. Dunlop, M. Franx, J. Fynbo, O. Le Fèvre	0.75	*J H Ks*	756	no
VVVX	Extending VVV to higher Galactic latitudes http://vvvsurvey.org/	D. Minniti, P. Lucas	1700	*J H Ks*	1985	yes
VEILS	VISTA Extragalactic Infrared Survey http://www.ast.cam.ac.uk/~mbanerji/VEILS/veils_index.html	M. Banerji	9	*J Ks*	1153	yes
GCAV	Galaxy Clusters at VIRCAM http://www.GCAV.it	M. Nonino	30	*Y J Ks*	560	no
VISIONS	VISTA star formation atlas https://visions.univie.ac.at/	J. Alves	550	*J H Ks*	553	yes
SHARKS	Southern Herschel-Atlas Regions *K*-band survey http://sharks.roe.ac.uk/	I. Oteo	300	*Ks*	1200	no

Table 2. Overview of the Cycle 2 VISTA Public Surveys. The columns illustrate the Public Survey acronym (column 1), the survey title (column 2), the PI name (column 3), the area covered (column 4), the filters (column 5), the total hours requested (column 6) and the request for multi epoch observations (column 7).

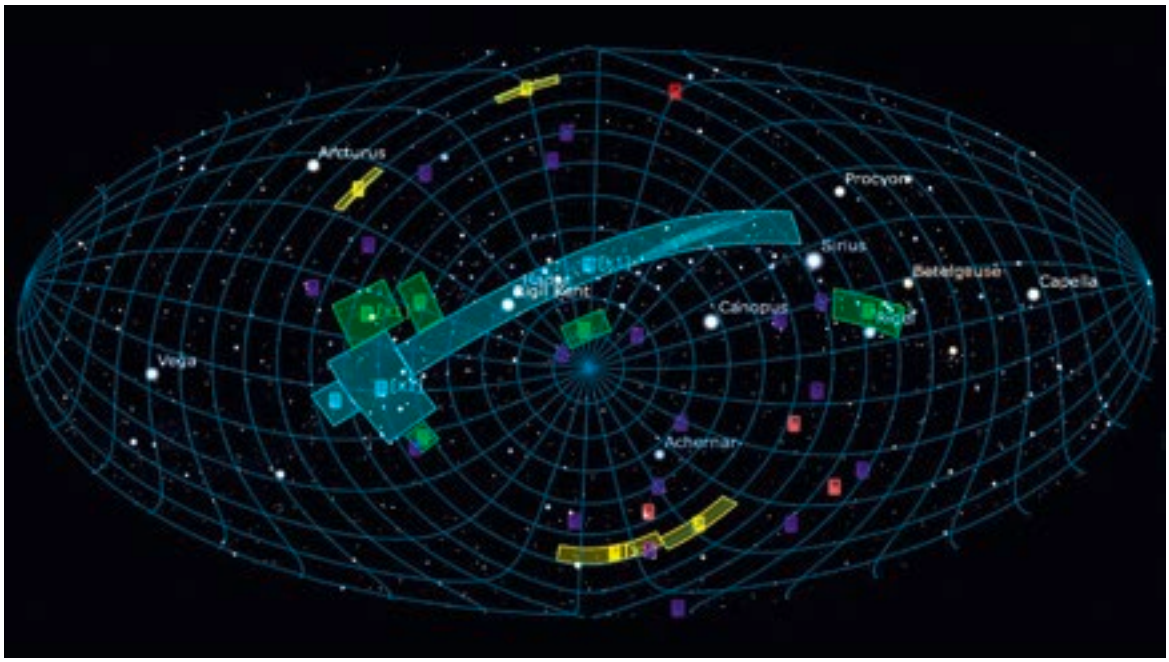

Figure 5. Sky coverage of the Cycle 2 VISTA Public Surveys. The colour coded footprints of their targeted areas are: VVVX (light-blue); VISIONS (green); SHARKS (yellow); GCAV (violet); VEILS (light-red), UltraVISTA (red). As pointings for VINROUGE are set by gravitational-wave triggers, they cannot be included here.

1. VINROUGE — VIsta Near-infraRed Observations Unveiling Gravitational wave Events — PI Nial Tanvir (University of Leicester)

This survey will conduct near-infrared follow-up imaging of the error regions for gravitational wave (GW) detections identified by the Laser Interferometer Gravitational-Wave Observatory (LIGO)-Virgo Collaboration. It will specifically target events that are likely to be due to a merger of a compact binary pair including at least one neutron star. Such systems are also expected to give rise to r-process kilonovae/macronovae, with spectral energy distributions peaking in the near-infrared in the days following the merger. Detection of an electromagnetic (EM) counterpart would trigger considerable further follow-up, providing the route to the redshift and host environment, and heralding a new era of GW-EM astrophysics. The Public Survey strategy will evolve over the course of the survey, as the behaviour of kilonovae is better characterised, and its strategy will be tailored to the parameters of each event. The total time requested by this survey project is 420 hours, nominally for up to ten triggers, resulting in a coverage of ~300 square degrees. The baseline plan is to image the first visit in three filters (*Y*, *J*, *Ks*) and one filter (*J*) at a repeat epoch to probe variability. Typically the limiting magnitude of the images is expected to reach J_{AB} = 21.

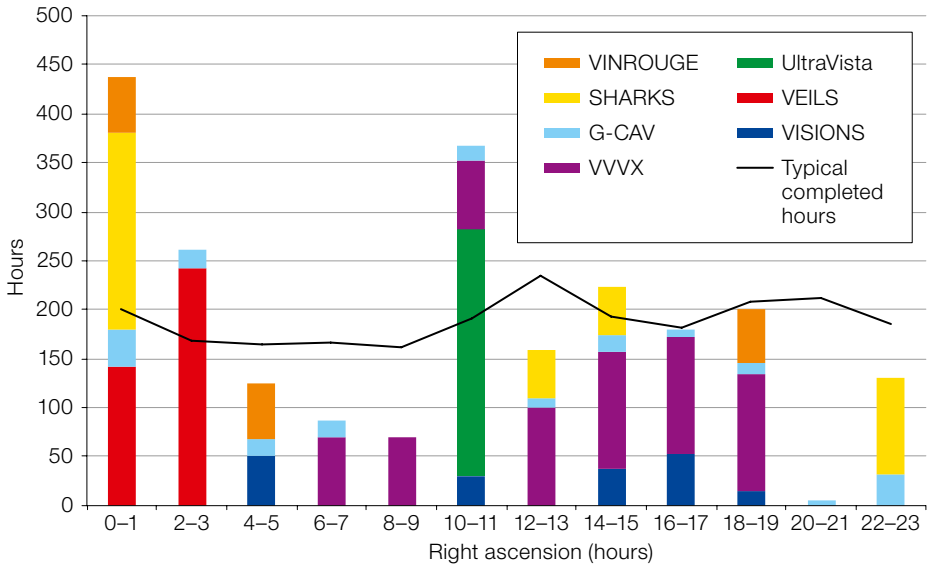

Figure 6. Requested hours per RA bin per year for the Cycle 2 VISTA Public Surveys. The continuous black line shows the typical available hours, based on the performance of VISTA in the previous 4.5 years. The RA range for VINROUGE shown here is set by the time of the year during which gravitational wave alerts may be triggered by the LIGO-Virgo collaboration.

2. Completing the legacy of UltraVISTA — PI Jim Dunlop (University of Edinburgh), Marijn Franx (Leiden Observatory), Johan Fynbo (University of Copenhagen), Olivier Le Fèvre (Laboratoire d'Astrophysique de Marseille)

The purpose of this survey is to complete the legacy of UltraVISTA by delivering the deepest degree-scale near-infrared imaging of the sky, within the unparalleled Cosmic Evolution Survey (COSMOS) field. This three-year programme will bring the *J*, *H* and *Ks* imaging across the full 1.5 square degrees footprint of VIRCAM to the same depths as has been achieved within the ultra-deep strips of the Cycle 1 UltraVISTA programme at Data Release 4; i.e., $J = 26.0$, $H = 25.7$, $Ks = 25.3$ (AB mag, 5σ, 1.8-arcsecond apertures). This will be well matched to the depths of the optical imaging from the new Subaru Hyper-SuprimeCam deep survey, and to the depths of the SPitzer Large Area Survey with Hyper-Suprime-Cam (SPLASH) using the Spitzer telescope. This 756-hour survey will deliver new results on the galaxy UV luminosity function out to redshift, $z = 8$ and the galaxy stellar mass function out to redshift, $z = 6$. It will also be a key resource for the study of dust-enshrouded star-forming galaxies, and for identifying spectroscopic targets for NASA's James Webb Space Telescope (JWST). This project maximises the value of the VISTA time already invested in the COSMOS field, and will secure the long-term legacy of VISTA for studies of the distant Universe.

3. VVVX — The VVV eXtended ESO Public Survey — PIs Dante Minniti (Universidad Andres Bello, Santiago de Chile), Philip Lucas (University of Hertfordshire)

The Cycle 1 Survey, VVV, mapped the Milky Way bulge and the adjacent southern mid-plane repeatedly over six years. The new VVVX survey, will fill the gaps left between the VVV and VHS areas and extend the baseline of VVV further, enabling proper motion measurements of < 0.3 milliarcseconds per year in the optically obscured regions where the Gaia satellite mission is limited by extinction. VVVX will take ~ 2000 hours, and cover 1700 square degrees of the southern sky, for the range of Galactic longitude, $20° \leq l \leq 130°$ (7 h < RA < 19 h). VVVX will provide a deep *JHKs* catalogue of about 2×10^9 point sources, as well as a *Ks*-band catalogue of ~ 10^7 variable sources. Within the area overlapping with the Cycle 1 VVV survey, VVVX will produce a 5-D map of the surveyed region by combining positions, distances and proper motions of well-understood distance indicators (for example, red clump stars, and RR Lyrae and Cepheid variables) in order to unveil the inner structure of the Milky Way. The VVV and VVVX catalogues will complement those from Gaia with very red sources and will feed spectroscopic targets for the forthcoming ESO high-multiplex spectrographs, MOONS and 4MOST.

4. VEILS — The VISTA Extragalactic Infrared Legacy Survey — PI Manda Banerji (University of Cambridge)

This is a deep *J* and *Ks*-band transient and wide-field survey with the following primary goals: to understand the epoch of reionisation and the build-up of massive galaxies; and constrain the cosmological equation of state using Type Ia supernovae and active galactic nuclei dust lags. VEILS will cover 9 square degrees over three fields: the European Large Area ISO Survey (ELAIS) S1 (RA = 00 h 30 m; Dec = −43° 00′); the Chandra Deep Field South, CDF-S (RA = 03 h 36 m; Dec = −28° 00′); and XMM-Newton Large scale Synoptic Survey field, the XMM-LSS (RA = 02 h 22 m; Dec = −06° 00′). The proposed per-epoch survey depths are $J < 23.5$ and $Ks < 22.5$ mag in all fields and in total 33–50 epochs per field per filter are expected over the entire duration of the survey. VEILS will take a total of 1153 hours (128 nights) in < 1 arcsecond seeing conditions to complete the survey.

5. GCAV — Galaxy Clusters At VIRCAM — PIs Mario Nonino (INAF, Trieste)

GCAV is a 560-hour infrared survey of a sample of 20 galaxy clusters, evenly distributed over the 0-24h RA range, which will mainly explore galaxy evolution over a broad, and largely unexplored, range of cluster environments.

All of the selected clusters have already been observed by the Advanced Camera for Surveys (ACS) and Wide Field Camera 3 (WFC3) on the Hubble Space Telescope (HST) by the following programmes: Cluster Lensing And Supernovae Search with Hubble (CLASH), Hubble Frontier Fields (HFF) and the Frontier Fields and Reionisation Lensing Cluster Survey (RELICS). Furthermore, a wealth of ground based ancillary data, from optical imaging and spectroscopy to radio observations, is available for most of the proposed clusters. The total area coverage is about 30 square degrees and the expected

depths are 24.5, 24.0, and 23.0 mag for *Y*, *J* and *Ks* respectively (5σ in point sources). The wide-area coverage coupled with the expected depths will also open up further scientific studies, for example, the search for high redshift quasars, lensed quiescent galaxies, L and T dwarfs, as well as infrared Galactic star counts and colours.

6. VISIONS — VISTA Star Formation Atlas — PI João Alves (University of Vienna)

VISIONS is a sub-arcsecond near-infrared survey of all nearby (< 500 parsecs) star formation complexes accessible from the southern hemisphere. This atlas will become the community's reference star formation database, covering the mass spectrum down to a few Jupiter masses and spatial resolutions reaching 100–250 au. The survey will cover a total of ~ 550 square degrees distributed over the six star forming complexes of Ophiuchus, Lupus, Corona Australis, Chamaeleon, Orion, and the Pipe Nebula. These are due to be completed within three years of the start of observations.

VISIONS is separated into three phases. The first phase will conduct *H*-band imaging of the target regions distributed over six epochs, with an effective exposure time of 60 seconds and a limiting magnitude of *H* ~ 19 mag. The immediate objective is to derive positions and proper motions of the embedded and dispersed young stellar population that is inaccessible to Gaia, as well as to provide photometry to complement the first generation VHS survey that fully covered all target regions in the *J*- and *Ks*-bands. In the second phase, VISIONS will carry out a set of deep observations that will image the high-column density regions of the star-forming complexes. The deep imaging in *J*-, *H*-, *Ks*-bands of 57 pointings, with a 600-second exposure time per pointing, will reach limiting magnitudes of *J* ~ 21.5 mag, *H* ~ 20.5 mag, and *Ks* ~ 19.5 mag. The third phase is to observe a set of additional six control fields with the same limiting magnitudes and a similar strategy as the deep observations, for statistical comparison with the galactic field population. The total requested time for VISIONS amounts to 553 hours.

7. SHARKS — Southern H-ATLAS Regions *Ks*-band Survey — PI Ivan Oteo (University of Edinburgh)

SHARKS is a wide and deep VISTA Public Survey over the South Galactic Pole and the fields covered by the GAlaxy and Mass Assembly (GAMA) and Herschel-Astrophysical Tetrahertz Large Area Survey (H-ATLAS) in the *Ks*-band. This survey covers 300 square degrees to a 5σ depth of *Ks* ~ 22.7 AB mag in 1200 hours. The SHARKS fields will also be followed up by a number of future deep and/or wide far-IR and radio surveys.

The main goals of this survey are as follows: to provide the best possible counterpart identification for ~ 90 % of the sources detected in the redshift range, $0 < z < 3$, by H-ATLAS, the Low Frequency Array (LOFAR), the Square Kilometre Array (SKA), and the Australian SKA Pathfinder (ASKAP); to produce a sample of a thousand strong lenses for cosmography studies; and, to study the evolution of the most massive structures in the Universe. The depth of the deepest available observations over the proposed fields (VIKING survey, *Ks* < 21.2 AB mag at 5σ) is currently not enough to accomplish any of these aims. The SHARKS fields will also overlap with future optical observations (using the Large Synoptic Survey Telescope) and with observations in the near-infrared (using ESA's Euclid mission), representing a complementary dataset with an extensive legacy.

Science data products from Cycle 2 surveys

The science policies concerning the return of science data products also apply to the VISTA Cycle 2 surveys. A short summary of the timeline for the delivery of their data products from their survey management plans is presented here. The first delivery of data products such as images and source lists is expected 1.5 years after the start of observations of the surveys, i.e., in October 2018. The aperture-matched multi-band catalogues and light curves should become available a year later in a second data release. The catalogues may not be limited to VISTA near-infrared photometry, as several teams have committed to delivering multi-wavelength data, including optical (for example, HST), radio (for example, LOFAR) or X-ray measurements. The time domain also plays a major role in setting the legacy value of the VISTA Cycle 2 surveys. For example, the multi-messenger astronomy nature of the GW-EM observations by VINROUGE, or the delivery of photometric catalogues with proper motions for millions of Milky Way stars in the Bulge by VVVX and their synergy with the results from Gaia, will have a transformational impact on the science carried out by the ESO community.

Acknowledgments

We would like to thank our La Silla Paranal colleagues for their work in supporting the science operations of the ESO Public Surveys. We wish to acknowledge our colleagues from the Department of Engineering for the development of the tools required for carrying out Phase 1, Phase 2 and Phase 3 for the ESO Public Surveys, and the ESO library team for the careful monitoring of refereed publications. We would like to thank the members of the Public Survey Panels, particularly the Chairs, Duccio Macchetto and Danny Lennon, for their work and support on the definition of the survey scientific programme with VISTA. Finally, we wish to thank the principal investigators of the Public Surveys and their collaborators, including the data centres at the Cambridge Astronomy Survey Unit (CASU[2]), the Wide Field Astronomy Unit (WFAU[3]) and the Traitement Élémentaire Réduction et Analyse des PIXels (TERAPIX[4]), for their hard work.

References

Arnaboldi, M. et al. 1998, The Messenger, 93, 30
Arnaboldi, M. et al. 2007, The Messenger, 127, 28
Arnaboldi, M. et al. 2014, The Messenger, 156, 24
Capaccioli, M. & Schipani, P. 2011, The Messenger, 146, 2
Cirasuolo, M. et al. 2011, The Messenger, 145, 11
de Jong, R. 2011, The Messenger, 145, 14
Retzlaff, J. et al. 2016, SPIE, 9910, 09
Romaniello, M. et al. 2016, The Messenger, 163, 5
Sutherland, W. et al. 2015, A&A, 575, 27

Links

[1] ESO Public Surveys: http://www.eso.org/sci/observing/PublicSurveys/sciencePublicSurveys.html
[2] Cambridge Astronomy Survey Unit: http://casu.ast.cam.ac.uk/
[3] Wide Field Astronomy Unit: http://www.roe.ac.uk/ifa/wfau/
[4] TERAPIX: http://terapix.iap.fr/
[5] Phase 3 releases: http://www.eso.org/sci/observing/phase3/data_releases.html
[6] ESO Science Archive Facility: http://archive.eso.org/wdb/wdb/adp/phase_main/form
[7] telbib: http://telbib.eso.org
[8] ESO Science Newsletter: http://www.eso.org/sci/publications/newsletter/

DOI: 10.18727/0722-6691/5021

The Cherenkov Telescope Array: Exploring the Very-high-energy Sky from ESO's Paranal Site

Werner Hofmann[1]
for the CTA Consortium

[1] Max-Planck-Institut für Kernphysik, Heidelberg, Germany

The Cherenkov Telescope Array (CTA) is a next-generation observatory for ground-based very-high-energy gamma-ray astronomy, using the imaging atmospheric Cherenkov technique to detect and reconstruct gamma-ray induced air showers. The CTA project is planning to deploy 19 telescopes on its northern La Palma site, and 99 telescopes on its southern site at Paranal, covering the 20 GeV to 300 TeV energy domain and offering vastly improved performance compared to currently operating Cherenkov telescopes. The combination of three different telescope sizes (23-, 12- and 4-metre) allows cost-effective coverage of the wide energy range. CTA will be operated as a user facility, dividing observation time between a guest observer programme and large Key Science Projects (KSPs), and the data will be made public after a one-year proprietary period. The history of the project, the implementation of the arrays, and some of the major science goals and KSPs, are briefly summarised.

Introduction

In the coming years, up to 99 of the Cherenkov Telescope Array (CTA) telescopes with dish sizes between 4 metres and 23 metres will be installed at the Paranal site, in the flat areas east of route B-710 (Figure 1). CTA will be the premier observatory for imaging the Universe at very high energies (VHE), covering the electromagnetic spectrum at energies from 10's of GeV to 100's of TeV. More information can be found in Acharya et al. (2013) and on the CTA website[1].

CTA employs Imaging Atmospheric Cherenkov Telescopes (IACTs) — large telescopes with ultraviolet–optical reflecting mirrors that focus flashes of Cherenkov light produced by γ-ray initiated atmospheric particle cascades (air showers) onto nanosecond-response cameras (Figure 2). Compared to space-based detectors that are limited to detection areas of around a square metre, Cherenkov telescopes use the Earth's atmosphere as a detection medium and provide detection areas in excess of 10^5 square metres, capable of coping with the very low flux of VHE γ-rays. Today's instruments use arrays of IACTs to image a cascade from different viewing angles, improving angular and energy

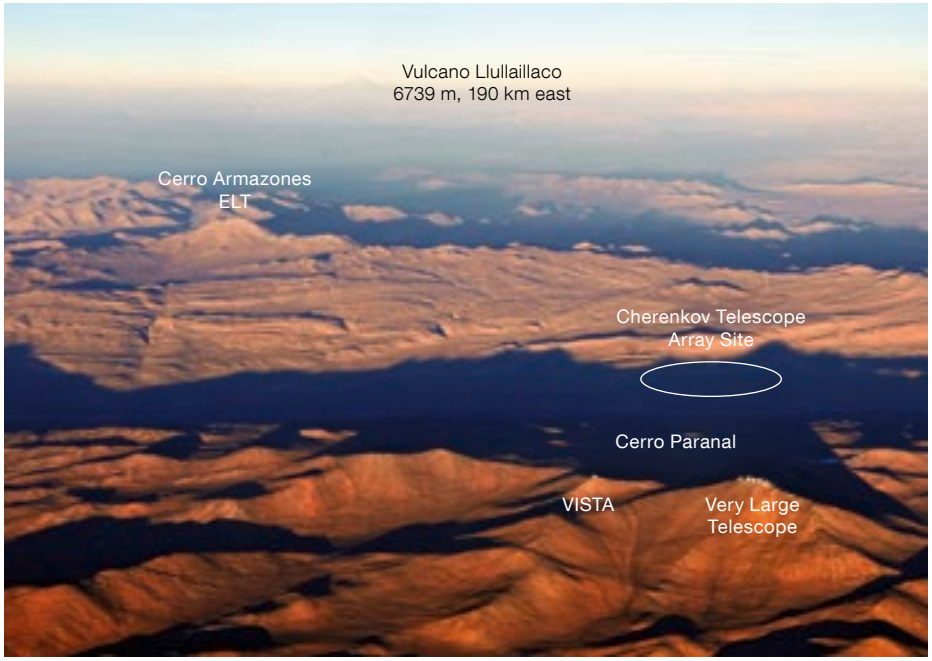

ESO/M. Tarenghi

Figure 1. The location of the CTA southern array, in the valley between Cerro Paranal and Cerro Armazones.

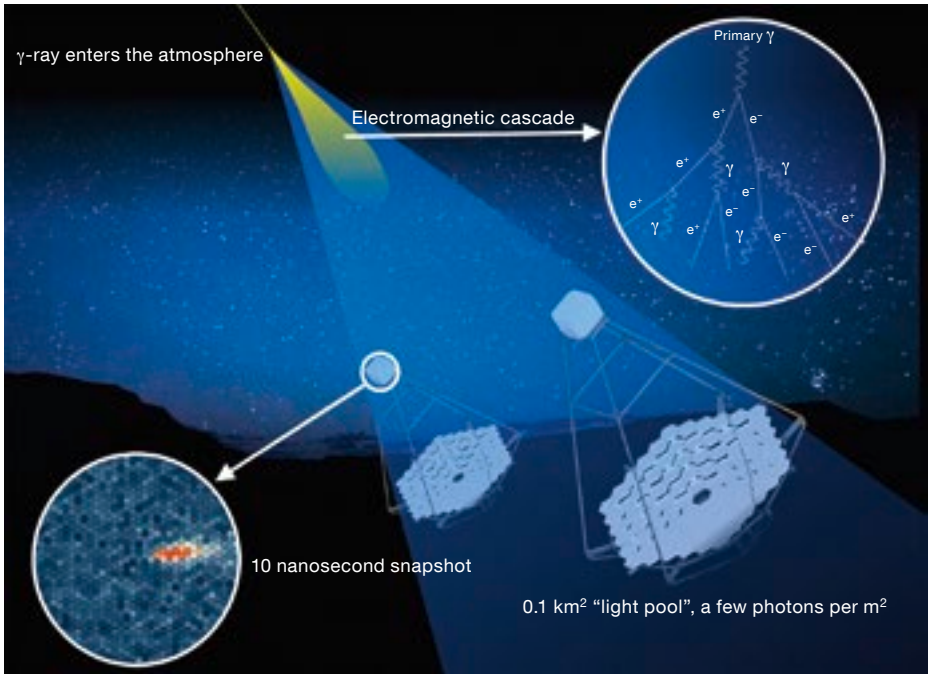

Figure 2. Detection of primary γ-rays using the Cherenkov light from the γ-ray induced air showers. A telescope will "see" the γ-ray if it is located in the ~ 250-metre diameter Cherenkov light pool. The different views of the air shower provided by multiple telescopes allow reconstruction of the shower geometry and hence of the direction of the incident γ-ray.

resolution of the γ-rays, as well as increasing the rejection of similar cascades initiated by cosmic-ray particles.

Ground-based γ-ray astronomy at very high energies is a young branch of astronomy that has developed very rapidly since the detection of the first cosmic VHE source in 1989 by the Whipple telescope (Hillas, 2013). The initial concepts for CTA as the first major open observatory for this waveband were formulated in 2005, motivated by the success of existing IACTs, such as the High Energy Stereoscopic System (HESS), the Major Atmospheric Gamma Imaging Cherenkov (MAGIC) and the Very Energetic Radiation Imaging Telescope Array System (VERITAS). These instruments have demonstrated that observations at these extreme energies are not only technically viable and competitive in terms of precision and depth, but also scientifically rewarding and with broad scientific impact. Their success has resulted in a rapid growth in the interested scientific community. Topics addressed with γ-ray observations include[2]:

(i) The origin and role of relativistic cosmic particles. Particles in our Galaxy and beyond are traced by the γ-rays they emit when interacting with gas or with radiation fields; this allows us to address questions like: what are the sites of high-energy particle acceleration in the Universe? what are the mechanisms for cosmic particle acceleration? and what role do accelerated particles play in feedback mechanisms related to star formation and galaxy evolution?
(ii) Probing extreme environments, for example, the physical processes that are at work close to neutron stars and black holes and the characteristics of relativistic jets, winds and explosions. γ-ray interactions can also be used to explore the radiation fields and magnetic fields in extreme cosmic voids, and their evolution over cosmic time.
(iii) Exploring frontiers in fundamental physics, such as: searching for dark matter particles annihilating into γ-rays, allowing us to probe the nature and distribution of dark matter; investigating mechanisms affecting photon propagation over cosmological distance, such as quantum gravitational effects causing tiny variations of the speed of light with photon energy; and photon-axion oscillations in cosmic magnetic fields.

CTA is envisaged as a general-purpose observatory for the VHE waveband, building on the techniques and technologies demonstrated by the currently operating IACTs, and improving on essentially all aspects of their performance. CTA will be the first truly open VHE observatory, providing accessible data products and support services to a wide scientific community. It will exploit large arrays of Cherenkov telescopes on two sites to provide all-sky coverage, broad energy coverage and unprecedented precision.

Some history

The CTA project was proposed and developed by the CTA Consortium (CTAC) that was formally established in 2008. The Consortium has now grown to over 1300 scientists and engineers from more than 200 institutes in 32 countries, involved in the design and prototyping of the telescopes and the associated auxiliary instruments and software, as well as in the characterisation of sites for the telescopes. Of ESO's 16 Member States, 13 are also represented in the CTA Consortium. In 2014, the CTA Observatory (CTAO) gGmbH was founded in Heidelberg, to provide a legal framework for the operation of the CTA Project Office, and for the contracts towards implementation of CTA. The CTAO gGmbH is governed by its Council of representatives of the shareholders from Austria, the Czech Republic, France, Germany, Italy, Japan, Spain, Switzerland and the United Kingdom, and from the Netherlands and South Africa as Associate Members. Work towards CTA was and is supported by the European Union under FP7 and H2020; since 2008, CTA is listed in the roadmap of the European Strategy Forum on Research Infrastructures (ESFRI).

A comprehensive programme of site search and site evaluation was conducted by the CTA Consortium from 2010 to 2013, resulting in a shortlist of sites and detailed input to a Site Selection Committee appointed by the CTA Resource Board (RB) of agency representatives (the RB preceded the CTAO Council). In July 2015, the RB decided to enter into detailed contract negotiations around hosting the southern array on the Paranal site in Chile and the northern array at the Instituto de Astrofisica de Canarias (IAC), Roque de los Muchachos Observatory in La Palma, Spain. The hosting agreement with IAC was signed in September 2016; the hosting agreement with ESO was approved in late 2016 by both the CTAO and ESO Councils. It is envisaged that ESO will become a scientific partner in CTA, expanding ESO's portfolio of wavebands and leveraging the scientific and operational synergies with its optical telescopes and the Atacama Millimeter/submillimeter Array (ALMA). ESO will operate the southern telescope array for CTAO and will receive observation time on CTA's arrays as well as voting rights in the CTAO's governing bodies. Also in 2016, the decision was taken to locate the CTA Headquarters at Bologna in Italy; the Science Data Management Centre will be hosted at Zeuthen near Berlin, Germany.

The full economic cost for implementing CTA is estimated at 400 M€; however, even with a reduced number of telescopes, CTA will provide a state-of-the-art astronomical facility, and a funding level of 250 M€ was established as the threshold for starting the implementation. Signature of a Memorandum of Understanding (MoU) towards construction and operation is underway and currently accounts for over 200 M€; the 250 M€ threshold should be reached in the near future.

The telescope arrays

In all aspects, CTA represents a significant step forward with respect to current instruments, and the combined effect is expected to be transformational for the field. For example, the improved γ-ray collection area, the background rejection power and the larger field of view increase the survey speed of CTA by a factor of several hundred with respect to current instruments. Sensitivity to point sources of γ-rays will be up to an order of magnitude higher than current instruments. The angular resolution of CTA will approach one arcminute at high energies — the best resolution of any instrument operat-

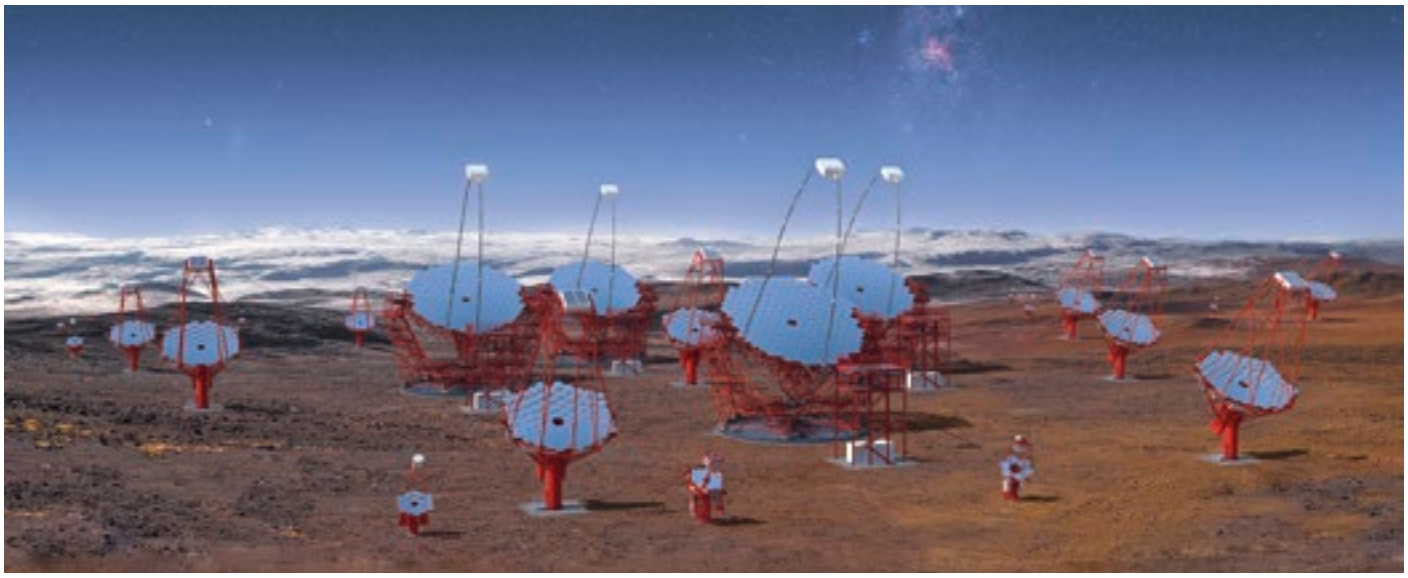

CTA/Gabriel Pérez Díaz/IAC/SMM/ESO/B.Tafreshi

Figure 3. (Above) Artist's rendering of the southern CTA site.

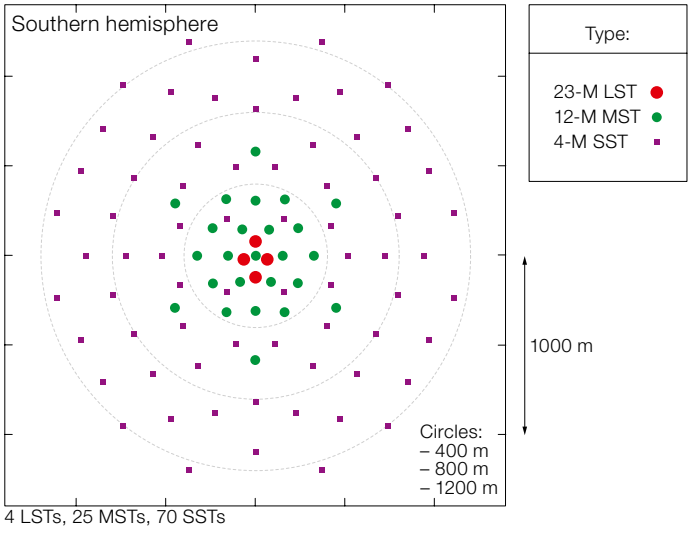

Figure 4. (Right) Layout of the southern telescope array, combining 4 LSTs, 25 MSTs and 70 SSTs.

ing above the X-ray band — allowing detailed imaging of a large number of γ-ray sources.

CTA will take the IACT technique to its next level, by deploying extended arrays of Cherenkov telescopes (Figures 3 and 4). In the current arrays, with at most five telescopes spaced by about 100 metres (compared to the ~250-metre diameter of the Cherenkov light pool), the bulk of the recorded air showers have impact points outside the footprint of the array, implying that usually only two telescopes record the shower, and that the angle between stereoscopic views of the cascade is modest, impacting the spatial reconstruction. CTA will for the first time deploy telescopes across areas that exceed the size of the Cherenkov light pool, resulting in:

– a dramatically increased rate of air showers contained within the footprint of the telescope array;
– an increased number of views of the air shower from different viewing angles, improving both the reconstruction of air-shower parameters and the rejection of cosmic-ray induced air showers as the major source of sensitivity-limiting background;
– a lower effective energy threshold since, for contained showers, there are always telescopes in the region of highest density of Cherenkov light.

For wide usable energy coverage, it is desirable for the effective γ-ray detection area to increase with γ-ray energy, compensating for the rapid drop of γ-ray flux with increasing energy (for typical sources, the γ-ray flux drops with energy, E, like $dN_\gamma/dE \sim E^{-2}$ or faster). Hence, rather than deploying one type of Cherenkov telescope on a regular grid, the CTA arrays use a graded approach:

– The lowest energies are covered by an arrangement of four Large-Sized Telescopes (LSTs, of 23-metre dish diameter), capable of detecting γ-rays as low as 20 GeV.
– The 0.1 to 10 TeV range is covered by larger arrays of 25 (south) and 15 (north) Medium-Sized Telescopes (12-metre MSTs).
– The highest energy γ-rays are detected by a multi-kilometre square array of 70 Small-Sized Telescopes (4-metre SSTs) in the south.

The small telescopes are only foreseen for the southern array (Figure 4), since the highest energies are most relevant for the study of Galactic sources. The use of three different sizes of telescope proved to be the most cost-effective solution, and it allows each telescope type to be optimised for a specific energy range. The detailed specifications of the telescopes and the layout of the CTA arrays are the result of a multi-step optimisation process, extending over several years and using 10's of millions of CPU-hours

Telescope	Large	Medium		Small		
	LST	MST	SCT	SST-1M	ASTRI SST-2M	GCT SST-2M
Number North array	4	15	TBD		0	
Number South array	4	25	TBD		70	
Optics						
Optics	Parabolic mirror	Modified Davies-Cotton	Schwarzschild-Couder	Davies-Cotton	Schwarzschild-Couder	Schwarzschild-Couder
Primary mirror diameter (m)	23	12	9.7	4	4	4
Secondary mirror diameter (m)	—	—	5.4	—	1.8	2
Eff. mirror area after shadowing (m^2)	370	90	40	7.4	6	6
Focal length (m)	28	16	5.6	5.6	2.1	2.3
Focal plane instrumentation						
Photo sensor	PMT	PMT	Silicon	Silicon	Silicon	Silicon
Pixel size (degr.), shape	0.10, hex	0.18, hex	0.07, square	0.24, hex	0.17, square	0.15–0.2, square
Field of view (degr.)	4.5	7.7/8.0	8.0	9.1	9.6	8.5–9.2
Number of pixels	1855	1764/1855	11328	1296	1984	2048
Signal sampling rate	GHz	250 MHz/GHz	GHz	250 MHz	S&H	GHz
Structure						
Mount	alz-az, on circular rail	alt-az positioner	alt-az positioner	alt-az positioner	alt-az positioner	alt-az positioner
Structural material	CFRP/steel	steel	steel	steel	steel	steel
Weight (full telescope, tons)	100	85	~85	9	15	8
Max. time for repositioning (s)	20	90	90	60	80	60

Table 1. Parameters of the different CTA telescopes currently under prototyping. For details of telescope technology, see Gamma, 2016[3].

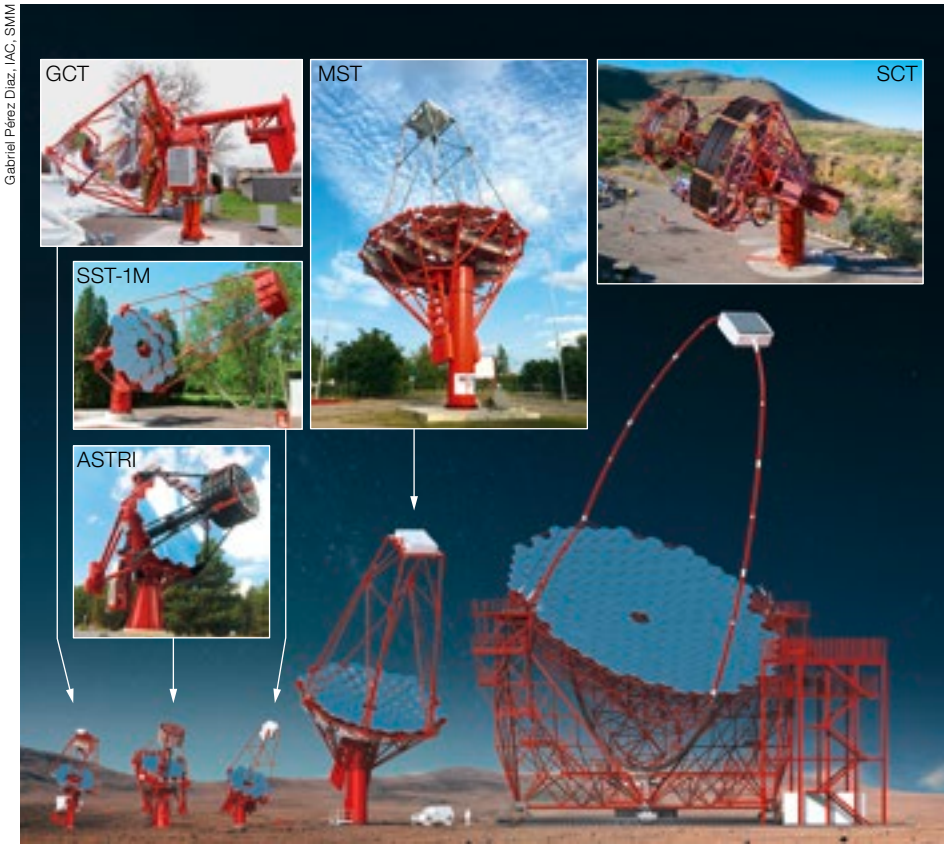

Gabriel Pérez Díaz, IAC, SMM

Figure 5. Main image: CAD models of the different CTA telescopes, shown to scale. The Small-Sized Telescopes (SST, from left: GCT, ASTRI, SST-1M) have a mirror diameter of about 4 metres, the Medium-Sized Telescope (MST, middle) has a 12-metre mirror, and the Large-Size Telescope (LST) a 23-metre mirror. Insets: Prototypes of CTA telescopes under test: GCT (at Meudon), ASTRI (on Sicily), SST-1M (at Warsaw), MST (at Berlin), and SCT (in Arizona). Construction of an LST prototype has started on La Palma (not shown).

for detailed simulations of the air showers and the response of the telescopes (Bernlöhr et al., 2013).

The parameters of the telescopes are summarised in Table 1. The different telescopes (Figure 5) have rather different design drivers. For example, the main drivers for the LSTs are the huge light-collecting power and rapid repositioning requirements (needed in particular for follow-up of γ-ray bursts), and for the SSTs the large number of elements implies tight constraints on unit cost and maintenance effort. Three different SST designs are being prototyped, the Gamma-ray

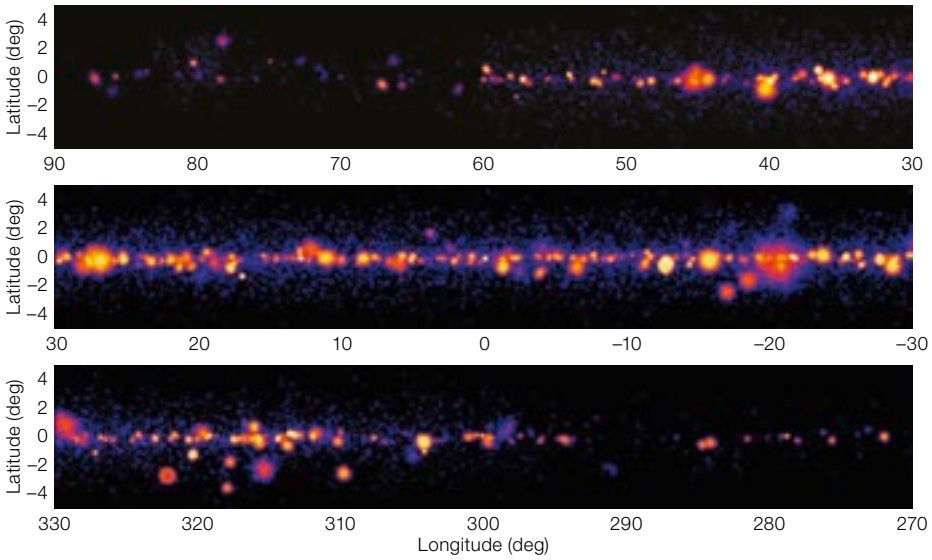

Figure 6. Simulation of the Milky Way seen with CTA in very-high-energy γ-rays.

Cherenkov Telescope (GCT) and the Astrofisica con Specchi a Tecnologia Replicante Italiana (ASTRI) dual-mirror telescopes and the SST-1M single-mirror variant. The dual-mirror telescopes use Schwarzschild-Couder (SC) optics, realised for the first time in CTA's Cherenkov telescopes. Also, a dual-mirror version of the MST is being considered (SCT); compared to the classical single-mirror Cherenkov telescopes; the novel dual-mirror telescopes offer improved imaging quality and allow a smaller plate scale and rather compact cameras. The LST and MST with their large (3-metre) cameras use photomultipliers with very high quantum efficiency to detect the Cherenkov light, whereas the smaller sensor areas of the SSTs and the SCT are covered with silicon sensors.

The CTA Observatory

The CTA facility will be open to a wide community of scientific users: from astronomy and astrophysics, to astroparticle physics, particle physics, cosmology and plasma physics. CTA observation time and data products will be provided to users through several different modes:

– The Guest Observer Programme is a proposal-based system that will give users access to time for observations requiring anywhere between a few hours and hundreds of hours.
– The Key Science Projects (KSPs) defined by the CTA Consortium are large programmes that ensure that the key science issues are addressed in a coherent fashion, generating legacy data products. KSPs require anything between 100 and 1000 hours of observation time.
– The Director's Discretionary Time will represent a small fraction of observation time that will be used for, for example, unanticipated targets of opportunity or outstanding proposals from non-member countries.
– Archive Access to CTA data will be made available worldwide after a proprietary period of about one year.

Observations will take place in service mode; the user may request specific telescope configurations, and specify trigger conditions, time constraints arising from coordinated observations with other observatories, etc. Users will receive processed and calibrated data in the form of photon-candidate event lists similar to the products of other photon-counting instruments, provided in the Flexible Image Transport System (FITS) format, together with relevant instrument response functions and auxiliary data, as well as science analysis tools.

Science data, calibration data and auxiliary data will be permanently stored in the CTA data archive and made available to archive users after the proprietary period. The data archive will remain available beyond the operational period of the CTA Observatory. High-level data, such as sky maps, light curves, and source catalogues will be made available in a Virtual Observatory (VO) compliant format. Alerts from CTA on noteworthy astronomical events (for example the detection of transients) will be sent to the wider community in the VO Event format.

The CTA Key Science Projects

The detailed volume *Science with the Cherenkov Telescope Array* is about to be published. Proposed CTA KSPs include: (i) the Dark Matter Programme; (ii) the Galactic Centre Survey; (iii) the Galactic Plane Survey; (iv) the Large Magellanic Cloud Survey; (v) the Extragalactic Survey; (vi) Transients; (vii) Cosmic-ray PeVatrons; (viii) Star-forming Systems; (ix) Active Galactic Nuclei; (x) Clusters of Galaxies; and (xi) Beyond gamma-rays. In the following, only the survey KSPs are briefly introduced; these will form a basis for subsequent guest observer proposals.

The combination of CTA's wide field of view (FoV) and its unprecedented sensitivity ensures that CTA can deliver surveys 1–2 orders of magnitude deeper than existing surveys very early in the life of the CTA Observatory. CTA surveys will open up discovery space in an unbiased way and generate legacy datasets of long-lasting value. The following surveys form part of the KSPs:

– The Extragalactic Survey — covering one quarter of the sky to a depth of ~ 6 mCrab. No extragalactic survey has ever been performed using IACTs. A 1000-hour CTA survey of such a region will reach the same sensitivity as the decade-long HESS programme of inner-Galaxy observations, and cover a solid angle ~ 40 times larger, providing a snapshot of activity in an unbiased sample of galaxies.
– The Galactic Plane Survey (GPS) — consisting of a deep survey (~ 2 mCrab) of the inner Galaxy and the Cygnus region, coupled with a somewhat shallower survey (~ 4 mCrab) of the entire Galactic Plane (see Figure 6). For the typical luminosity of known Milky Way TeV sources of $10^{33–34}$ erg s^{-1}, the CTA GPS will provide a distance reach

of ~ 20 kpc, detecting essentially the entire population of such objects in the Galaxy and providing a large sample of objects one order of magnitude fainter. The excellent angular resolution of CTA is critical here if it is to avoid being limited by source confusion rather than flux.
– The Galactic Centre Survey — consisting of a > 500 hours deep exposure of a ± 1 degree window around Sgr A*, covering the Galactic Centre source, the centre of the Dark Matter halo, multiple supernova remnants and pulsar wind nebulae, central radio lobes and arc features. An additional 300 hours extended survey covers a 10 by 10 degree region around Sgr A*, including the edge of the Galactic Bulge, the base of the Fermi Bubbles, the radio spurs and the Kepler supernova remnant.
– The Large Magellanic Cloud (LMC) Survey — providing a face-on view of an entire star-forming galaxy, resolving regions down to 20 pc in size with sensitivity down to luminosities of ~ 10^{34} erg s^{-1}. CTA aims to map the diffuse LMC emission as well as individual objects, providing information on relativistic particle transport.

These surveys will establish the populations of VHE emitters in Galactic and extragalactic space, providing samples of objects large enough to understand source evolution and/or duty cycle. Data products from the survey KSPs include catalogues and flux maps which will serve as valuable long-term resources for a wide community. The value of these surveys is not only that they provide the basis for a population synthesis of cosmic particle accelerators, but also that they enable discovery of key objects — the equivalents of the Hulse-Taylor pulsar or the Double Pulsar found in radio pulsar surveys.

Construction of the CTA

The Design Phase of CTA has been concluded; the project is currently near the end of the Pre-Construction Phase in which instrument designs were evolved to production readiness and were reviewed in the Science Performance and Requirements Review, the Preliminary Design Review and the final Critical Design Review — all performed by CTA's Science and Technical Advisory Committee.

The forthcoming Pre-Production Phase covers the deployment of approximately 10 % of the final number of telescopes with the aim of verifying and optimising production schemes, as well as exercising and optimising deployment, testing software, etc. Based on the Pre-Production Readiness/Deployment Reviews, Pre-Production telescopes will be installed on the sites; after retrofitting to final production status where relevant, they are planned to be used in the final CTA arrays.

Once Pre-Production is successfully established for a given telescope type, this element moves to the Production Phase. To first approximation, telescopes are not dependent on each other for operation and the cumulative completion of the full scope of the arrays may progress gradually. Science operation will start with partial arrays, before deployment of the full arrays is completed. Telescopes are successively handed over from the construction project to operations. Prior to user science operation, the performance of the (initially partial) arrays will be verified and documented. It is anticipated that construction activities will start in 2018, with the first data from partial arrays becoming available in 2021.

In summary, CTA will provide a next-generation VHE γ-ray observatory with unprecedented capability. CTA perspectives in relativistic astrophysics include the in-depth understanding of known VHE γ-ray emitters and their mechanisms, detection of new object classes and discovery of new phenomena. As with many facilities breaking new ground, the most important discoveries may not be the ones discussed in today's science case documents.

References

Acharya, B. S. et al. 2013, Astroparticle Physics, 43, 3
Bernlöhr, K. et al. 2013, Astroparticle Physics, 43, 171
Hillas, A. M. 2013, Astroparticle Physics, 43, 19

Links

[1] CTA Observatory: www.cta-observatory.org
[2] For an overview of CTA science, see articles in the Special CTA edition of Astroparticle Physics, 43, 1-356, 2013
[3] Contributions of CTA to the 6th International Symposium on High-Energy Gamma-Ray Astronomy (Gamma 2016), arXiv:1610.05151

The panorama from the planned site of the Cherenkov Telescope Array looking towards the Very Large Telescope on Cerro Paranal.

Near-infrared three-filter (*Y*-, *J*- and *Ks*-band) colour-composite image of the centre of the Small Magellanic Cloud obtained with the Visible and Infrared Survey Telescope for Astronomy (VISTA). See Photo Release eso1714a for more information.

ESO/VISTA VMC

DOI: 10.18727/0722-6691/5022

To be or not to be Asymmetric? VLTI/MIDI and the Mass-loss Geometry of AGB Stars

Claudia Paladini[1]
Daniela Klotz[2]
Stephane Sacuto[2,3]
Eric Lagadec[4]
Markus Wittkowski[5]
Andrea Richichi[6]
Josef Hron[2]
Alain Jorissen[1]
Martin A. T. Groenewegen[7]
Franz Kerschbaum[2]
Tijl Verhoelst[8]
Gioia Rau[2]
Hans Olofsson[9]
Ronny Zhao-Geisler[10]
Alexis Matter[4]

[1] Institut d'Astronomie et d'Astrophysique, Université libre de Bruxelles, Belgium
[2] Department of Astrophysics, University of Vienna, Austria
[3] Department of Physics and Astronomy, Division of Astronomy and Space Physics, University of Uppsala, Sweden
[4] Laboratoire Lagrange, Université Côte d'Azur, Observatoire de la Côte d'Azur, CNRS, Nice, France
[5] ESO
[6] National Astronomical Research Institute of Thailand, Chiang Mai, Thailand
[7] Koninklijke Sterrenwacht van België, Brussel, Belgium
[8] Belgian Institute for Space Aeronomy, Brussels, Belgium
[9] Department of Earth and Space Sciences, Onsala Space Observatory, Sweden
[10] Department of Earth Sciences, National Taiwan Normal University, Taipei, Taiwan

The Mid-infrared Interferometric instrument (MIDI) at the Very Large Telescope Interferometer (VLTI) has been used to spatially resolve the dust-forming region of 14 asymptotic giant branch (AGB) stars with different chemistry (O-rich and C-rich) and variability types (Miras, semi-regular, and irregular variables). The main goal of the programme was to detect deviations from spherical symmetry in the dust-forming region of these stars. All the stars of the sample are well resolved with the VLTI, and five are asymmetric and O-rich. This finding contrasts with observations in the near-infrared, where the C-rich objects are found to be more asymmetric than the O-rich ones. The nature of the asymmetric structures so far detected (dusty discs versus blobs) remains uncertain and will require imaging on milli-arcsecond scales.

Background

Stars with low to intermediate initial mass ($\lesssim 8\ M_{\odot}$), including our Sun, undergo a short evolutionary phase, called the AGB, towards the end of their lives and undergo several mass dredge-up events. Stars on the AGB usually have O-rich chemistry. However, after the third dredge-up, stars with initial masses between 1 and $4\ M_{\odot}$ can reach a C/O ratio > 1, and their spectra are then dominated by C-bearing molecular and dust species.

The atmosphere of a star on the AGB can be as large as a few au, and it is stripped away by a stellar wind on a typical timescale of thousands of years. Observations of the following evolutionary stages, the post-AGB and planetary nebula, show some very asymmetric envelopes and emission nebulae around the central star. For many years, AGB stellar mass loss was considered to be mainly symmetric. It is accepted in the planetary nebula community that binary interaction can be responsible for the asymmetric morphology (Jones & Boffin, 2017), but the population of binaries on the AGB does not match that in the post-AGB phase. In fact, because of the pulsation of the star itself and the dust around the AGB star, the companions are difficult to detect.

Between 2009 and 2013, the Herschel Space Telescope imaged the interface between the outer atmosphere and the interstellar medium for a sample of AGB stars within the MESS (Mass-loss from Evolved StarS) guaranteed observing time programme (Groenewegen et al., 2011). The MESS programme identified four different geometries: ring, fermata, eye and irregular (Cox et al., 2012). The ring shape is due to the interaction between different episodic mass-loss events; the fermata (so named because of its similarity to the symbol used in music) is caused by interaction between the stellar wind and the interstellar medium; the eye shape is due to a mixture of the previous two mechanisms, and possibly the interaction with an unseen companion; and the irregular shape applies to objects showing extended and non-detached material (as opposed to rings).

Observations carried out using other techniques (from near-infrared interferometric campaigns to radio and sub-millimetre studies — examples include: Cruzalèbes et al., 2015; Lykou et al., 2015; Kervella et al., 2014; Ramstedt et al., 2014; and Maercker et al., 2012) showed a very complex picture. Altogether it became clear that observations needed to probe all spatial scales for a defined sample of stars in order to understand the physics of the outflow.

The VLTI/MIDI survey

Our VLTI/MIDI Large Programme (Paladini et al., 2017) observed a subsample of the MESS targets to understand how asymmetric structures develop within a very few stellar radii (2–10 $R_{\star}$) of the atmosphere as a result of the mass-loss process. The questions we wanted to answer were: (i) whether the mass loss is an episodic process; (ii) where the asymmetric structures form, and what is the mechanism responsible; (iii) how do the asymmetries change as the star moves up the AGB; and (iv) whether the asymmetric structures detected by Herschel are connected to the ones eventually observed in the inner atmospheres of AGB stars.

Of course, performing a study of the global geometry with a two-telescope beam combiner is very challenging. However, MIDI was the only facility available worldwide with the angular resolution needed to resolve the inner dust-forming region of these stars. We carried out an extensive preparatory study to select the right baselines to sample the same spatial frequencies in all targets necessary for simple morphology studies. For this we used the Jean-Marie Mariotti Centre (JMMC) tool Aspro2[1] and the ESO VisCalc[2] tool. An in-house tool optimised for MIDI was also developed to analyse the data (GEometrical Model Fitting for INterferometric Data [GEM-FIND]; Klotz et al., 2012).

A total of 115 hours on the Auxiliary Telescopes was devoted to observing the

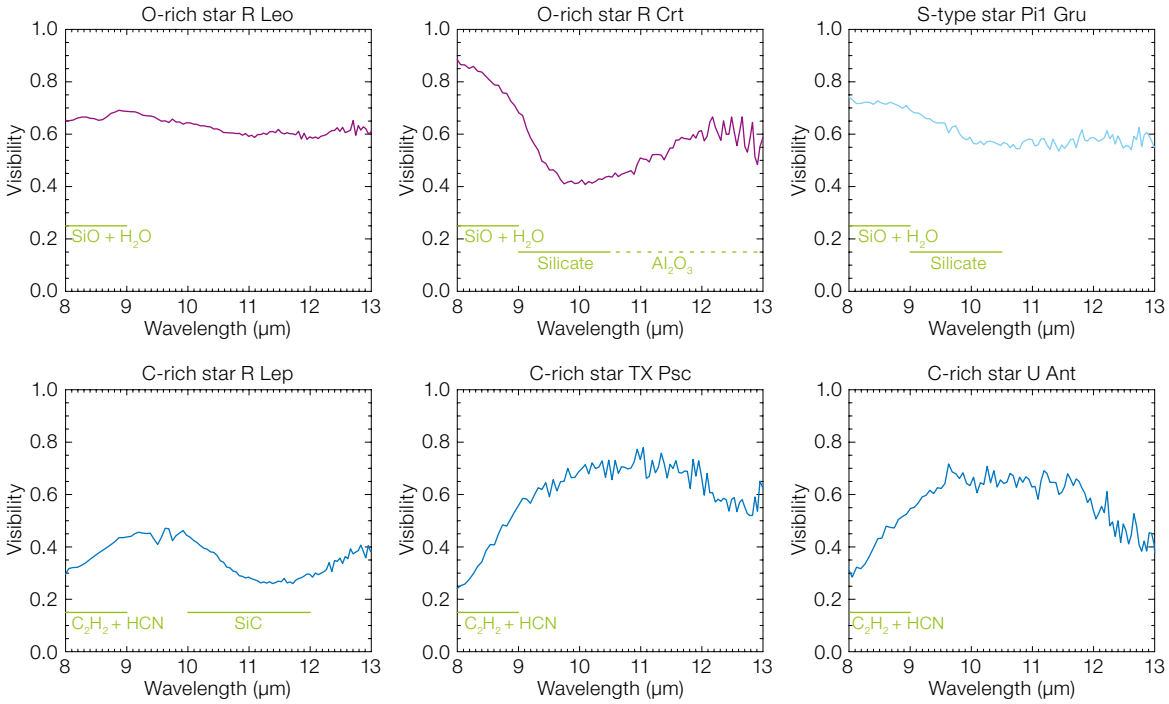

Figure 1. Some examples of the MIDI visibility spectra of AGB stars with different chemistry observed within the programme. The molecular and dust features characterising the visibility spectra are highlighted. The typical error bar is of the order of 10 %. From Paladini et al. (2017).

14 targets initially selected. The objects have different chemistry: five are O-rich stars with C/O < 1; two are S-type stars with 0.5 < C/O < 1; and seven are C-rich stars with C/O > 1. When available for any of the selected targets, archival data were also analysed.

Visibility versus wavelength

The MIDI observables are photometry, visibility amplitudes and differential phases spread across the *N*-band (8–13 μm). The analysis of the visibilities (also called the visibility spectrum) provides information about the brightness and angular size of the molecular and dust components of the envelope. Figure 1 shows the typical visibility spectra of the O-rich cases (upper row), where SiO and water molecules dominate the region between 8 and 9 μm. Silicate dust emission in the integrated spectrum usually corresponds to a drop in the visibility around 10 μm. Such a visibility drop indicates that the envelope is more extended and/or brighter in that wavelength range.

The C-rich counterparts of the sample (examples in the lower row in Figure1) have different visibility spectrum morphology. A drop in the visibility between 8 and 9 μm, where C_2H_2 and HCN molecules contribute, is observed for all the C-stars. Evolved Mira variables, such as R Lep, show a drop in the visibility around 11 μm, where the SiC dust feature appears. Stars without SiC emission in the integrated spectrum have a visibility more like that of TX Psc (Figure 1, lower row, central panel).

Peculiar cases

In the literature to date, all the features identified in the mid-infrared spectra of AGB stars have always been mirrored in the visibility spectrum. However, we observed two interesting and unexpected cases in our sample. The Infra-Red Astronomical Satellite (IRAS) and MIDI spectra of the C-rich star U Ant show the typical 11.3 μm silicon carbide dust feature, but there is no trace of such a feature in the visibility spectrum (Figure 1, lower row, right panel). It might therefore be that the interferometer is resolving out the dust shell in this case.

Another peculiar star in our sample is the C-star S Sct. While SiC dust is clearly detected in the Infrared Space Observatory (ISO) spectrum, there is no trace of such a feature in the MIDI spectrum and in the visibility. Perhaps a recent episodic strong stellar wind might have dissolved the shell, but no such event has been reported in the literature.

Follow-up observations with the VLT Imager and Spectrometer for mid-InfraRed (VISIR) and the VLTI second-generation instrument Multi AperTure mid-Infrared SpectroScopic Experiment (MATISSE), see Lopez et al. (2006) and Kasper et al. (2013), as well as detailed dynamic modeling (for example, Rau et al., 2017), should help to solve the mystery of these two stars.

Variability

The rich archive of MIDI observations gave us the chance to study the interferometric and spectroscopic variability for some targets. Comparing visibility spectra taken at different visual phases, but with the same projected baseline and position angle, gives information on the size variation of the target. On the other hand, the variability in the integrated spectra corresponds to variation in the colour (temperature).

The only case of interferometric variability detected in our sample is shown in

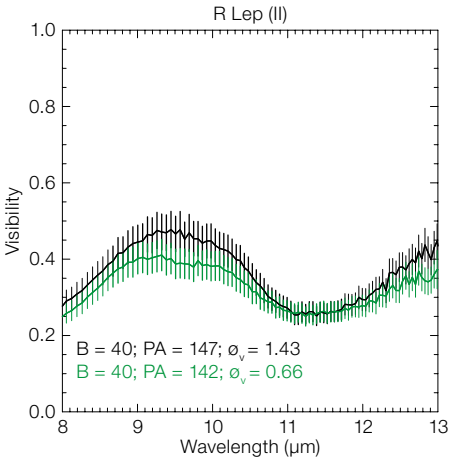

Figure 2. Interferometric variability for the C-rich Mira star R Lep. Comparison between two visibility spectra observed at different visual phases, with the same position angle and projected baseline, is shown.

Figure 2. The observations of the C-rich Mira star R Lep indicate that the molecular environment (8–10 μm) is slightly smaller before minimum visual phase (green line). No size variation is observed, however, in the SiC dust emission wavelength region (~11 μm).

These findings confirm that interferometric variability is connected to pulsation, as previously reported by Ohnaka et al. (2007) for V Oph.

We observed flux variation within photometric cycles for four targets. In all the cases the *N*-band magnitude variation is of the order of 0.8–1 mag. For the semi-regular variable RT Vir, the fluxes observed with MIDI at different visual phases follow a sinusoid where the *N*-band maximum is slightly shifted with respect to the visual maximum (Figure 3). These findings agree with previous work (Le Bertre, 1993; Karoricova et al., 2011, and references therein).

Morphology

The main goal of our investigation was to study the geometry of the targets, with a focus on the detection of non-spherical symmetry. A model-independent way to achieve this goal consists in comparing visibilities probing the same spatial frequency at different position angles. A second approach is to use the differential phase observed; objects with a spherical brightness distribution have differential phases equal to zero or 180 degrees. Alongside these two direct methods, we tested the data with spherical, elliptical, and two-component geometrical models.

The differential phase of the two O-rich stars, RT Vir and R Leo, immediately indicates that the stellar environment of these stars is very complex. The analysis of the other objects showed that all the carbon stars were surprisingly symmetric. Both the S-type objects are asymmetric, as is one of the remaining O-rich stars. In summary, we find that asymmetric structures in the *N*-band wavelength domain are more common among the stars with O-rich chemistry.

This result is illustrated in Figure 4 on an IRAS colour-colour diagram.

Near-infrared observations point to the fact that carbon stars are very asymmetric and O-rich objects are not; thermal infrared data show that the percentage of asymmetries between AGB stars with different chemistry is nearly the same (Blasius et al., 2012). This result can be interpreted in terms of the dust composition and characteristics of the stars with different chemistry. The O-rich dust in the near-infrared is nearly transparent, as one sees deeper into the envelope, and not as many asymmetries are expected in that wavelength range. On the other hand, the C-rich dust absorbs the radiation in the near-infrared, making the stars appear blob-like. In the mid-infrared, the O-rich dust is more blobby than in the C-rich cases because there are stronger non-linear effects in the radiative acceleration.

Prospects

Our Large Programme has shown that the stellar wind produces asymmetric structures in the very inner part of the dust-forming region. However, the nature of such asymmetries (dust clumps versus circumstellar discs) will require an imaging campaign with MATISSE. Our programme initially included a VISIR campaign, designed to fill in the gap between the spatial scales of MIDI and Herschel (see Figure 5 for the colour-colour plot of

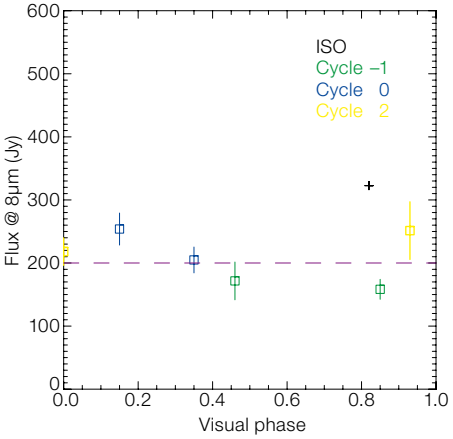

Figure 3. Spectroscopic variability observed with MIDI over several cycles for the O-rich semiregular variable RT Vir. From Paladini et al. (2017).

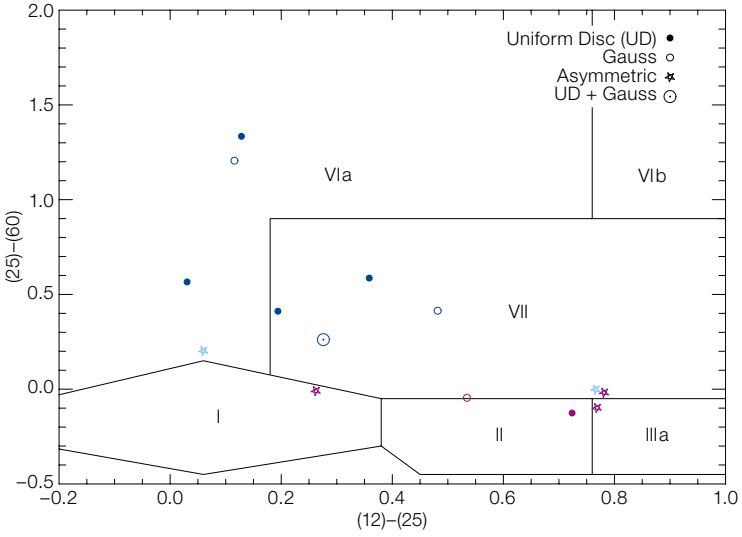

Figure 4. The targets analysed in the programme plotted in the IRAS colour-colour diagram (van der Veen & Habing, 1988). The lower part of the diagram is populated with O-rich stars (magenta) and S-type stars (bright blue). The C-rich objects are located in boxes VIa and VII. Asymmetric targets (stars) are concentrated in the lower part of the diagram.

object morphology). However, adverse weather conditions, and the decommissioning of VISIR for upgrade, prevented us from carrying out this part of the programme. Future observations in this direction are planned.

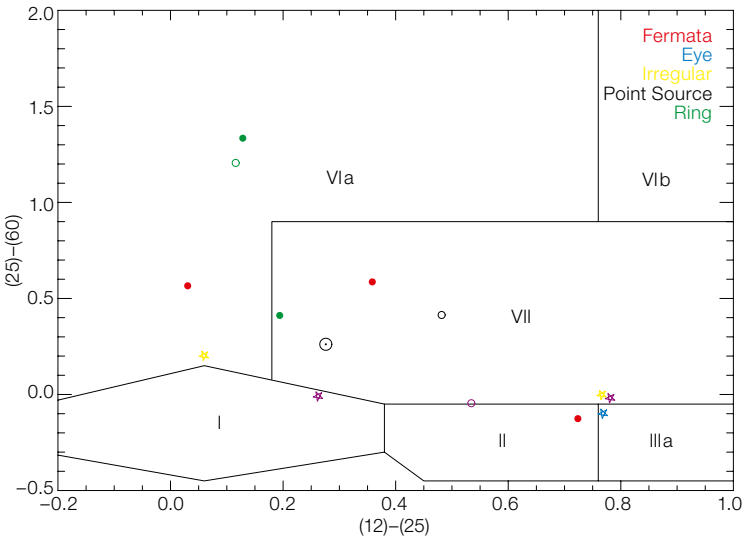

Figure 5. Same as Figure 4 (van der Veen & Habing, 1988) but colour-coded by the Herschel morphology identified in Cox et al. (2012). Linking the Herschel and MIDI observations will require the intermediate spatial scales probed by VISIR.

Acknowledgements

This work was supported by the Austrian Science Fund FWF under the project AP23006, the Belgian Federal Science Policy Office via the PRODEX Programme of ESA, the Belgian Fund for Scientific Research F.R.S.- FNRS, and the European Union's Seventh Framework Programme under Grant Agreement 312430. This research has made use of the SIMBAD database, operated at CDS Strasbourg, France. We acknowledge with thanks the variable star observations from the AAVSO International Database contributed by observers worldwide and used in this research. We thank the ESO Paranal team for supporting our VLTI/MIDI observations. F. Bufano, L. Burtscher, M. Cesetti, S. Höfner, T. Lebzelter, J.-B. Le Bouquin, G. C. Sloan, and K. Tristam are thanked for their key contributions.

References

Blasius, T. D. et al. 2012, MNRAS, 426, 4
Cox, N. L. J. et al. 2012, A&A, 537, A35
Cruzalèbes, P. et al. 2015, A&A, 446, 3277
Groenwegen, M. A. T. et al. 2011, A&A, 526, A162
Jones, D. & Boffin, H. 2017, NatAs, 1, 117
Karovicova, I. et al. 2011, A&A, 532, A134
Kervella, P. et al. 2014, A&A, 564, 88
Klotz, D. et al. 2012, Proc. SPIE, 8445, 84451
Le Bertre, T. 1993, A&AS, 97, 729
Lykou, F. et al. 2015, A&A, 576, 46
Lopez, B. et al. 2006, Proc. SPIE, 6268, 62680
Maercker, M. et al. 2012, Nature, 490, 212
Ohnaka, K. et al. 2007, A&A, 484, 371
Paladini, C. et al. 2017, A&A, 600, 136
Ramstedt, S. et al. 2014, A&A, 570, 14
Rau, G. et al. 2017, A&A, 600, 92
van der Veen, W. E. C. J. & Habing, H. J. 1988, A&A, 194, 125

Links

[1] JMMC interferometric tool Aspro2: http://www.jmmc.fr/aspro_page.htm
[2] ESO VisCalc tool: https://www.eso.org/observing/etc/

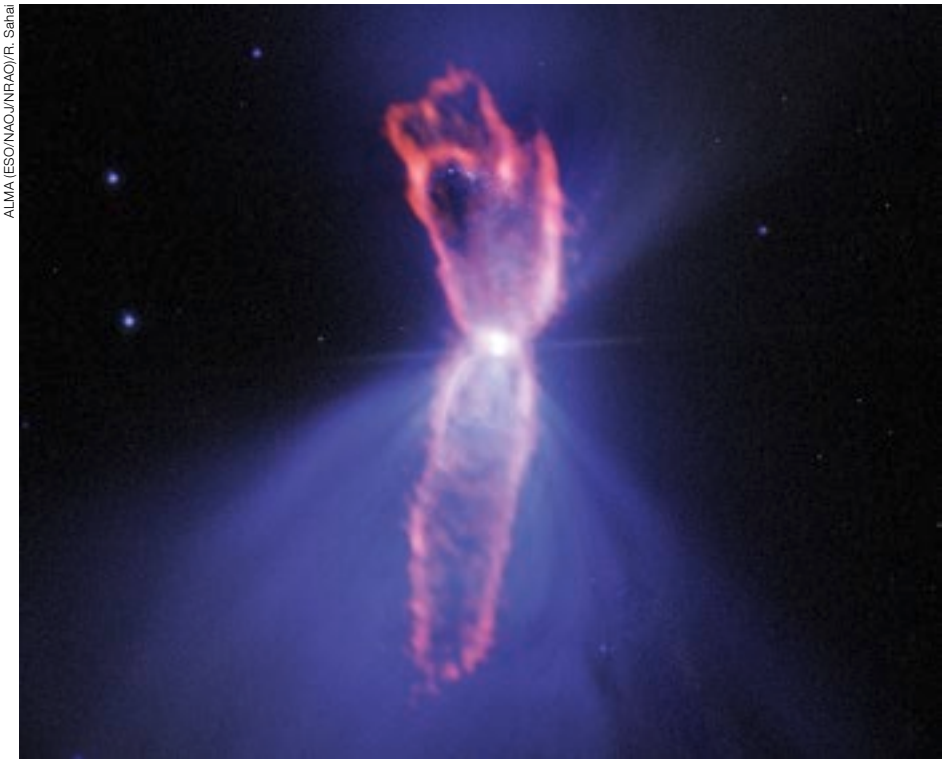

ALMA (ESO/NAOJ/NRAO)/R. Sahai

Composite Atacama Millimeter/submillimeter Array (ALMA) and NASA/ESA Hubble Space Telescope (HST) image of the pre-planetary nebula, the Boomerang, which was ejected by an evolved low mass star. The background bipolar structure (purple) is from the HST visible light image, while the narrow elongated CO (3-2) emission mapped by ALMA is shown in orange. The outflow has exceptionally low brightness temperature (≲ 10 K). See Picture of the Week potw1724 for more details.

DOI: 10.18727/0722-6691/5023

Towards a Sharper Picture of R136 with SPHERE Extreme Adaptive Optics

Zeinab Khorrami[1,2]
Farrokh Vakili[1]
Thierry Lanz[1]
Maud Langlois[3,4]
Eric Lagadec[1]
Michael R. Meyer[5,6]
Raffaele Gratton[7]
Jean-Luc Beuzit[8]
David Mouillet[8]

[1] School of Physics and Astronomy, Cardiff University, United Kingdom
[2] Université Côte d'Azur, OCA, CNRS, Lagrange, France
[3] Université de Lyon, Université Lyon 1, CNRS, CRAL UMR5574, Saint-Genis Laval, France
[4] Université Aix Marseille, CNRS, Laboratoire d'Astrophysique de Marseille, UMR 7326, France
[5] Institute for Astronomy, ETH Zurich, Switzerland
[6] Department of Astronomy, University of Michigan, Ann Arbor, U.S.A.
[7] INAF — Astronomical Observatory of Padua, Italy
[8] Université Grenoble Alpes, CNRS, Institut de Planétologie et d'Astrophysique de Grenoble, France

The SPHERE extreme adaptive optics instrument was used to observe the central core of the Large Magellanic Cloud, R136, in the near-infrared. This challenging observation demonstrated the capabilities of SPHERE for imaging distant clusters. More than one thousand sources have been detected in *Ks*- and *J*-band images in the small field of view of IRDIS covering almost 2.7 × 3.1 pc of the core of R136. Based on isochrone fitting of the colour-magnitude diagram, ages of 1 and 1.5 Myr for the inner 3-arcsecond core and the outer core of R136 fit our data best. The mass function slope is −0.96 ± 0.22 over the mass range of 3 to 300 $M_{\odot}$. Using SPHERE data, we have gone one step further in partially resolving the core of R136, but this is certainly not the final step and higher resolution is still required.

30 Doradus, in the Large Magellanic Cloud (LMC), is one of the most massive and optically brightest H II regions in the Local Group. In the heart of 30 Doradus, the most massive and compact star cluster R136 is located. This cluster hosts the most massive stars known in the Local Universe (Crowther et al., 2016; Crowther et al., 2010). R136 provides a unique opportunity to study the formation of massive stars and their feedback on cluster formation and evolution.

We used the second-generation Very Large Telescope (VLT) SpectroPolarimetric High-contrast Exoplanet REsearch (SPHERE) instrument to observe the central core of R136 in the near-infrared. Using the small field of view (FoV) of the SPHERE InfraRed Dual-band Imager and Spectrograph (IRDIS), more than one thousand sources have been detected in *Ks*- and *J*-band data in the core of R136 (10.9 × 12.3 arcseconds) covering almost 2.7 x 3.1 pc at the distance of R136 (50 kpc).

SPHERE's extreme adaptive optics (AO) system results in the same resolution with the VLT Melipal telescope in the *Ks*-band as the Hubble Space Telescope (HST) yields in the visible (0.055 arcseconds). In the *J*-band the resolution of 0.035 arcseconds exceeds that of the HST, and does so with a better pixel sampling of 12.25 milli-arcseconds per pixel.

Observations

We collected data in Guaranteed Time Observation (GTO) runs to image R136 using the classical imaging mode of IRDIS (Langlois et al., 2014). Observations were performed in September 2015, with high dynamic and high angular resolution imaging in *J*- and *Ks*-bands, over a FoV of 10.9 × 12.3 arcseconds, centred on the core of the cluster (Figure 1). The seeing was 0.63 ± 0.1 arcseconds during the observations and the night was rated as clear. Less than 10 % of the sky (above 30 degree elevation) was covered by clouds, and the transparency variations were lower than 10 %.

The SPHERE data consist of 300 frames, each of 4.0 s exposure, in the two IRDIS broad-band *Ks* and *J* filters (BB-*Ks*, BB-*J*). The Wolf-Rayet star R136a1 was used to guide the AO loop of SPHERE, confirming its better-than-nominal performance that surpasses previous NAOS-CONICA (NACO) and Multi-conjugate Adaptive optics Demonstrator (MAD) observations. The air mass during these observations ranged from 1.54 to 1.67. The average Strehl ratio (SR) in the *J*- and *Ks*-bands was determined to be 0.40 ± 0.05 and 0.75 ± 0.03, respectively.

In order to qualify our data, we compared the reduced *Ks*-band images with published images of R136 from HST (with the Wide Field Planetary Camera 3, WFC3) in the *V*-band and with the MAD imaging (Campbell et al., 2010) in the *Ks*-band (Figure 2). This comparison confirms that our data present better spatial resolution and point-spread function (PSF) sampling which are more suitable for applying deconvolution techniques. For the photometry, we used the Starfinder package (Diolaiti et al., 2000), implemented in the Interactive Data Language (IDL). Starfinder is designed for the analysis of AO images of crowded fields such as the Galactic Centre (Pugliese et al., 2002). It enables determination of the empirical local PSF from several isolated sources in the image and uses this PSF to extract other stellar sources across the FoV.

Three well-isolated stars (no neighbours within 0.47 arcseconds) were used to extract the PSF in the *J*- and *Ks*-band data separately. The extracted PSFs from the *J*- and *Ks*-band data were used as input for the stellar source detection by Starfinder. The full width half maximum (FWHM) of the extracted PSFs are 54.71 and 65.16 milli-arcseconds in the *J*- and *Ks*-band data, respectively. As a consequence, 1110 and 1059 sources were detected in the *J*- and *Ks*-bands, respectively, with a signal-to-noise ratio (S/N) better than two. The AO correction efficiency degrades as a function of distance from R136a1, which is the reference star for the AO loop. At the borders of the FoV, the isoplanatic limits are approached. Overall, the PSF is not centro-symmetric at large distances from R136a1. We took these distortions into account to estimate the local statistical errors, which become significant for those sources that are more distant from the centre of the image than typically 3 arcseconds.

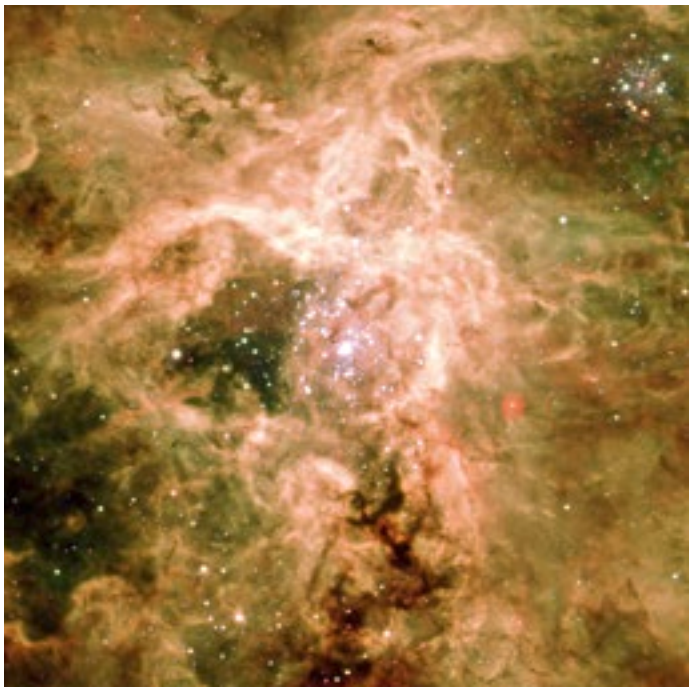

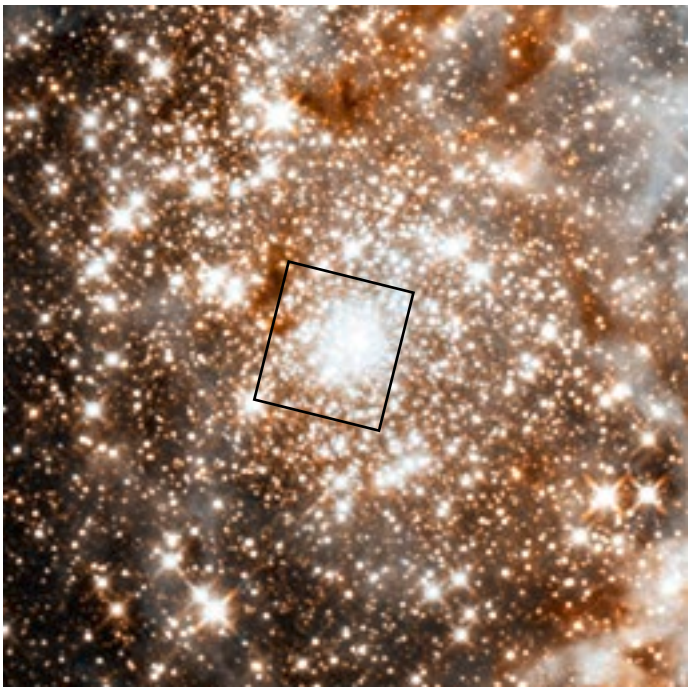

NASA, ESA, F. Paresce (INAF-IASF, Bologna, Italy), R. O'Connell (University of Virginia, Charlottesville), and the Wide Field Camera 3 Science Oversight Committee

Figure 1. (Upper left) Zooming into the core of R136 (275 arcseconds), from a large-field *BVR* image with FORS1 to the core of R136 (upper right) from an HST WFC3 *JH*-band image (59 arcsecond field-of-view), showing the area imaged by SPHERE IRDIS.

Figure 2. (Lower) Comparison of images of the R136 core with the highest available angular resolution. The FoV of all the images in the upper row is the same as the IRDIS data (10.9 × 12.3 arcseconds); the lower row of images are zoomed into the very core of R136 (FoV of 1.5 × 1.5 arcseconds). From left to right: HST/WFC3 (*V*-band), MAD (*Ks*-band), and SPHERE/IRDIS (*Ks*-band).

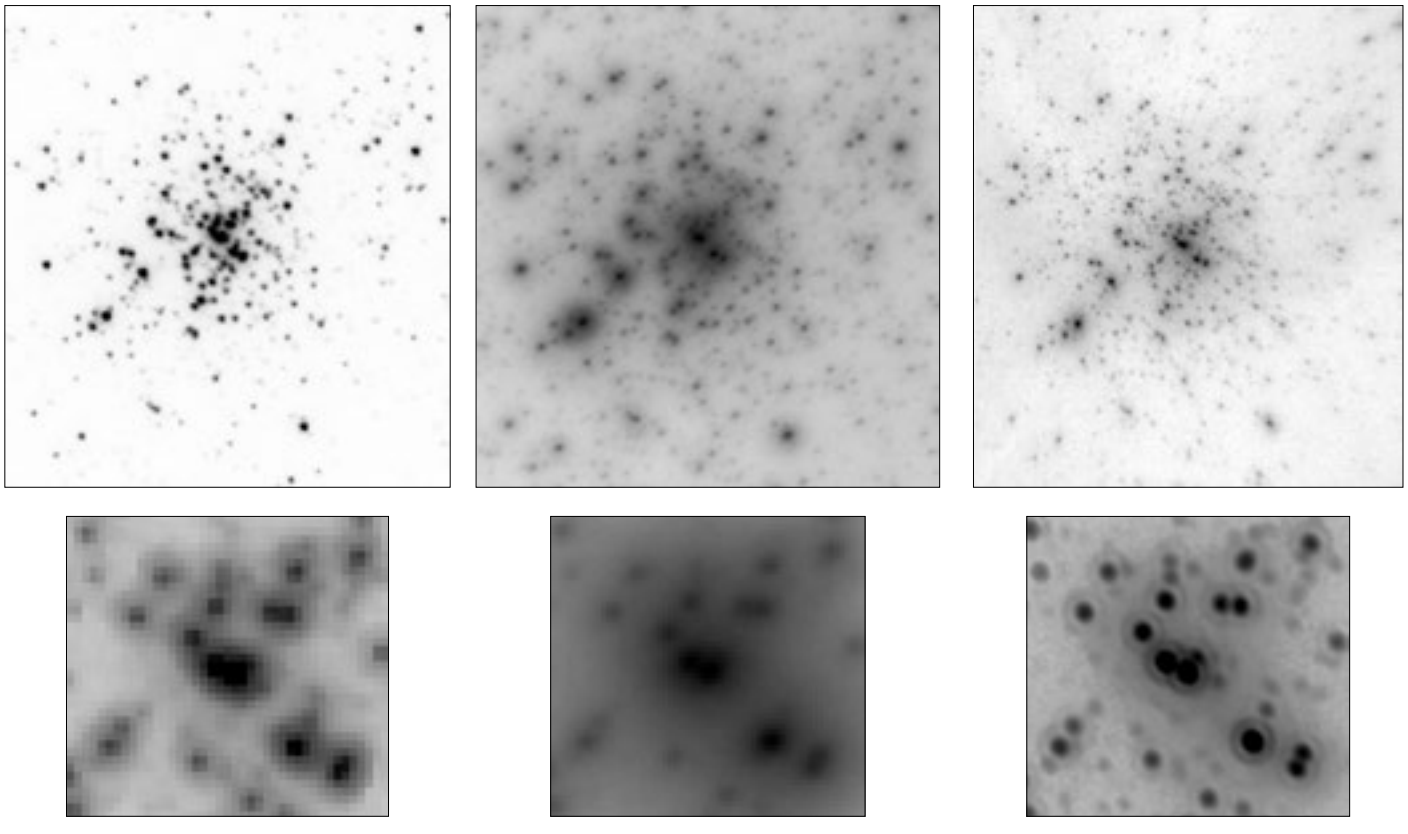

Age and extinction

To estimate the stellar ages and the extinction in the core of R136, we used the effective temperature (T_{eff}) and luminosity (log L) of 54 stars that were studied spectroscopically by Crowther et al. (2016). We also chose a grid of isochrones at different ages (from 0.1 up to 8 Myr) with the LMC metallicity (Z = 0.006) from the latest sets of PARSEC evolutionary models (Bressan et al., 2012), a theoretical library[1] that includes the latest set of stellar phases from pre-main sequence to main sequence and covering stellar masses from 0.1 to 350 $M_{\odot}$. By fitting the isochrones to each star, we estimated its age and intrinsic colour with error bars. An age range of $1.8\ ^{+1.2}_{-0.8}$ Myr is the most probable for these stars. The extinction in J- and Ks-bands is 0.45 ± 0.5 and 0.2 ± 0.5 mag, respectively.

Figure 3 (upper) shows the colour-magnitude diagram (CMD) of detected sources in J- and Ks-band IRDIS data with their error bars. The CMD is plotted for the whole FoV (818 sources), in the very core of the cluster (r < 3 arcseconds), and outside (r > 3 arcseconds), from left to right. The PARSEC isochrones at four different ages (0.6, 1.0, 1.5 and 2.0 Myr) are also plotted in this figure using a distance modulus of 18.49 to R136 and central extinction values in J (0.45 mag) and K (0.2 mag).

We note that, based on the CMD isochrone fitting, ages of 1 Myr for the inner core (r < 3 arcseconds) and 1.5 Myr outside the core (r > 3 arcseconds) fit the data best. Interestingly, the age of stars in the very core (r < 3 arcseconds) is younger than in its outer region. This result appears to be consistent with the older population found beyond the core of R136, like the northeast clump observed by Sabbi et al. (2012), and, at a greater distance (3 arcminutes), the old cluster Hodge301, studied by Grebel & Chu (2000). In future it should be possible to understand this apparent age trend in R136, and also in the 30 Dor region, in terms of formation. Moreover, a key question is how the younger population in the centre of the cluster can be explained by star cluster formation scenarios (Wünsch et al., 2017). We note that this age difference between the two regions can also be explained by an observational bias, because the central region of R136 is very compact and bright so the incompleteness level is very low.

Considering the errors on the extinction, we can estimate the stellar mass range for each star at a given age. We estimated the stellar masses only for com-

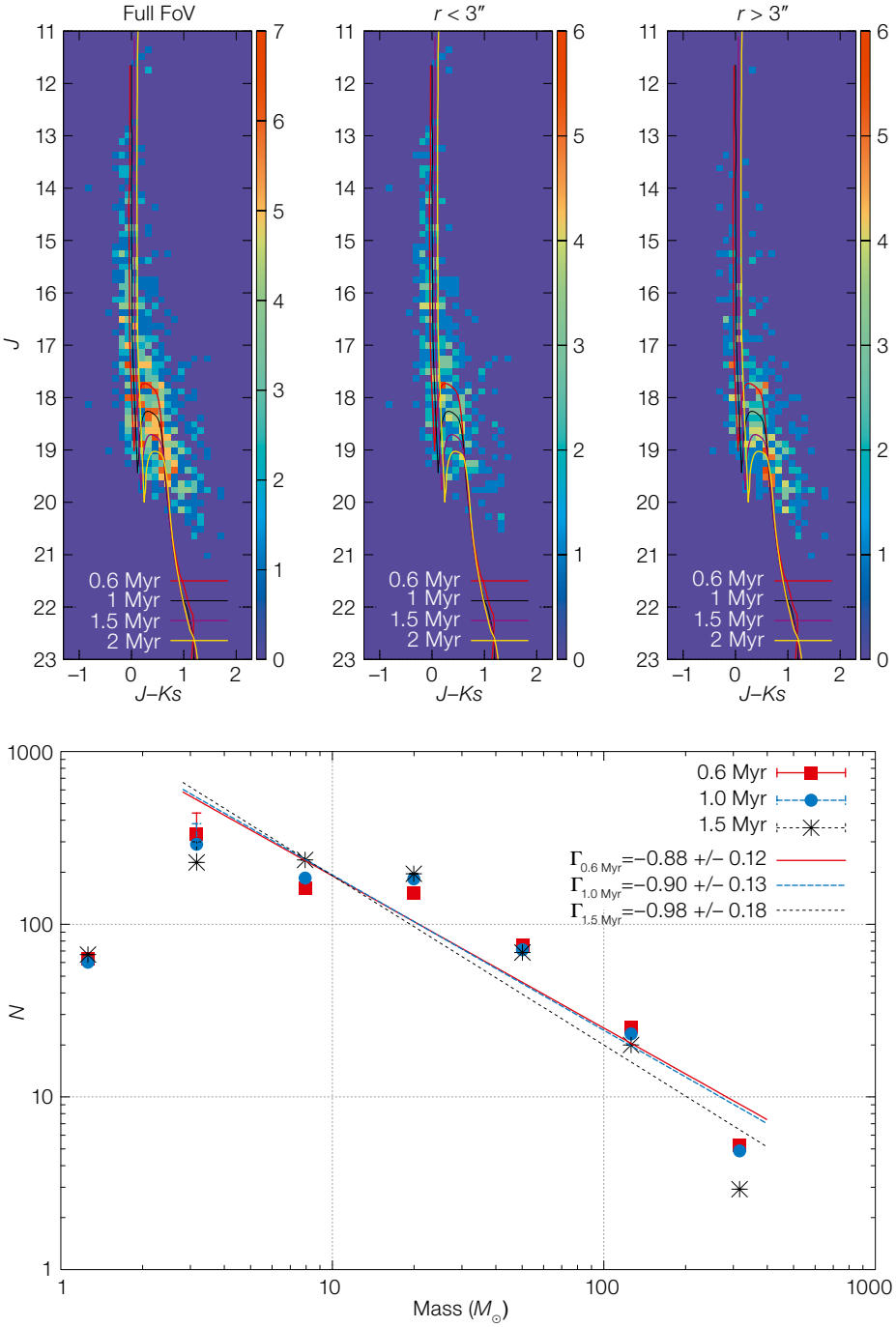

Figure 3. Upper: Colour-magnitude diagram (CMD) in 3D showing the number density of stars. The CMD is plotted for the whole FoV (left), in the very core of the cluster (r < 3 arcseconds, centre) and outside (r > 3 arcseconds, right). Solid red, black, pink, and yellow lines depict PARSEC isochrones (corrected for distance modulus of 18.49 and central values of extinctions, A_J = 0.45 mag and A_K = 0.2 mag) at the ages of 0.5, 1, 1.5 and 2 Myr, respectively. Lower: Generalised histogram of the stellar masses (mass function, MF) at 0.6, 1 and 1.5 Myr. PARSEC models were used to estimate the stellar-mass range for each source using the extinction range.

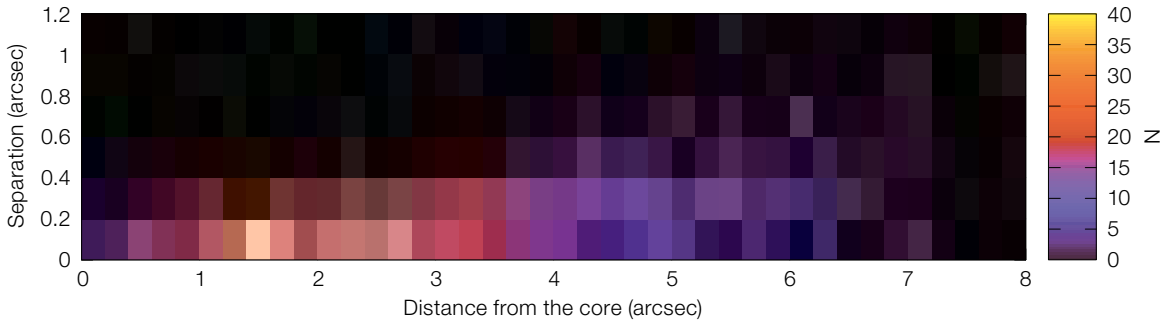

Figure 4. Histogram of the separation of the close detected sources versus their distance from the core of R136.

mon sources between *J* and *Ks* data, using their magnitudes fitted to PARSEC isochrones at three different ages: 0.6, 1, and 1.5 Myr. The histogram of mass, i.e. the mass function (MF), is plotted on the basis of a Gaussian distribution for each stellar mass. The Gaussian uncertainty in the mass of each star was accounted for when constructing the MF.

Figure 3 (lower) shows the generalised histogram of the mass (MF) at three different ages (0.6, 1, and 1.5 Myr). The MF slopes for the 1 and 1.5 Myr isochrones are $\Gamma_{1\ \mathrm{Myr}} = -0.90 \pm 0.13$ and $\Gamma_{1.5\ \mathrm{Myr}} = -0.98 \pm 0.18$, respectively, for the mass range of 3 – 300 $M_{\odot}$. These values are lower limits to the steepness because of incompleteness and the central concentration of bright stars. The derived MF is limited by the resolution of the instrument and also by the detection limit of the observation. In future, using higher angular resolution data, we may resolve binaries and low-mass stars, which affect the shape of the MF.

Visual companions

For each star detected in both *J*- and *Ks*-bands, we determined the distance between the star and its closest neighbour. Figure 4 shows the number of detected neighbouring stars in *Ks* and *J* versus their separation in arcseconds. More than 250 star pairs have a closest neighbour at a separation of less than 0.2 arcseconds. Over 90 % of massive objects (brighter than 16.7 mag in *Ks* and 15 mag in *J*) have a closest neighbour at a separation less than 0.2 arcseconds.

Figure 4 shows the separation between close-by stars versus their distance from R136a1 in the core. This figure indicates that even the sources at larger radii have close visual companions, so that the large number of close visual companions is not just an effect of 2D projection on the sky across the FoV.

The most massive stars, R136a1, R136b and R136c, have visual companions detected in the near-infrared. R136a3 is also resolved as two stars with the PSF fitting technique. Both stars of the pair have a high correlation coefficient (above 70 %) with the input PSF. The separation between the R136a3 primary and secondary is about 58.9 ± 2.1 milli-arcseconds, which is larger than the FWHM of the PSF. We note that even the closest visual companions, like R136a3, are physically distant from each other (0.059 arcseconds corresponds to 2890 au). This visual separation implies a period of more than 10^4 yr for a binary system, so that these sources are probably not gravitationally bound to each other.

Future prospects

Using SPHERE data, we have gone one step further and partially resolved the core of R136, but this is certainly not the final step. R136 needs to be observed in the future with higher resolution, such as with the Extremely Large Telescope (ELT) and the James Webb Space Telescope (JWST) over a wide wavelength range (and field of view). JWST, while more sensitive than our VLT observations, will remain confusion-limited in the core. However, it will provide sensitive observations from 1–28 µm, over a field of several square arcminutes, enabling us to place the R136 cluster in context. The ELT, with its enhanced spatial resolution, will be our best chance to resolve the core, assess the low-mass end of the initial mass function (IMF), and put models of dynamical evolution to serious test. This future work may help us understand massive star formation, the impact massive stars have on their environment, and, ultimately, the formation and evolution of massive star clusters as possible sites for the emergence of stellar black hole binaries whose mergers have recently been detected as sources of gravitational waves.

References

Beuzit, J.-L. et al. 2008, SPIE, 7014, 701418
Bressan, A. et al. 2012, MNRAS, 427, 127
Campbell, B. et al. 1992, AJ, 104, 1721
Campbell, M. A. et al. 2010, MNRAS, 405, 421
Cassinelli, J. P., Mathis, J. S. & Savage, B. D. 1981, Sci, 212, 1497
Grebel, E. K. & Chu, Y.-H. 2000, AJ, 119, 787
Crowther, P. A. et al. 2010, MNRAS, 408, 731
Crowther, P. A. et al. 2016, MNRAS, 458, 624
Diolaiti, E. et al. 2000, A&AS, 147, 335
Feitzinger, J. V. et al. 1980, A&A, 84, 50
Hunter, D. A., Shaya, E. J. & Holtzman, J. A. 1995, ApJ, 448, 179
Khorrami, Z. et al. 2016, A&A, 588, L7
Langlois, M. et al. 2014, SPIE, 9147, 91479P
Sabbi, E. et al. 2012, ApJ, 754, L37
Savage, B. D. et al. 1983, ApJ, 273, 597
Weigelt, G. & Baier, G. 1985, A&A, 150, L18
Wünsch, R. et al. 2017, ApJ, 835, 60

Links

[1] PARCSEC evolutionary models: http://stev.oapd.inaf.it/cgi-bin/cmd

DOI: 10.18727/0722-6691/5024

1000 High-redshift Galaxies with Spatially-resolved Spectroscopy: Angular Momentum over 10 Billion Years

Chris Harrison[1,2]
Mark Swinbank[2]

[1] ESO
[2] Centre for Extragalactic Astronomy, Durham University, United Kingdom

A sample of ~1000 high-redshift (z ~ 0.3–1.7) star-forming galaxies has been observed with three-dimensional spectroscopy using the KMOS and MUSE spectrographs in order to explore the dynamical properties of galaxies across cosmic time. A summary of the survey is presented along with one set of results that explores the relationship between the angular momentum of the star-forming gas and galaxy morphology. This work expands previous angular momentum studies that mostly focused on local galaxies, to cover the past 10 billion years of cosmic time.

Galaxy formation, morphologies and angular momentum

Galaxies have a range of morphological types, including ellipticals, spheroidals and late-type spirals, which form the morphological "Hubble Sequence". Identifying the dominant physical processes that were responsible for the formation of the Hubble Sequence has been one of the major goals of galaxy formation studies for decades. In the cold dark matter paradigm, baryonic galaxies (i.e., the stars and gas) form at the centres of dark matter halos. If unperturbed, the baryons inside dark matter halos should cool and collapse, weakly conserve angular momentum and form a galaxy disc which follows an exponential light profile.

However, the angular momentum (i.e., the product of the mass, velocity and radial distance) of the baryons can also be redistributed through mergers, inflows, outflows and chaotic motions. From the dynamics of gas and stars of nearby galaxies, it has been shown that angular momentum appears to be the fundamental property defining the local Hubble Sequence (for example: Fall & Romanowsky, 2013; Cortese et al., 2016; see Figure 1). Indeed, Fall & Romanowsky (2013) show that local spiral discs retain ~80 % of their initial angular momentum, but this drops to only ~10 % for early-type ellipticals/spheroidals. As visualised in Figure 1, the Hubble Sequence of galaxy morphologies appears to follow a strict sequence of increasing angular momentum for a fixed mass.

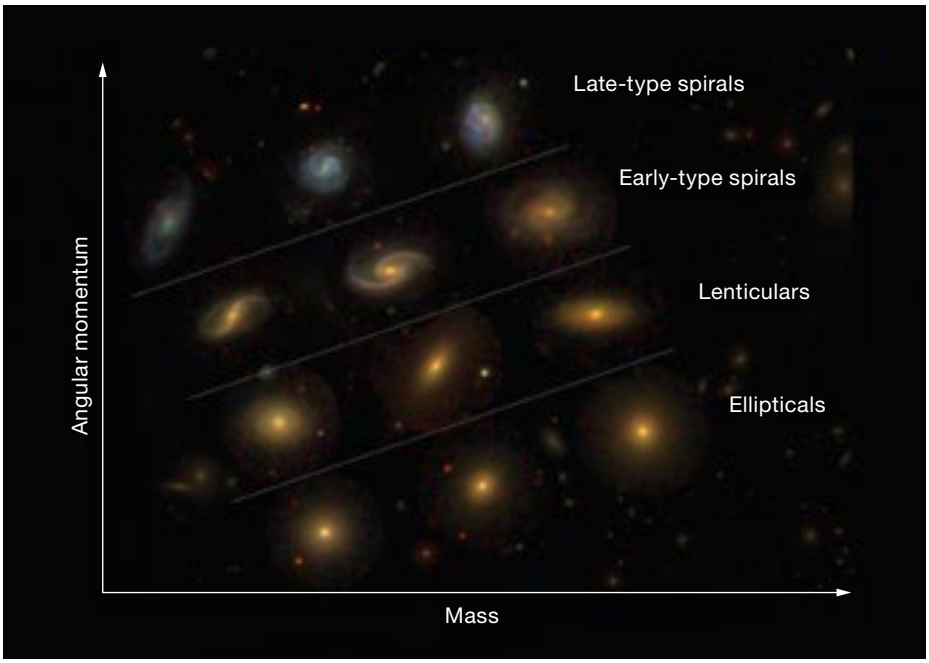

L. Cortese and Sloan Digital Sky Survey

Figure 1. A schematic diagram showing the relative position of low-redshift galaxies with different morphologies in the angular momentum versus stellar mass plane.

The need for high-redshift integral field surveys

Morphological surveys of high-redshift galaxies, in particular using the Hubble Space Telescope (HST), have suggested that the Hubble Sequence began to emerge when the Universe was just under half of its present age (i.e., a redshift of z ~ 1.5; for example Mortlock et al., 2013). This is the epoch when spirals and ellipticals appear to become as common as irregular/clumpy galaxies. Consequently there is a clear need to expand local dynamical studies of angular momentum to galaxies in the distant, high-redshift Universe. Furthermore, recent simulations suggest that most of the angular momentum redistribution (that later defines galaxy morphologies) occurs at high redshift (for example, Lagos et al., 2017). If true, then the redistribution of angular momentum in high-redshift galaxies plays a dominant role in the formation the Hubble Sequence. Moreover, constraining the angular momentum of galaxies around this epoch (and any corresponding evolution) provides a critical test of galaxy formation models.

The most efficient way to obtain the required dynamical measurements for large samples of high-redshift galaxies is to use spatially-resolved spectroscopy, via integral field unit (IFU) data, to map bright emission lines such as Hα or [O II] 3727 Å. Motivated by this, we set out to obtain measurements for almost 1000 galaxies out to z ~ 1.7, covering ~10 billion years of cosmic time, using two IFU instruments on the Very Large Telescope (VLT): the *K*-band Multi-Object Spectrograph (KMOS); and the Multi Unit Spectroscopic Explorer (MUSE).

Dynamics of 1000 high-z emission-line galaxies with KMOS and MUSE

For our studies, we constructed a sample of high-redshift (z = 0.3–1.7) star-forming galaxies with IFU data using two approaches: firstly, using KMOS Guaranteed Time Observations (GTO); and secondly, using archival MUSE observations. The KMOS spectrograph (Sharples et al.,

2013) has been in operation at the VLT since late 2012. KMOS has 24 near-infrared (~ 800–2500 nm) IFUs that can be moved independently within a 7-arcminute field of view. This enables the dynamics of large samples of high-redshift galaxies to be determined (at a rate that is ~ 20× faster than previously possible). The MUSE IFU (Bacon et al., 2010), which has been in operation since 2014, provides spectral coverage of the optical wavelengths, spanning 477–930 nm and a contiguous field of view of 60 by 60 arcseconds. This combination of field of view and spectral coverage for an IFU means that large samples of high-redshift star-forming galaxies can be detected in emission lines — serendipitously — during any observation of an extragalactic field. Our results on the angular momentum of our combined MUSE and KMOS samples are presented across two papers — Harrison et al. (2017) and Swinbank et al. (2017) — and consist of data from the three observational surveys detailed below.

KMOS Redshift One Spectroscopic Survey (KROSS)

KROSS is a 30-night KMOS GTO project that was led by Durham University and the University of Oxford, with contributions from the University of Edinburgh (Stott et al., 2016). The project ran from Period 92 to 95, and consists of a final sample of 743 star-forming galaxies at z = 0.7–1.1 (Harrison et al., 2017). All targets were observed in the *YJ*-band, targeting the Hα emission line. The bright Hα emission line enables us to map the two-dimensional gas dynamics on 3–10 kpc scales within these galaxies. Of the final sample, about 80 % are detected in Hα emission, providing a sample of 586 galaxies for which dynamical measurements — and consequently angular momentum constraints — can be derived (Harrison et al., 2017).

KMOS Galaxy Evolution Survey (KGES)

KGES is an ongoing Durham University project utilising ~ 25 nights of GTO time on KMOS between Periods 95 and 100. Building on KROSS, the observations are designed to measure the dynamics of ~ 300 star-forming galaxies at z = 1.3–1.7. The first 17 galaxies from this survey are presented in Swinbank et al. (2017), and the results from the first half of the survey will be presented in Tiley et al. (2017).

MUSE serendipitous sources

In order to extend the redshift and mass range of our KMOS survey, we exploited MUSE observations of 17 extragalactic "deep" fields that were observed during commissioning, Science Verification and Period 94. These fields include standard extragalactic "deep" fields (such as COSMOS), as well as high-redshift galaxies, quasars and cluster fields. By searching through the data cubes for the [O II] 3727 Å emission line, we identified 364 star forming galaxies at z = 0.3–1.7 with sufficient data quality to perform dynamical analyses and consequently obtain angular momentum constraints (Swinbank et al., 2017).

Angular momentum of high-redshift star-forming galaxies

Using our KMOS and MUSE IFU data we produced maps of the emission-line gas intensity, velocities and velocity dispersions (i.e., random motions) for each galaxy. Examples can be seen in Figure 2. These maps were used to identify the

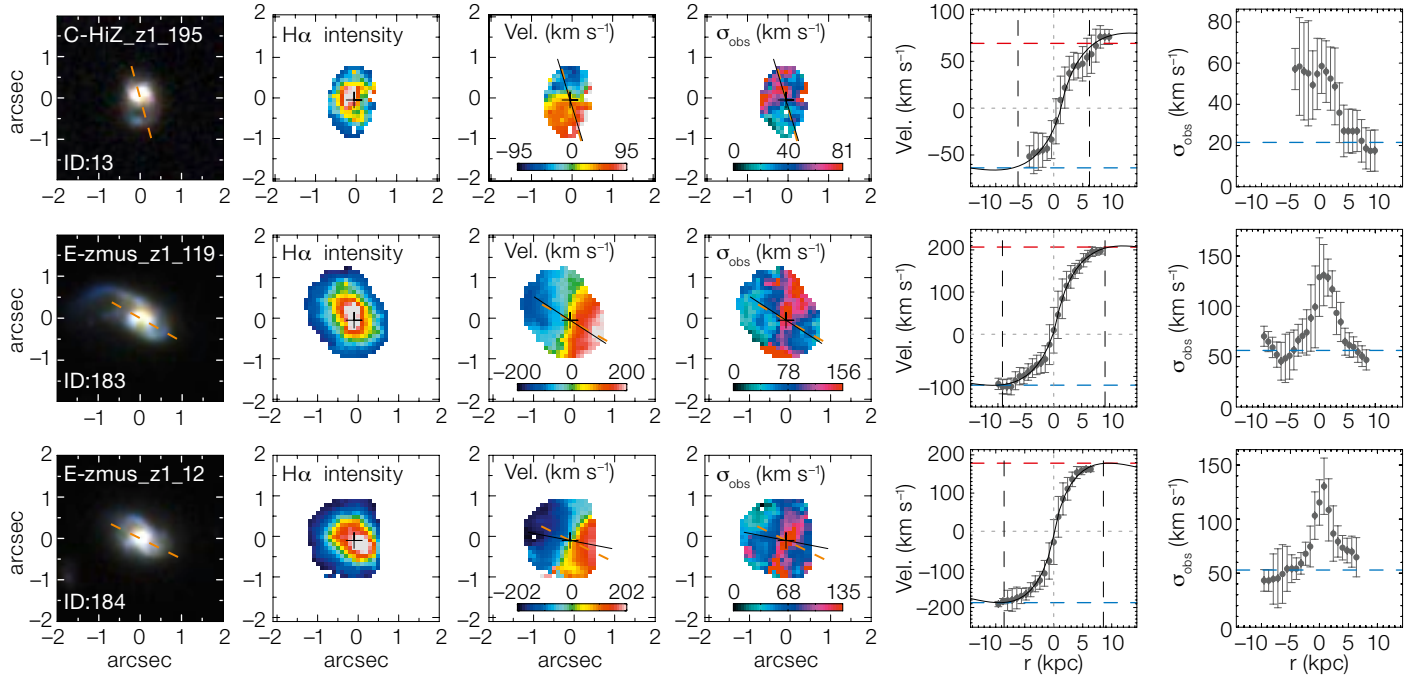

Figure 2. HST and KMOS data for three example objects. From left to right: (1) HST image (dashed line shows major axis); (2) Hα intensity map; (3) velocity map; (4) velocity dispersion map (solid line shows dynamical axis); (5) one-dimensional velocity profile (with model rotation curve overlaid); (6) one-dimensional dispersion velocity profile (with dashed lines showing intrinsic velocity dispersion).

dynamical ("rotational") axes of the gas and one-dimensional velocity profiles were extracted along these axes. Rotation velocities are measured at twice the half-light radii for each galaxy. The rotation velocity, in combination with the galaxy's size, enables the angular momentum to be calculated. Throughout the analyses, great care was taken to remove any artificial "blurring" or "smearing" due to instrumental and atmospheric effects during the observations.

In Figure 3 we plot the specific angular momentum (i.e., the angular momentum per unit mass) as a function of the stellar mass for each galaxy in our sample. The relationship between angular momentum and galaxy mass for our high-redshift galaxies shows the same trend (i.e., slope) as seen in local galaxies (for example, Fall & Romanowsky, 2013). However, as discussed below, on average the high-redshift galaxies appear to have lower angular momentum than the spiral galaxies seen today (when the stellar masses are considered).

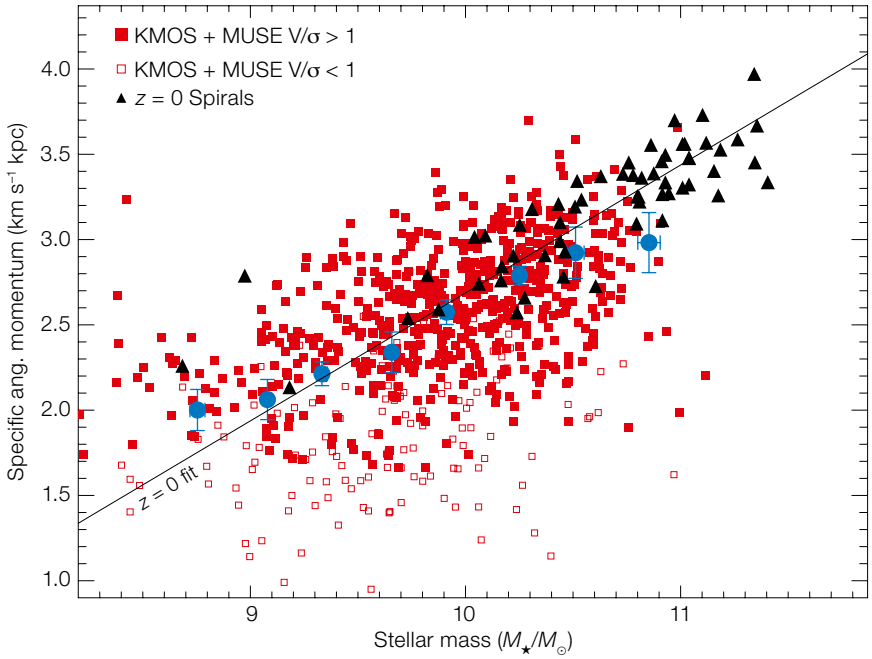

Figure 3. Specific angular momentum (angular momentum per unit stellar mass; $j_* = J/M_*$) for the combined sample of high-redshift galaxies in the KMOS and MUSE samples. The high-redshift sample is split into those galaxies which are dominated by rotation (filled squares) and those that are dominated by dispersion support (open squares). Local spiral galaxies are shown as filled triangles. The run of the median specific angular momentum of the high-redshift galaxies is shown by the large blue points. The full KMOS + MUSE sample reveals a similar relationship between stellar mass and angular momentum as for local spirals.

Angular momentum and morphology

By comparing the rotational velocities with the intrinsic velocity dispersions (see Figure 2), we determine whether the star-forming gas in each galaxy is predominantly "rotationally dominated", or the galaxy is "dispersion dominated". This is an important way to categorise the galaxies as it is strongly related to whether the galaxies are "discy" in nature. In Figure 3, the filled points show the galaxies that are dominated by rotation, versus those which are dominated by dispersion (open symbols). This shows that "discier" galaxies appear to have the most angular momentum. This is in qualitative agreement with the results sketched in Figure 1 for local galaxies — spiral galaxies have more angular momentum for a fixed mass than elliptical galaxies.

In order to test this result further, we isolated the galaxies with the most angular momentum per unit mass and those with the least angular momentum per unit mass and compared their HST images (see Figure 4 for examples). The galaxies with the highest angular momentum have the most prominent discs and spiral-like morphologies. This may not be unexpected, but shows that the emergence of the Hubble Sequence in the high redshift Universe is closely related to the angular momentum of the star-forming gas. However, note that the discs in our high-redshift sample (see Figure 4) are not smooth, but consist of several "clumps" which may be the result of their relatively low angular momentum compared to their low redshift-counterparts (see below). In summary, the strong relationship between angular momentum, mass and morphology that is observed locally appears to be falling into place as early as redshift $z \sim 1.5$.

The evolution of angular momentum

The galaxies in our sample span a range of redshifts from $z \sim 0.3$–1.7. To test how the specific angular momentum evolves with time, we split the sample into four redshift bins. However, to account for any underlying evolution of the stellar masses, we adopt the ratio of angular momentum of the stellar component to stellar mass ($j_*/M_*^{2/3}$), which should remove the expected underlying stellar mass evolution with redshift. In Figure 5 we plot this mass-normalised angular momentum as a function of redshift (and time). Also included on the plot are the locations of local galaxies of various morphological types (early and late type spirals). Figure 5 reveals that selecting star-forming galaxies at increasing redshift (and time) results in selecting systems with decreasing angular momentum. To test how this compares to predictions from numerical models, we also include the evolution of angular momentum of model galaxies from the EAGLE[1] simulation (Schaye et al., 2015), selected in the same way as the galaxies in our observed sample. In both the data and the model, as star-forming galaxies increase their specific angular momentum, their morphologies transform into smooth spiral discs.

In summary, our results have shown that the fraction of rotationally supported disc-like galaxies at high-redshift is high, yet most of these galaxies appear clumpy (examples in Figure 4). We attribute the clumpy nature of the high-redshift galax-

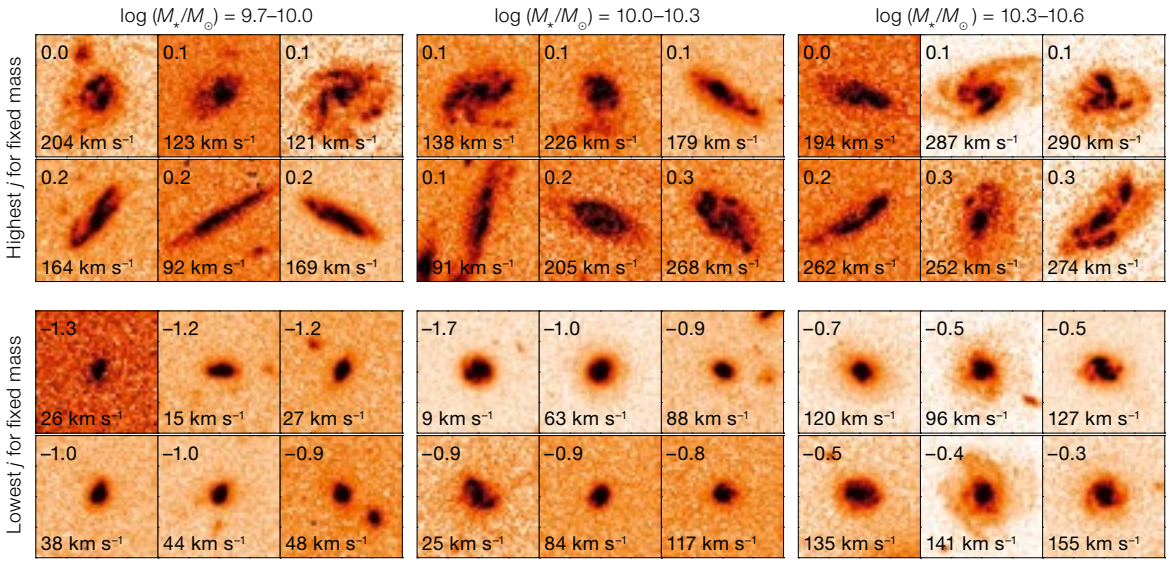

Figure 4. *I*-band HST images for the six galaxies from the sample with the lowest (lower panels) and highest (upper panels) specific angular momentum for three stellar mass bins. This shows that the galaxies with the highest angular momentum have the most prominent discs and spiral-like morphologies. The value in the lower left corner of each panel is the (inclination corrected) rotational velocity, and in the upper left, the value of $\Delta \log (j_*)$.

ies to the low angular momentum of the gas, which results in globally unstable, turbulent systems. With decreasing redshift, the angular momentum of gas discs appears to gradually increase (such as in Figure 5), and this appears to play a major role in defining the disc stability and morphology (Figure 4). As the specific angular momentum of growing discs increases below $z \sim 1$, the galaxy discs must evolve from globally unstable clumpy, turbulent systems into the stable, flat regular spirals we see today.

Ongoing work and prospects

The efficiency of KMOS and MUSE means that the next few years will see a continued increase in the sample sizes of galaxies with well resolved dynamics, but also in the range of stellar mass, star formation rate and redshift. In the near future, the launch of the James Webb Space Telescope will also allow the first systematic study of the stellar kinematics of high-redshift galaxies to be carried out, building on the work here which focuses on the star-forming gas kinematics. Confronting the gaseous and stellar content of galaxies will provide a critical measure of the interaction between star formation and gas dynamics, and further improve the constraints linking galaxy morphologies and angular momentum–mass–morphology relationships in galaxies around the peak epoch of galaxy formation at $z \sim 1.5$.

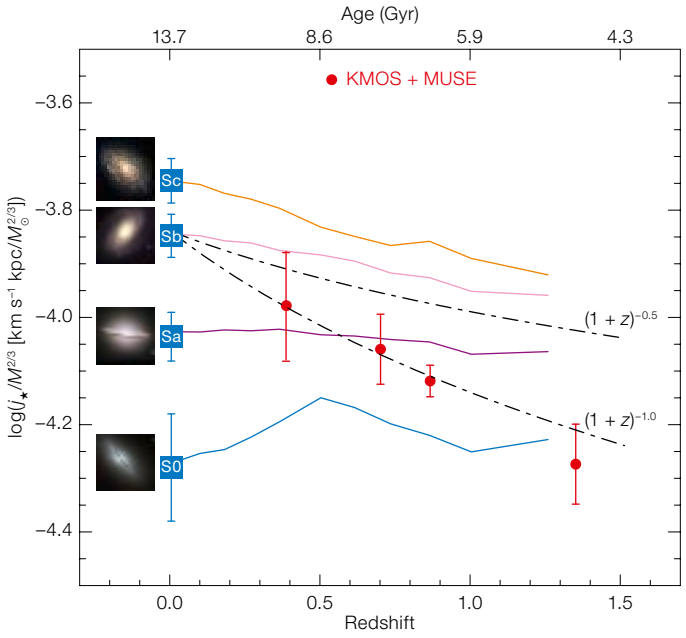

Figure 5. The redshift evolution of the specific angular momentum (normalised by mass) from $z = 0$ to $z = 1.5$. The $z = 0$ galaxies are split into their morphological types (from S0 to Sd). To compare with model predictions, the evolution of angular momentum for galaxies in the EAGLE simulation is overlaid. Toy-model tracks that show evolution according to $(1 + z)^{-n}$ with $n = 0.5$ and $n = 1.0$ are also shown.

Acknowledgements

Based on observations data obtained under ESO programmes: 060.A-9100; 060.A-9302; 060.A-9306; 060.A-9318; 060.A-9321; 060.A-9323; 060.A-9325; 060.A-9326; 060.A-9331; 060.A-9334; 060.A-9338; 060.A-9460; 092.B-0538; 093.B-0106; 094.B-0061; 094.A-0141; 094.A-0280; 095.B-0035; 095.A-0570; 095.A-0748. The authors acknowledge support from the UK Science and Technology Facilities Council (ST/L00075X/1) and the Leverhulme Foundation.

References

Bacon, R. et al. 2010, SPIE Conf. Ser., 7735, 8
Cortese, L. et al. 2016, MNRAS, 463, 170
Fall, M. S. & Romanowsky, A. J. 2013, ApJ, 769, 26
Harrison, C. M. et al. 2017, MNRAS, 467, 1965
Lagos, C. d. P. et al. 2017, MNRAS, 464, 3850
Mortlock, A. et al. 2013, MNRAS, 433, 1185
Schaye, J. et al. 2015, MNRAS, 446, 521
Sharples, R. et al. 2013, The Messenger, 151, 21
Stott, J. P. et al. 2016, MNRAS, 457, 1888
Swinbank, A. M. et al. 2017, MNRAS, 467, 3140

Links

[1] EAGLE Project: http://icc.dur.ac.uk/Eagle/

DOI: 10.18727/0722-6691/5025

The VIMOS Public Extragalactic Redshift Survey (VIPERS): Science Highlights and Final Data Release

Luigi Guzzo[1]
The VIPERS Team*

[1] Università degli Studi di Milano, Italy

The VIMOS Public Extragalactic Redshift Survey (VIPERS) released its final set of nearly 90 000 galaxy redshifts in November 2016, together with a series of science papers that range from the detailed evolution of galaxies over the past 8 Gyr to the growth rate and the power spectrum of cosmological structures measured at about half the Hubble time. These are the results of a map of the distribution of galaxies and their properties which is unprecedented in its combination of large volume and detailed sampling at $0.5 < z < 1.2$. In this article, the survey design and data properties are briefly summarised and an overview of the key scientific results published so far is provided. The VIPERS data, obtained within the framework of an ESO Large Programme over the equivalent of just under 55 nights at the Very Large Telescope, will remain the largest legacy of the VIMOS spectrograph and its still unsurpassed ability to reach target densities close to 10 000 spectra per square degree.

* L. Guzzo[1, 2], B. Garilli[3], M. Scodeggio[3], B. Granett[2, 1], M. Bolzonella[4], S. de la Torre[5], U. Abbas[6], C. Adami[5], D. Bottini[3], A. Cappi[4, 7], O. Cucciati[4], I. Davidzon[5, 4], P. Franzetti[3], A. Fritz[3], A. Iovino[2], J. Krywult[8], V. Le Brun[5], O. Le Fèvre[5], D. Maccagni[3], K. Malek[9], F. Marulli[10], M. Polletta[3], A. Pollo[9, 11], L. Tasca[5], R. Tojeiro[12], D. Vergani[13], A. Zanichelli[14], S. Arnouts[5], J. Bel[15], E. Branchini[16], J. Coupon[17], G. De Lucia[18], A. Gargiulo[3], C.P. Haines[2], A. Hawken[2, 1], O. Ilbert[5], E. Jullo[5], A. Marchetti[3], C. Marinoni[15], H. J. McCracken[19], Y. Mellier[19], L. Moscardini[10], T. Moutard[20, 5], J. A. Peacock[21], W. J. Percival[22], A. Pezzotta[2, 23], S. Rota[3], G. Siudek[24], G. Zamorani[4].

[1] Università degli Studi di Milano, Italy; [2] INAF — Osservatorio Astronomico di Brera, Milano, Italy; [3] INAF — IASF Milano, Italy; [4] INAF — Osservatorio Astronomico di Bologna, Italy; [5] LAM, Marseille, France; [6] INAF — Osservatorio Astronomico di Torino, Italy; [7] Université de Nice, Obs. de la Cote d'Azur, France; [8] Jan Kochanowski University, Kielce, Poland; [9] National Centre for Nuclear Research, Warsaw, Poland; [10] Dip. di Fisica e Astronomia, Università di Bologna, Italy; [11] Astron. Observatory, Jagiellonian University, Cracow, Poland; [12] School of Physics and Astronomy, University of St. Andrews, UK; [13] INAF — IASF Bologna, Italy; [14] INAF — IRA Bologna, Italy; [15] CPT Université de Provence, Marseille, France; [16] Università Roma 3, Rome, Italy; [17] Dept. of Astronomy, University of Geneva, Switzerland; [18] INAF — Osservatorio Astronomico di Trieste, Italy; [19] Institut d'Astrophysique de Paris, France; [20] Dept. of Astron. & Physics, St. Mary's Univ., Halifax, Canada; [21] Institute for Astronomy, University of Edinburgh, UK; [22] Inst. of Cosmology and Gravitation, Univ. of Portsmouth, UK; [23] Università di Milano-Bicocca, Italy; [24] Centre for Theoretical Physics, Warsaw, Poland.
See http://vipers.inaf.it for a full list of the VIPERS team including former and associated members.

Introduction

Galaxy redshift surveys represent one main pillar of the current "standard" Λ Cold Dark Matter (CDM) cosmological model, in combination with observations of distant supernovae and the Cosmic Microwave Background (see for example Planck Collaboration, 2016). The amplitude of galaxy clustering on different scales is a probe of both the initial conditions and the physical processes that governed the growth of cosmic fluctuations since the Big Bang. Surveys like the 2dF Galaxy Redshift Survey (Colless et al., 2001) and the Sloan Digital Sky Survey (SDSS) led this effort at the turn of the millennium. The SDSS in particular, in its subsequent incarnations the Luminous Red Galaxy (LRG) survey (Eisenstein et al., 2011) and, more recently, the Baryon Oscillation Spectroscopic Survey (BOSS: Alam et al., 2015), progressively increased the cosmological yield by maximising the sampled volume at the expense of restriction to specific, sparse sub-populations of galaxies. It was the original SDSS main sample of 10^6 objects with measured redshifts, however, that also allowed the properties of galaxies and their scaling relationships to be defined with exquisite accuracy, thanks to its broad selection function, good resolution spectra and multi-band imaging (York et al., 2003).

The VIPERS project was started in 2008 (Period 82), with the goal of extending such precise measurements of both structure and galaxy properties to redshifts approaching unity. VIPERS was built upon the experience of earlier VIsible Multi-Object Spectrograph (VIMOS) surveys, such as the VIMOS Very Deep Survey (VVDS: Le Fèvre et al., 2005) and *z*COSMOS (Lilly et al., 2009), pushing the data size, reduction techniques and management infrastructure to an even higher level (see Garilli et al., 2012 and Guzzo et al., 2014).

The VIPERS project

The way to achieve this goal has been to measure redshifts for galaxies with $i_{AB} < 22.5$ mag., further limited to redshift $z > 0.5$ through a robust *ugri* colour preselection. This nearly doubled the density of galaxies at $0.5 < z < 1.2$, compared to the pure magnitude-limited sample and was made possible by the accurate five-band photometry provided by the Canada France Hawaii Telescope Legacy Survey (CFHTLS) Wide data[1], on which VIPERS is based. The goal was to focus the effort at high redshifts by excluding the galaxies in the low-redshift volume that would not be competitive with the wide-angle samples already available. With an average sampling of 47 %, the VIPERS strategy has in fact yielded a spatial density close to $10^{-2}\ h^3\ \mathrm{Mpc}^{-3}$ (where h is the normalised Hubble constant) at the peak of the survey selection function.

A volume comparable to that of the 2dF Galaxy Redshift Survey, i.e., close to $5 \times 10^7\ h^{-3}\ \mathrm{Mpc}^3$, was secured by tiling an overall footprint of 23.5 square degrees with a mosaic of 288 VIMOS pointings over the W1 and W4 CFHTLS fields (192 and 96 pointings, respectively), which are shown in Figure 1. 372 hours of multi-object spectroscopy (MOS) observations (45 min exposure per field), and 68.5 hours of pre-imaging were invested on VLT Unit Telescope 3 (Melipal), corresponding to a total of about 55 night-equivalents.

Working at low resolution between 5500 and 9500 Å with the LR-Red grism (resolution, $R = 210$) resulted in a typical redshift root mean square (rms) error of $s_z = 0.00054\ (1 + z)$. This value has been directly estimated from about 3000 double measurements available in the final sample (Scodeggio et al., 2017). A few examples of VIPERS spectra are presented in Figure 2.

The final Public Data Release 2 (PDR-2) includes 86 775 measured redshifts for galaxies in the statistical VIPERS target

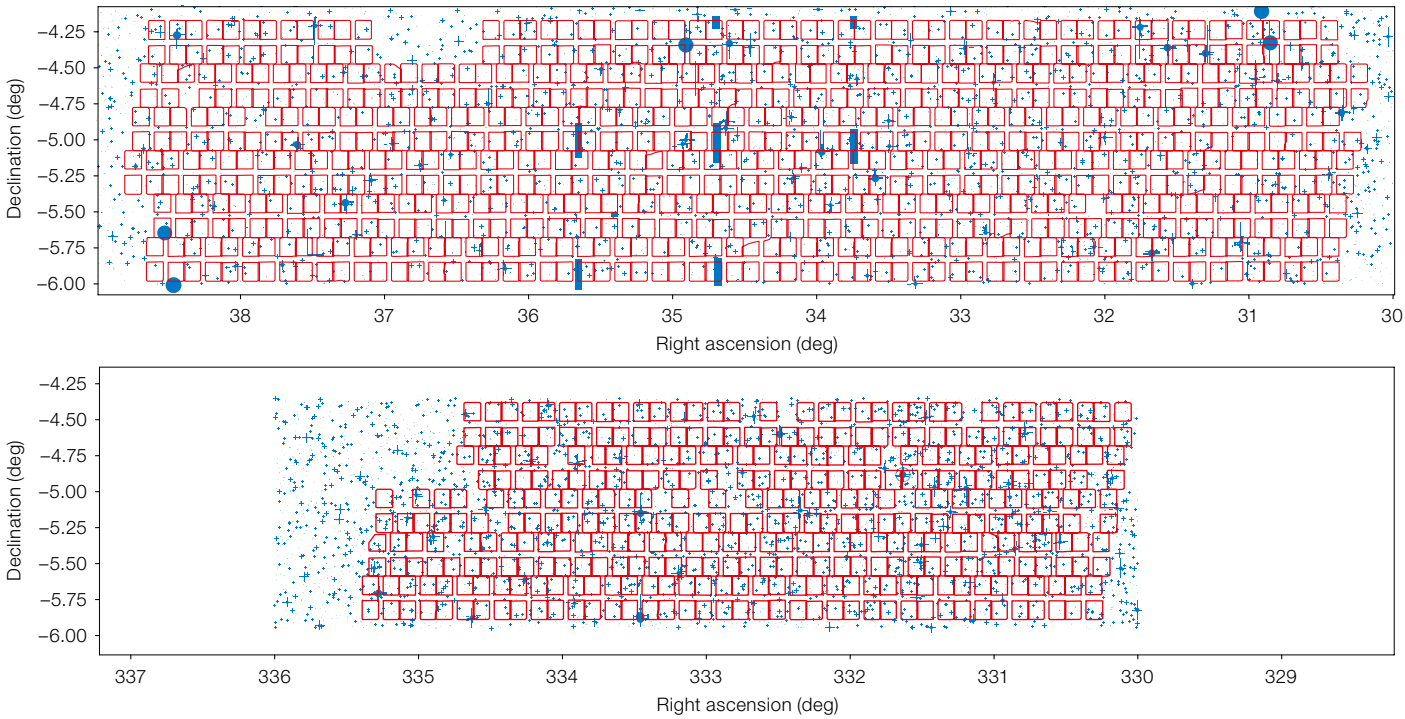

Figure 1. (Above) Layout of the 288 VIMOS pointings comprising the VIPERS survey, over the W1 (upper) and W4 (lower) fields of the CFHTLS photometric survey. From Scodeggio et al. (2017).

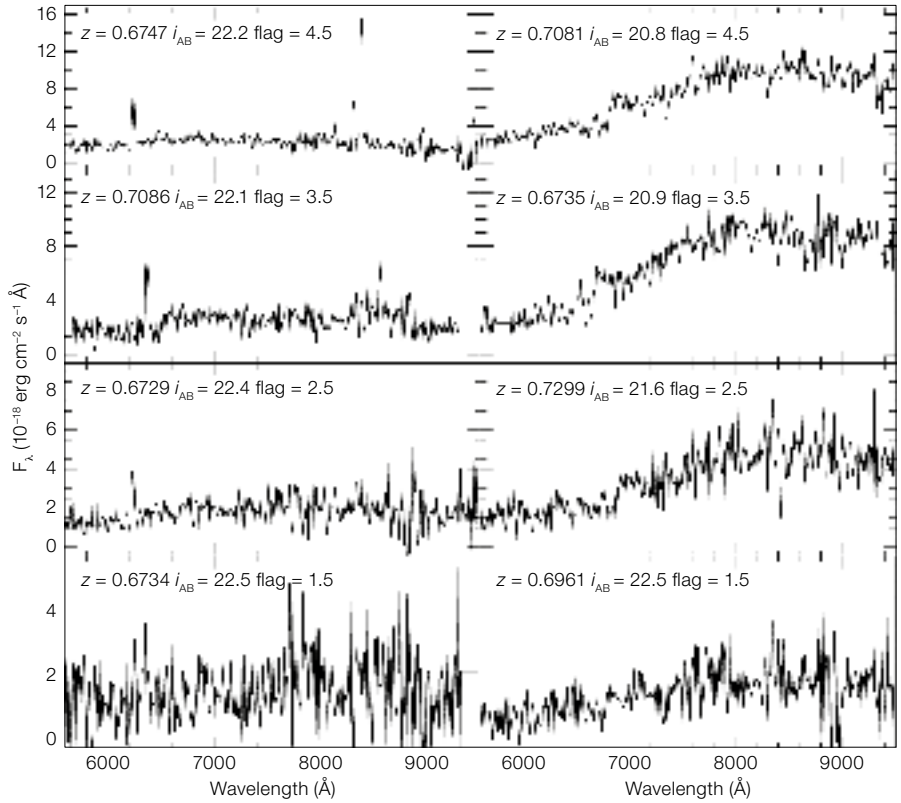

Figure 2. Examples of VIPERS spectra at z around 0.7, i.e. near the peak of the VIPERS redshift distribution. For different values of the redshift quality flags, examples of both a late-type and an early-type galaxy spectrum are shown. Note that objects with flag < 2 (bottom row) are not part of the statistical sample of highly reliable redshifts, as discussed in the text. The decimal part of the flag (0.5) indicates agreement with the photometric redshift. From Scodeggio et al. (2017).

sample. Of these, 78 586 (90.6 %) have been validated as highly reliable (confidence level > 96 %) and represent the sample to be used for statistical investigations. 2247 targets turned out to be stars, a very low residual contamination (2.5 %) that confirms the quality of the original star-galaxy separation (see appendix in Guzzo et al., 2014). More details of the PDR-2 sample can be found in Scodeggio et al. (2017); the survey construction and first data release were presented in Guzzo et al. (2014) and Garilli et al. (2014), respectively. The PDR-2 data are available both in the ESO Science Archive and, together with other complementary information, from the VIPERS website[2].

The combination of sampling and volume provided by VIPERS at these redshifts can be appreciated from the cone diagrams in Figure 3 and represents a unique feature among redshift surveys of the $z > 0.5$ Universe. In the same figure, galaxy positions are marked by circles of different size and colour, reflecting the actual luminosity and ultraviolet rest-frame

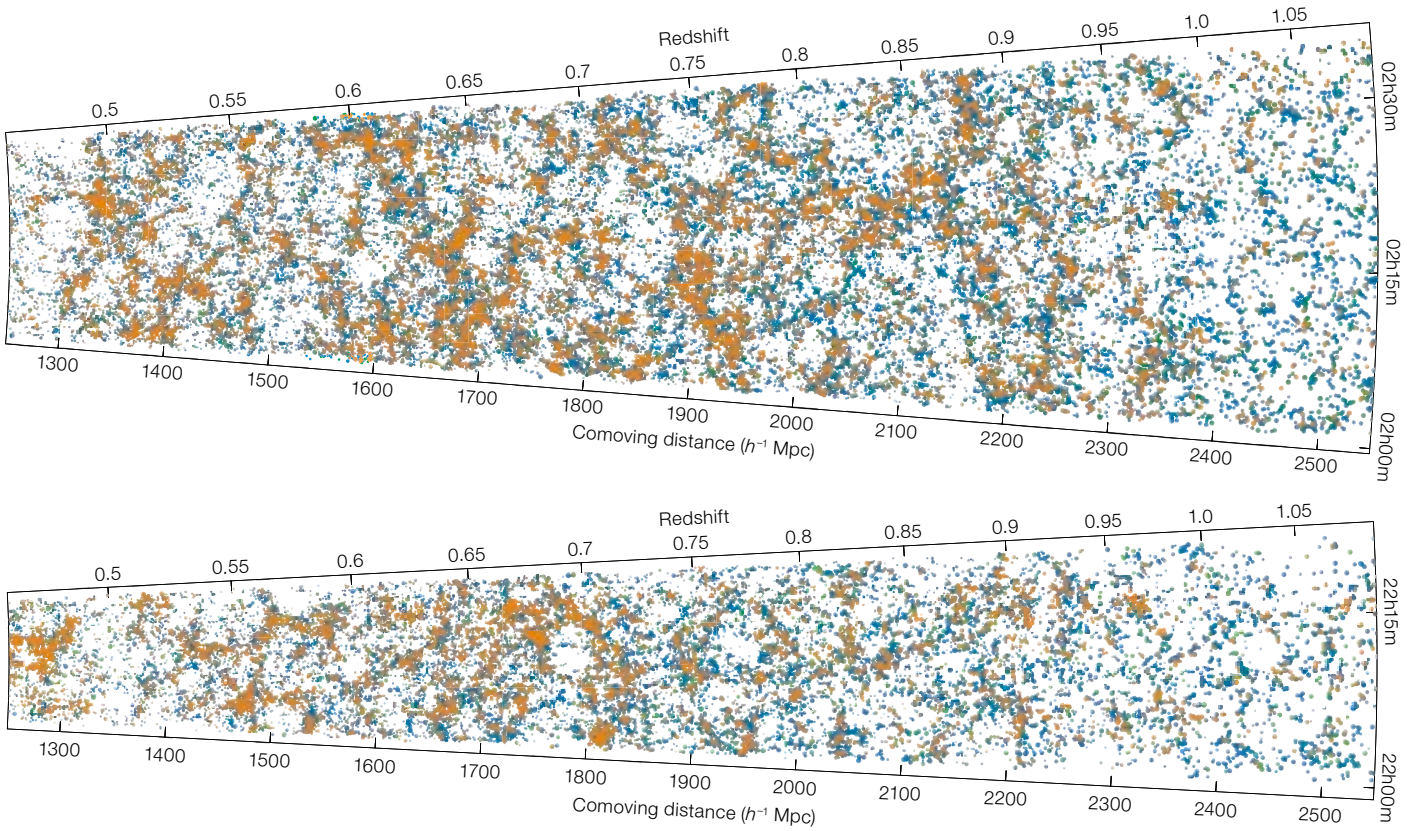

Figure 3. The detailed picture of the large-scale structure of the Universe at $0.45 < z < 1.1$, delivered by the VIPERS survey over the W1 and W4 CFHTLS fields (upper and lower, respectively). The opening angle corresponds to Right Ascension and the data are projected over ~2 degrees in declination. The size of each dot is proportional to the galaxy *B*-band luminosity and the dot colours reflect the intrinsic *U-B* colour of each galaxy. From Scodeggio et al. (2017).

colours of the galaxies, respectively, providing evidence of some of the unique information yielded by the VIPERS data. A first characterisation of such filamentary structure and its relation to galaxy properties is presented in Malavasi et al. (2017).

Straddling local surveys and Planck: a consistency test of the ΛCDM model

Figure 4 shows the estimate of the power spectrum of the galaxy distribution, $P(k)$, from four independent sub-samples of the VIPERS PDR-2 data over the redshift range $0.6 < z < 1.1$. At about half the Hubble time, this is the highest redshift where such a measure has been produced, straddling Planck and local measurements. This classic statistic contains information about the mean total density of matter in the Universe and the baryonic-to-dark matter fraction. The estimated posterior distribution of these quantities, obtained through a combined likelihood analysis of the four $P(k)$ estimates, is shown in Figure 5, compared to results from other surveys. Such a comparison provides an important test of the validity of the ΛCDM model. The position of the first acoustic peak measured by Planck constrains the combination $\Omega_M h^3$, while the galaxy power spectrum on large scales probes $\Omega_M h$. Therefore, although the error bars are currently large, the galaxy power spectrum measurements can help to resolve the tension between estimates of the Hubble constant made in the local Universe and at the last scattering surface.

Measuring the growth rate of structure with redshift-space distortions

Measurements of the growth rate of structure constitute a key observation to detect possible deviations from General Relativity (GR). A modification of the laws of gravity on large scales may represent an alternative to dark energy as an explanation of the apparent acceleration of cosmic expansion. Galaxy peculiar velocities that trace this growth manifest themselves by corrupting our redshift measurements: they add a Doppler component along the line of sight that distorts galaxy maps and the derived clustering measurements. Such redshift-space distortions (RSD: Kaiser, 1987; Peacock et al., 2001) produce a detectable anisotropy in the measured power spectrum, or its Fourier counterpart the two-point correlation function. This function can be estimated as a 2D map, $x(r_p,\pi)$, in which the distortion affects only the radial direction, i.e. the π axis, in Figure 6.

This figure shows a measurement based on the full VIPERS sample, which has been split into two redshift bins. The effect of RSD is evident in the flattening of $x(r_p,\pi)$ along the line of sight direction. This flattening is proportional to the growth rate of cosmic structure $f(z)$, which can be extracted through model fits and is characterised by gravity theory. In GR

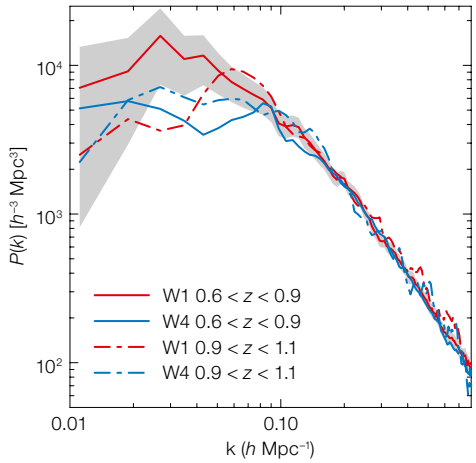

Figure 4. Estimates of the redshift-space power spectrum of the galaxy distribution $P(k)$ from four independent VIPERS subsamples (two redshift bins in each of W1 and W4 fields). A representative error corridor (shaded) is shown for one of the samples, and was obtained from the dispersion of a corresponding set of 150 mock catalogues. From Rota et al. (2017).

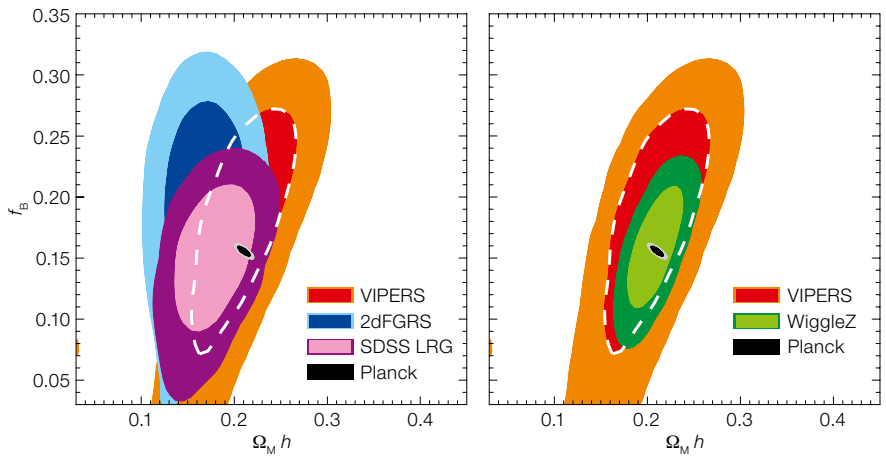

Figure 5. VIPERS constraints on the baryonic fraction f_B and the matter density parameter times the Hubble parameter $\Omega_M h$, obtained from a fit of a ΛCDM model with flat prior to the measured VIPERS power spectra. These are compared to similar measurements from other galaxy surveys and those from Planck observations. The left panel shows low-redshift constraints from the 2dFGRS at z = 0.2 and the SDSS LRG at z = 0.35. The right panel instead compares VIPERS to WiggleZ results at comparable redshift. See Rota et al. (2017) for details and references to the literature data.

we expect a growth rate $f(z) = [\Omega_M(z)]^{0.55}$. A more precise measurement of this quantity at z approaching unity was one of the original motivations for the VIPERS survey, following the early proof of concept from the VVDS-Wide data and its implications for the understanding of cosmic acceleration (Guzzo et al., 2008).

A first VIPERS estimate of the cosmic growth rate from RSD was obtained from the PDR-1 data (de la Torre et al., 2013).

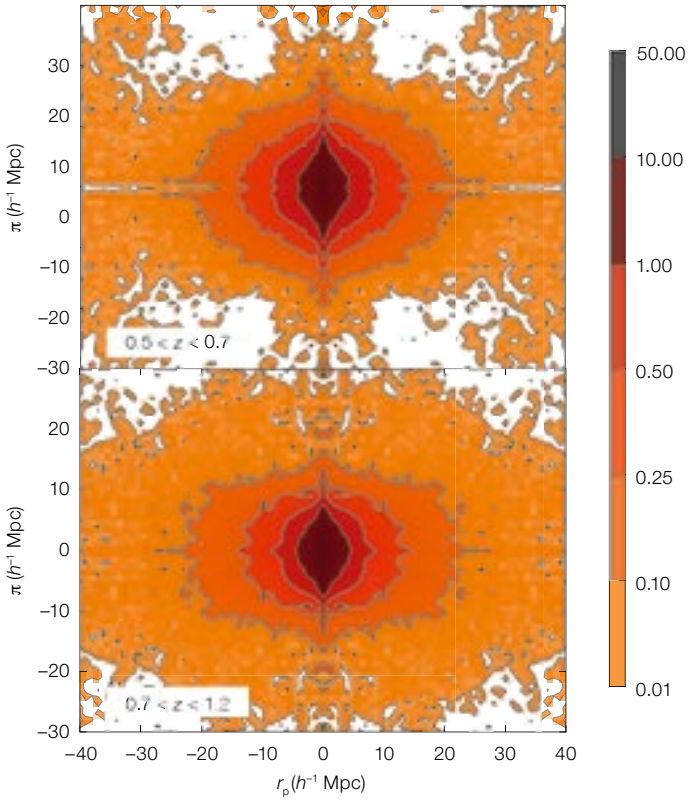

Figure 6. The redshift-space two-point correlation function $x(r_p,\pi)$ computed from the final VIPERS catalogue within two redshift bins, $0.5 < z < 0.7$ (upper) and $0.7 < z < 1.2$ (lower). The large-scale deviations from circular symmetry (i.e., oval shape) are the fingerprint of peculiar motions produced by the growth of cosmic structures. From de la Torre et al. (2017) and Pezzotta et al. (2017).

The richness of information and the broad selection function of VIPERS allow us to extend this result with the full data release by applying different estimation techniques to improve the systematics inherent in the analytic models (for example, de la Torre & Guzzo, 2012). Using the PDR-2 data, therefore, a series of RSD investigations using a variety of methods has been planned, some of which are still being completed. Pezzotta et al. (2017) present the measurement on the full sample with a focus on the required non-linear corrections and investigate in detail the systematic effects present in the VIPERS data.

In de la Torre et al. (2017), these investigations have been supplemented by measurements of galaxy-galaxy lensing performed on the parent photometric sample, the CFHTLS, allowing the growth rate of structure to be separated from the amplitude of matter fluctuations. While the RSD in the galaxy correlation function tell us how large-scale structures are collapsing, we are also looking at how the cosmic voids are expanding. A first catalogue of voids was built from PDR-1 (Micheletti et al., 2014) and then updated to PDR-2 in Hawken et al. (2017), where the void-galaxy cross-correlation has been fitted with a model to give a complementary measure of the growth of structure from the lowest density environments.

These different VIPERS estimates are shown in Figure 7, compared to similar measurements from the literature. The scatter in the different VIPERS values provides a direct indication of the level of systematic errors in the different techniques.

Two further RSD measurements using different galaxy tracers/techniques are in preparation. Both works aim at reducing the complex non-linear signal in the data, while keeping the modeling as simple as possible. The first shows that use of the luminous blue galaxies as tracers of RSD can sensibly reduce the impact of non-linearities (Mohammad et al., in preparation). In the second (Wilson et al., in preparation), the so-called "clipping" technique is used to linearise the density field before computing $P(k)$ and estimating redshift distortions.

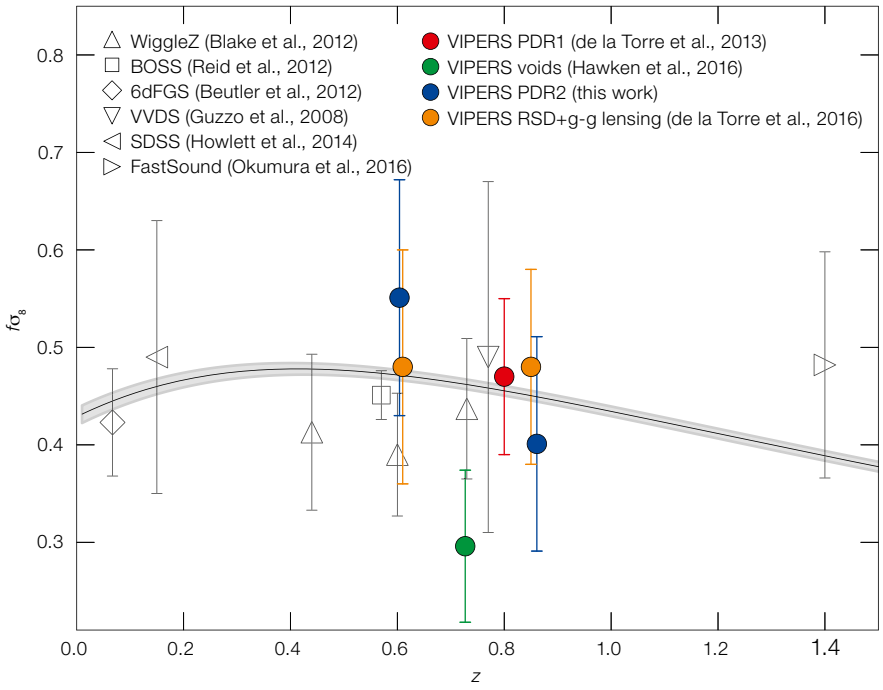

Figure 7. Published estimates of the growth rate of structure from redshift space distortions (RSD) in the VIPERS PDR-2 data, as summarised in Pezzotta et al. (2017). In addition to developing an improved modeling in this paper, RSD have been combined with galaxy-galaxy lensing (de la Torre et al. 2017) and also extracted in a completely independent way using galaxy outflows in cosmic voids (Hawken et al. 2017). These VIPERS measurements are compared to the earlier PDR-1 estimate and to a collection of similar results from the literature (see the journal paper for references). Two further analyses of RSD are currently in preparation (see text). The growth rate f is plotted in its conventional combination with the amplitude of clustering, $f\sigma_8$.

A detailed movie of galaxy transformations over the past 9 Gyr

The description of the physical properties of VIPERS galaxies is significantly enhanced by the availability of a series of ancillary photometric observations that complement the five high-quality bands of the CFHTLS. These include two ultraviolet bands (from the Galaxy Evolution Explorer [GALEX] satellite) and the near-infrared K-band (from the CFHT Wide-field InfraRed CAMera [WIRCAM]), which comprise the so-called VIPERS Multi-Lambda Survey (Moutard et al., 2016). These data are combined to perform reliable spectral energy distribution (SED) fits and, in turn, estimate luminosities, colours and stellar masses.

All these quantities, coupled to spectral information (like the amplitude of the 4000 Å break) and structural parameters from a morphological analysis (Krywult et al., 2017), have allowed us to look at the evolution of classic relationships observed at $z \sim 0$. In Haines et al. (2017), VIPERS and the SDSS have been combined to trace the evolution in redshift of the bimodality of galaxy properties, producing an unprecedentedly clear and coherent picture. This is visible in Figure 8 for the D4000 index, revealing the developing bimodality of galaxies into those whose optical light is still dominated by young stars (D4000 ~ 1.2; the blue cloud population) and the red sequence of old, passive galaxies (D4000 ~ 1.9). This figure shows the assembly of the red sequence, extending to ever lower masses, but also the decline of the blue cloud, its high-mass limit remarkably dropping by a factor of around 3 from $z \sim 1$ to today.

Important extra value has been added to VIPERS by the morphological analysis of the CFHTLS images, which allowed us to obtain reliable Sérsic indexes and effective radii for the majority of the objects in the catalogue (Krywult et al., 2017). Benefiting from this crucial information, in Gargiulo et al. (2017) we studied the evolution of the number density of massive ($> 10^{11}\ M_{\odot}$) passive galaxies (MPGs) and their stellar population ages, separating objects by surface stellar mass density. With an unprecedented sample of about 2000 such galaxies, VIPERS provides a novel picture of how the current population of massive red galaxies could have been formed (Figure 9). What emerges is that while compact objects in this class seem to be there from previous epochs and their number density does not change as a function of cosmic time, the less compact ones (left panel, green points) show instead a significant increase.

What is most interesting is that this observed increase quantitatively matches the parallel disappearance of star-forming objects within the same mass range, consistent with a scenario in which the least compact passive galaxies replace the massive star-forming ones, whose number density drops five-fold from $z = 1.0$ to $z = 0.5$, as shown in Figure 10 (from Haines et al., 2017). VIPERS provides statistically definitive evidence for the decline of this blue massive population between $z = 1$ and $z = 0.5$, consistent with the value measured at $z \sim 0$ from the SDSS. Comparison with the zCOSMOS-20K bright sample (Lilly et al. [2009] re-analysed by us in this work;

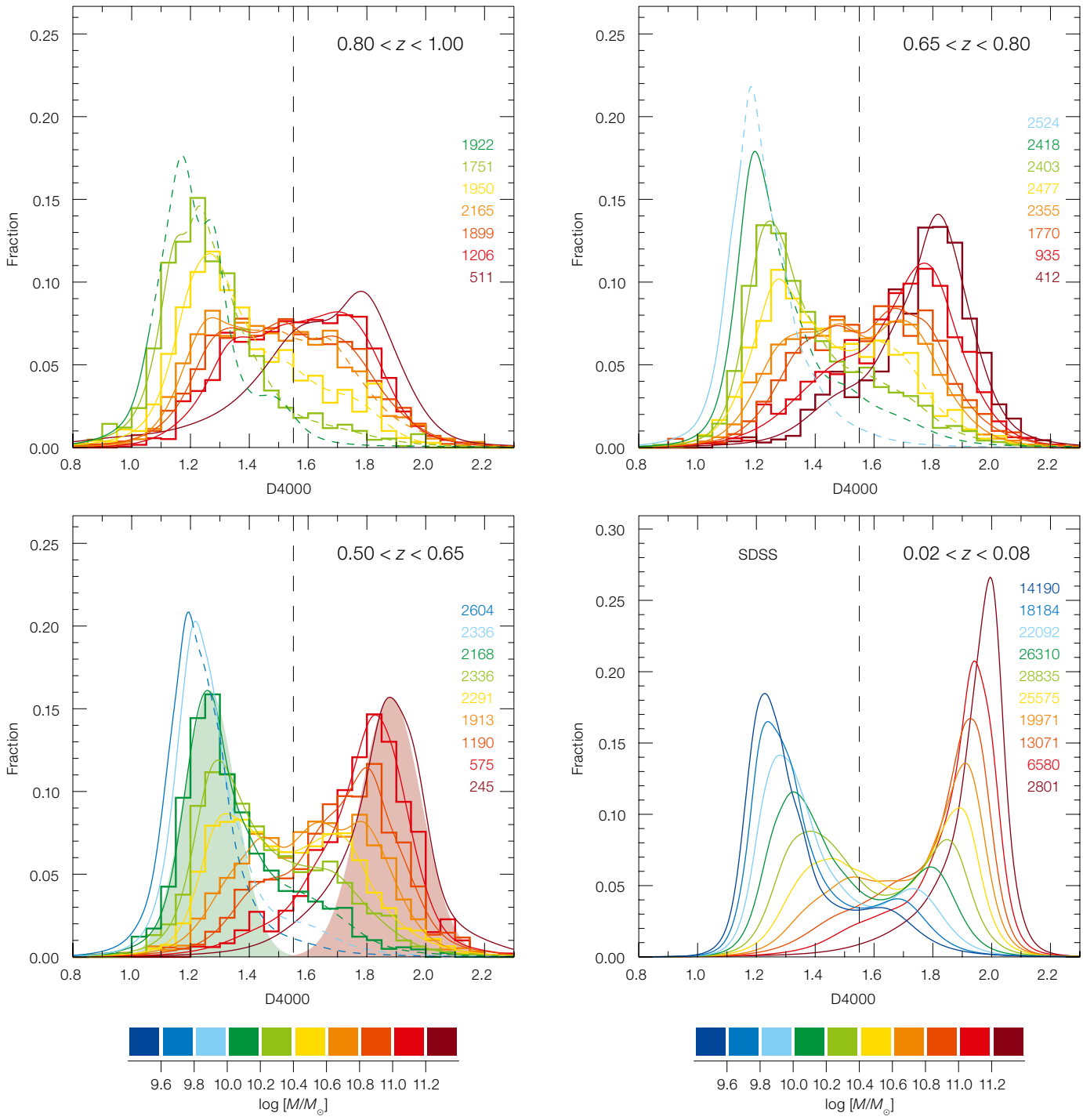

purple points) clearly demonstrates that the gain in our understanding of these rare, massive galaxies is due to the much larger volumes covered by VIPERS (Haines et al., 2017).

These works, together with the earlier studies of the colour-magnitude diagram (Fritz et al., 2014) and the stellar mass function (Davidzon et al., 2013), give a remarkably consistent picture of how galaxies migrate from the blue to the red sequences in the colour-magnitude diagram as a function of redshift. The measurements suggest that dry mergers are not the main mechanism to produce

Figure 8. The evolution from $z = 1$ of the bimodal distribution of the 4000 Å break amplitude (D4000), for galaxies in four redshift ranges with different stellar masses (see colour bar), as traced by combining VIPERS with the local SDSS DR7 data. The *y*-axis scale indicates the fraction of galaxies within bins of width 0.05 in D4000. The coloured numbers down the right-hand side indicate the number of galaxies in each stellar mass bin. From Haines et al. (2017) where further details can be found.

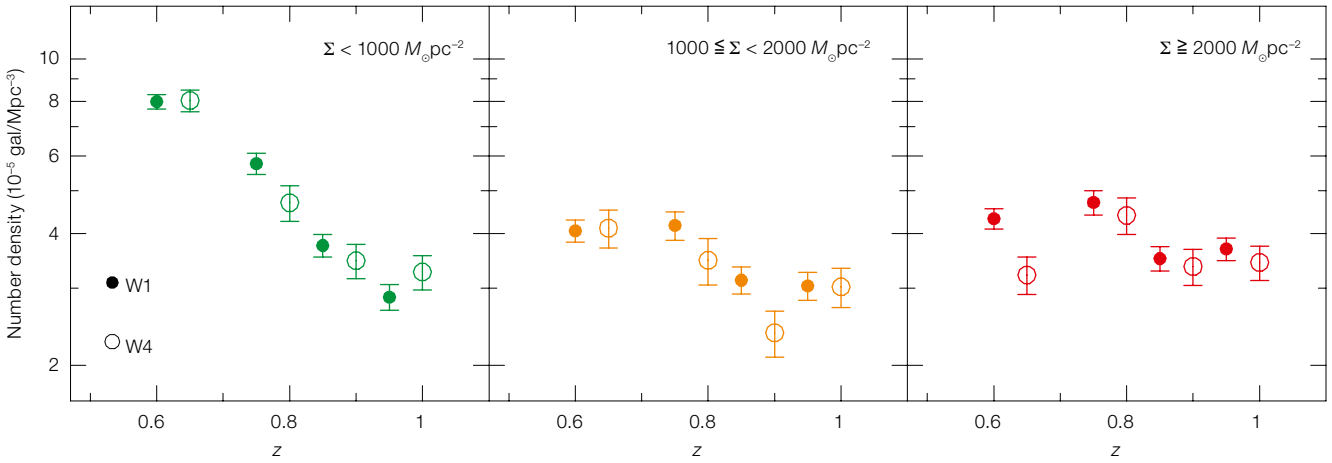

Figure 9. (Above) The evolution of the number density of massive ($M > 10^{11}\ M_\odot$) passive galaxies split into different classes of mass surface density. VIPERS shows that the abundance of the most compact of such galaxies (right panel) does not change with cosmic time, while the least compact of these objects do increase in number. The solid and open circles are for the W1 and W4 fields respectively, demonstrating the robustness of the observed trend, a consequence of the large survey volume, allowing samples of rare populations with unprecedented statistics. From Gargiulo et al. (2017).

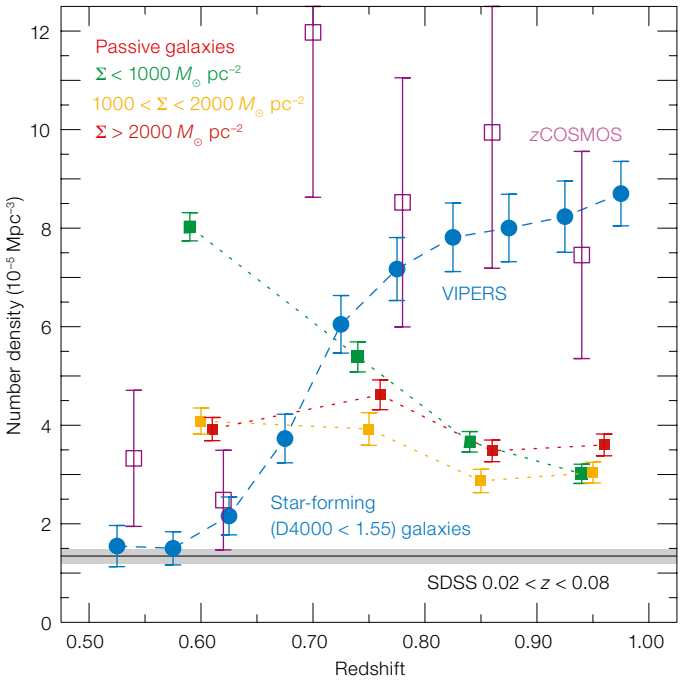

Figure 10. (Left) Same as Figure 9 but now for the evolution of the whole population of massive galaxies ($M_* > 10^{11}\ M_\odot$), including star-forming objects (blue points). These are compared to passive objects, again split as a function of mass surface density. The least compact passive galaxies appear to replace the massive star-forming ones, whose number density drops five-fold from $z = 1.0$ to $z = 0.5$; see text for details. From Haines et al. (2017).

the population of massive passive galaxies seen at low redshifts. This scenario is supplemented by a parallel study of the star formation history of massive galaxies (Siudek et al., 2016), while in another work in preparation we are trying to derive constraints on the quenching mechanism (Manzoni et al., in preparation). At the same time, the fraction of star-forming *vs.* passive galaxies is quantified as a function of local density (Cucciati et al., 2017), revealing that it is higher in low-density regions and for the most massive galaxies at redshift approaching unity.

Conclusions

Redshift surveys remain at the forefront of cosmological research in the 21st century. Huge cosmology-focused surveys, such as Euclid[3] and the Dark Energy Spectroscopic Instrument (DESI[4]), are being prepared with the goal of collecting tens of millions of redshifts in the distant Universe. Such projects will typically deliver low signal-to-noise (SNR) spectra with limited information, often targeting specific sub-populations of galaxies. This implies that complementary spectroscopic surveys with broader scope and selection functions will be necessary to assess to high statistical precision the evolution of the physical properties of the full population (see for example the report of the ESO Working Group on the Future of Multi-Object Spectroscopy, Ellis et al., 2017). These surveys will be similar in spirit to VIPERS, involving a detailed sampling of large-scale structure over large volumes to determine accurate information on galaxy properties, possibly enhanced by higher spectral resolution.

VIPERS has opened the way to such accurate statistical studies at $z > 0.5$, refining the scaling relationships that were only hinted at so far, owing to the limited size of deep samples, and enabling novel ways to look at the data, self-consistently modelling the galaxy properties and the underlying density field through a Bayesian approach (Granett et al., 2015). This is a necessary path, if the goal is to understand the full growth history of galaxies and the cosmic web they inhabit, providing the crucial link between the cosmological dark-matter skeleton and the objects we use to trace it.

Acknowledgements

We acknowledge the support of the ESO staff for all operations in Garching and at Paranal. We especially thank Michael Hilker and Marina Rejkuba for their constant help during several phases of the project.

References

Alam, S. et al. 2015, ApJS, 219, 12
de la Torre, S. & Guzzo, L. 2012, MNRAS, 427, 327
de la Torre, S. & VIPERS Team 2013, A&A, 557, 54
de la Torre, S. & VIPERS Team 2017, A&A, submitted, arXiv:1612.05647
Colless, M. et al. 2001, MNRAS, 328, 1039
Cucciati, O. & VIPERS Team 2017, in press, arXiv:1611.07049
Davidzon, I. & VIPERS Team 2013, A&A, 558, 23
Eisenstein, D. et al. 2011, AJ, 142, 72
Ellis, R. S. et al. 2017, arXiv:1701.01976
Fritz, A. & VIPERS Team 2014, A&A, 563, 92
Gargiulo, A. & VIPERS Team 2017, A&A, in press, arXiv:1611.07047
Garilli, B. et al. 2012, PASP, 124, 1232
Garilli, B. et al. 2014, A&A, 562, 23
Granett, B. R. & VIPERS Team 2015, A&A, 583, 61
Guzzo, L. et al. 2008, Nature, 451, 541
Guzzo, L. & VIPERS Team 2013, The Messenger, 151, 41
Guzzo, L. & VIPERS Team 2014, A&A, 566, 108
Hawken, A. & VIPERS Team 2017, A&A, in press, arXiv:1611.07046
Haines, C. P. & VIPERS Team 2017, A&A, in press, arXiv:1611.07050
Kaiser, N. 1987, MNRAS, 227, 1
Krywult, J. & VIPERS Team 2017, A&A, 598, 120
Le Fèvre, O. et al. 2005, A&A, 439, 845
Lilly, S. J. et al. 2009, ApJS, 184, 218
Malavasi, N. & VIPERS Team 2017, MNRAS, 465, 3817
Micheletti, D. & VIPERS Team 2014, A&A, 570, 106
Moutard, T. & VIPERS Team 2016, A&A, 590, 102
Peacock, J. A. et al. 2001, Nature, 410, 169
Pezzotta, A. & VIPERS Team 2017, A&A, in press, arXiv:1612.05645
Planck Collaboration 2016, A&A, 594, 1
Rota, S. & VIPERS Team 2017, A&A, in press, arXiv:1612.05644
Scodeggio, M. & VIPERS Team 2017, A&A, in press, arXiv:1612.05648
Siudek, M. & VIPERS Team 2017, A&A, 597, 107
York, D. et al. 2000, AJ, 120, 1579

Links

[1] CFHTLS: http://www.cfht.hawaii.edu/Science/CFHLS
[2] VIPERS web site: http://vipers.inaf.it
[3] Euclid satellite mission: http://sci.esa.int/euclid/
[4] DESI: http://desi.lbl.gov/

ESO/CFHT

A small region (42 × 41 arcminutes) of the Canada France Hawaii Telescope Legacy Survey W1 field, which was covered by VIPERS, centred at 2 h 27 m, –4° 24′, in a *u*-, *r*- and *z*-band colour composite. See Release eso1212.

Upper: The signature of the contract with SCHOTT for the ELT primary mirror segment blanks took place at ESO Headquarters on 30 May 2017.

Lower: And the contract signing with Safran Reosc for production of the ELT primary mirror segments on the same day. See Release eso1717 for details.

DOI: 10.18727/0722-6691/5026

Report on the Workshops

VLTI Community Days VLTI Winter School

held at ESO Headquarters, Garching, Germany, 6–10 March 2017

Antoine Merand[1]

[1] ESO

The infrastructure of the Very Large Telescope Interferometer (VLTI) is in the process of being upgraded and second-generation interferometric instruments are entering service (GRAVITY) or under construction (MATISSE). The VLTI Community Days presented these developments and began a discussion with the community on the future of the VLTI. Prior to the VLTI Community Days, a short Winter School was held to introduce early stage researchers to VLTI observation and data reduction.

VLTI Community Days

There have been two previous VLTI Community meetings — one at the European Week of Astronomy and Space Science (EWASS) in 2015 in La Laguna in Tenerife ("VLTI Community Day") and one combined with a PIONIER community meeting in 2014 in Grenoble. This meeting in Garching attracted nearly 60 members of the VLTI community, including ESO personnel. On the first day of the meeting, speakers from ESO updated the community on the status of the VLTI following the upgrades to the VLTI infrastructure over recent years (see ESO 2015 Annual Report[1]), as well as the forthcoming ones. The early results from the first of the second-generation VLTI instruments, GRAVITY, were presented by Frank Eisenhauer from the Max-Planck-Institut für extraterrestrische Physik (MPE), the Principal Investigator of the instrument. In particular, the community was impressed by the observations of the Galactic Centre[2]. Results with the first generation VLTI instruments, the MID-infrared Interferometric instrument (MIDI) and the Precision Integrated Optics Near-infrared Imaging ExpeRiment (PIONIER) were also presented. The status of the Multi Aper-Ture mid-Infrared SpectroScopic Experiment (MATISSE), the second-generation instrument still under construction and due for commissioning in 2018, was also presented.

The second day of the meeting was dedicated to the forthcoming evolution of VLTI operations, as well as the result of prospective exercises by ESO (the VLTI Roadmap, which was presented to the 89th Scientific Technical Committee [STC] in April 2017), and the report from the working group of the European Interferometry Initiative entitled "The future of interferometry"[3].

The last day of the meeting provided the opportunity for the community to present ideas and science cases for future instruments. Two projects were presented: the first was for an *L*-band high-contrast interferometric instrument, aimed at studying planet formation around young stars and, ultimately, the planets themselves. The second was for a visible high-spectral-resolution instrument, which would boost VLTI angular resolution, allowing exquisite images of stellar surfaces.

VLTI Winter School

The school, held from 6 to 8 March 2017, just prior to the VLTI Community Days, attracted about 15 participants, ranging from masters students to postdocs. The four half-day sessions aimed specifically at providing the necessary knowledge to apply for time with the latest VLTI instrument GRAVITY. The programme included an introduction to interferometry, observation preparation, and GRAVITY data reduction, as well as general interferometry data reduction and image reconstruction. The classes and practical sessions were given by members of the User Support Department and Paranal Science Operations, as well as participation from VLTI community experts.

Details of the programmes of both the Community Days and the Winter School, together with links to some of the presentations, are on the workshop webpage[4].

Links

[1] ESO Annual Report 2015: https://www.eso.org/public/products/annualreports/ar_2015/
[2] GRAVITY observations of the Galactic Centre: https://arxiv.org/abs/1705.02345
3 European Interferometry Initiative: http://www.european-interferometry.eu/working-groups/the-future-of-interferometry-in-europe
[4] Workshop webpage: http://www.eso.org/sci/meetings/2017/VLTI-2017.html

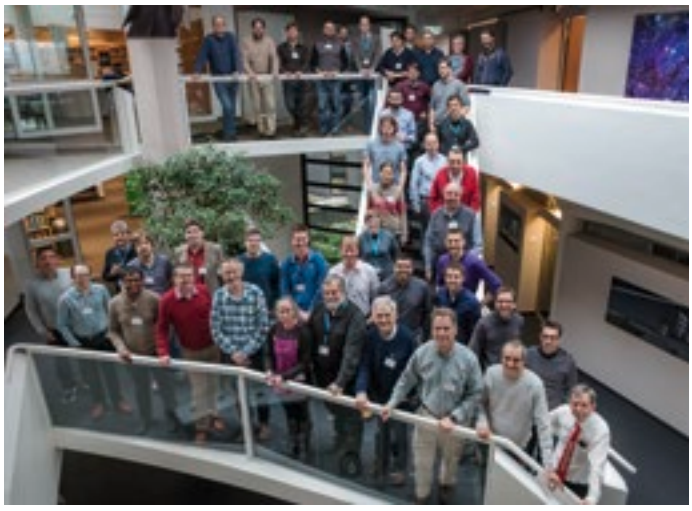

Figure 1. (Left) The participants at the VLTI Community Days pose in the entrance hall at ESO Headquarters.

Figure 2. (Above) All the participants at the VLTI Winter School, both students and lecturers together, in the Headquarters lobby.

DOI: 10.18727/0722-6691/5027

Report on the Workshop

Stellar Populations in Stellar Clusters and Dwarf Galaxies — New Astronomical and Astrophysical Challenges

held at ESO Vitacura, Santiago, Chile, 2–3 March 2017

Bruno Dias[1]
Ivo Saviane[1]

[1] ESO

Chile hosts many world-leading expert groups working on stellar populations and stellar clusters. This field has undergone something of a revolution during the last decade with the advent of large photometric and spectroscopic surveys, and preparations for relevant new facilities are underway. A Chilean meeting on stellar populations and star clusters was therefore timely. The goal was to bring together experts in the field for discussion and to encourage collaboration. The workshop was open to all astronomers and advanced students, especially those in Chilean institutes, limited to a maximum of 50 participants in order to foster discussion.

A significant fraction of the Chilean astronomical community is involved in the investigation of stellar populations in star clusters and dwarf galaxies, and in the last few years this research field has witnessed many developments. So in late 2016 we felt there was a need to discuss the new results in a national meeting, which took place in March this year.

Particular topics we wanted to discuss were, for example: the high-precision photometric and spectroscopic observations revealing multiple stellar generations in young and old Galactic and extragalactic massive clusters; the large surveys that are amassing impressive datasets on the Milky Way and Local Group galaxies (such as VISTA Variables in the *Via Lactea* [VVV[1]], Gaia-ESO[2], the Sloan Digital Sky Survey [SDSS], the Apache Point Observatory Galactic Evolution Experiment [APOGEE[3]], the GlObular clusTer Homogeneous Abundance Measurements survey [GOTHAM], etc.); and the associated theoretical efforts that are attempting to make sense of all this information. Observers and theoreticians are together trying to solve the puzzle of how star clusters form and evolve, and how this is connected with the history of their host galaxy.

Key questions that we wanted to address during the two days of the conference were: Are massive young clusters the prototypes of future globular clusters? What is missing in stellar evolution models, in particular concerning evolved stars, such as those in the asymptotic giant branch (AGB) and horizontal branch (HB) phases? What is the relationship between stars in clusters and dwarf galaxies, and stars in the Galactic halo and bulge? What are the fractions of Galactic clusters formed in situ and those that formed in dwarf galaxies captured by the Milky Way? What are the differences and similarities between star clusters in the Milky Way and Local Group galaxies? How can star clusters be used as tracers of the chemical and dynamical evolution history of their host galaxy? What is the best complement of instruments that is needed to answer these questions?

In order to promote focused discussions, the workshop was divided into five sessions: The Milky Way; The Magellanic Clouds; Dynamics and models; Extragalactic stellar populations; and a special session dedicated to the VVV survey. Each session was followed by a half-hour discussion where everyone had the opportunity to express their opinions and make plans for collaborations on topics triggered by the chair. The full programme can be found on the workshop webpage[4].

Some highlights from the various sessions are presented.

The Milky Way

Two sub-sessions were dedicated to this vast topic. We started with an invited talk by Patricia Tissera who discussed the chemical evolution of Milky Way-type galaxies. The results from the simulations show that the outer halo was mostly accreted, while the inner halo has a mix of histories (see for example, Scannapieco et al., 2011). The Disc was formed more recently and the Bulge was mostly formed *in situ* with a fraction accreted at high redshift. These stars contribute to the spheroidal, dispersion-dominated component while most of the stars formed *in situ* make up the bar structure. Patricia showed that a good way to disentangle populations formed *in situ* from those that have been accreted is to look at the [α/Fe] vs. [Fe/H] plot, thanks to its sensitivity to star formation efficiency (Tissera et al., in prep.).

This review was followed by a series of talks on multiple populations in globular and open clusters. The applicability of the sodium-oxygen anticorrelation as a default characteristic of Milky Way globular clusters was explored (see review by Gratton et al., 2012). Some young

Figure 1. The workshop participants, mostly from all regions in Chile with others from Argentina, Australia and Spain, photographed in the ESO Vitacura garden.

massive clusters (for example, Geisler et al., 2012; Schultheis et al., in prep.), and extragalactic clusters (Niederhofer et al., 2017; Salgado et al., in prep.) also show the anticorrelation. Dynamics and black holes were then discussed for the case of ω Centauri. To better understand the origin of multiple stellar populations, the search is on for special cases with a single stellar population. Different surveys of Milky Way populations were presented: APOGEE, GOTHAM, Gaia-ESO for spectroscopy, and Hubble Space Telescope (HST) for photometry of Bulge clusters. In particular, the GOTHAM survey has defined a new metallicity scale for Milky Way globular clusters (Dias et al., 2016a, b) and has established a non-linear calibration for Ca II triplet strength with metallicity (Vasquez et al., in prep.), essentially confirming the results of Saviane et al. (2012).

The Magellanic Clouds

The invited talk by Celeste Parisi reviewed the chemical evolution of the Magellanic Clouds. Recent studies argue in favour of a first close passage of the Clouds into the Milky Way neighbourhood, which contrasts with the classical scenario in which the Clouds are orbiting the Milky Way (for example, Besla et al., 2007; Diaz & Bekki, 2011). It is possible that the Clouds are the largest members of a group of dwarf galaxies that came into the Milky Way halo at late times. The peculiar metallicity gradients in the Clouds inspired discussion. This invited talk was followed by one on the VIsible photometric survey on SOAR star Clusters from tApii Coxi HuguA (VISCACHA) and the first results on the Small Magellanic Cloud (SMC). This survey reveals four components of star clusters, three of them related to the tidal history. All external regions present peculiar age and metallicity gradients, and each component seems to have a specific age-metallicity relation (Dias et al., 2016c).

The star formation region of 30 Doradus was discussed in the light of the findings of sequential star formation during the last two million years. The case of light element abundance variations in globular clusters was discussed with respect to Magellanic Cloud clusters, in particular for CN, CH and Na abundances (Salgado et al., in prep.). Finally, a different point of view was presented for the abundance spread in the subgiant branch, which is usually thought to explain the photometric evidence of multiple populations in clusters. The claim is that stellar variability plays an important role in this regard and the presence of multiple populations is only one of the possible interpretations (Salinas et al., 2016).

Dynamics and models

This was a short and intense session led by the invited speaker Michael Fellhauer, who stated that there is no accepted model for globular cluster formation. Models which focus on dynamics cannot explain the observations concerning the chemistry of stellar populations, as discussed above, but they certainly constrain the relation between globular clusters and dwarf galaxies, for example. He also discussed the formation of ultra-compact dwarf (UCD) galaxies, which either originated as threshed nucleated dwarfs after getting rid of dark matter (Bekki et al., 2001) or are merger products from intense starbursts forming many star clusters in a small confined area (Fellhauer & Kroupa, 2002). Dwarf spheroidal (dSph) galaxies could have formed from tidally disrupted discs, either through interactions with a major galaxy (ram-pressure and tidal stripping) or through dwarf-dwarf interactions (resonant stripping), or in isolation through merging and dissolution of star clusters inside a dark matter halo. In the first two formation scenarios, the basic building blocks in the Universe are dwarf discs, while in the last they are in fact the dSph galaxies.

There was also a talk on young stellar cluster formation and one on the possibility that gas filaments eject protostars. The effect of binaries was also addressed.

VVV

Dante Minniti discussed globular clusters in the VVV survey using data from the past six years, and announced the extension of the survey for the next few years, the VVVX ESO Public Survey (see Arnaboldi et al. p. 15). There could be thousands of young clusters and up to 100 globular clusters hidden in the infrared imaging data (Ivanov et al., 2017). Challenging Bulge clusters were analysed in a following talk, the conclusion of which was that dust must be studied in different environments. Another talk on young star clusters showed evidence of 120 $M_{\odot}$ stars in small clusters. There were also two talks on the characterisation of variable sources from within the survey.

Extragalactic populations

The last session of the two days covered globular cluster systems in other galaxies and the Milky Way neighbourhood. The first topic was addressed in the invited review by Thomas Puzia. He came back to the formation of globular clusters, offering at least three channels: *in situ* via mergers; as a leftover from stripped dwarfs; or formed in primordial dark matter halos. He showed evidence that most globular clusters are found in luminous and low-metallicity galaxies (see review by Brodie & Strader, 2006).

Galactic neighbours are increasing in number, as more than 40 new dwarfs and 20 globular clusters were discovered in the past few years (see, for example, Bechtol et al., 2015; Koposov et al., 2015). More tidal streams around globular clusters have been characterised, supporting the disruption scenario for dwarf galaxies and globular clusters in the Milky Way halo. Moreover, the effect of different star formation histories on the mass-to-light ratio was discussed. This effect directly impacts on the stellar mass estimation of dwarf galaxies.

Take-home messages

From two intense days of discussions with 50 participants, we can safely say that the meeting was rather successful, thanks to a few key factors:
– We chose a topic which is very popular among the Chilean community (and beyond);
– The short, two-day span focused the talks and discussions;

– The chairs did an excellent job of moderating the discussions and launching interesting themes at the end of each session.

While it is not possible to convey here the full range of the discussions, a few main topics emerged during the workshop:

1. Many new results about multiple stellar populations in globular clusters were presented, but there is no theoretical model that can explain all the evidence. This is in no small part due to the sheer computational power that is required to simulate physical processes from the stellar to the galactic scale, and over long time scales;
2. Spectroscopic tagging of stellar populations is becoming one of the key tools to uncover the past evolution of the Milky Way and its sub-components;
3. More and more, the spectroscopic data are delivered by large surveys (such as, VVV(X), APOGEE, Gaia-ESO, GOTHAM, etc.);
4. Surveys are revealing that we lack basic data for many Galactic components, even after decades of research efforts (such as for globular clusters). Perhaps hundreds of young clusters and globular clusters are hidden in the highly extincted regions of the Milky Way;
5. Variable stars are a powerful tool to find those hidden clusters and other structures, so many results can be expected as the detection and characterisation of variables progresses;
6. The accumulation of large spectroscopic datasets is both a blessing and a challenge for the simulations of galaxy evolution that need to reproduce them;
7. Nevertheless, simulations of Milky Way-type galaxies are reaching significant maturity, and we can expect an ever-improving match to observations in the near future;
8. Both known Milky Way streams, and the search for new ones with wide-field imaging surveys, were discussed. In agreement with recent observational results, simulations predict that outer galactic halos are mostly formed by accretion;
9. Photometric and spectroscopic surveys are helping to disentangle the complex evolution history of the Magellanic Clouds. Stellar populations from external regions (star clusters in particular) are useful tools to characterise the tidal interaction history of both galaxies.

Acknowledgements

We thank the ESO Office for Science in Chile for allowing us to host the conference at the ESO premises, and we are grateful to the local organising committee (Paulina Jirón, María Eugenia Gómez, and César Muñoz) for ensuring that all practical issues were smoothly managed behind the scenes. We are also thankful to the scientific organising committee members (Javier Alonso-García, Jura Borissova, Márcio Catelan, Doug Geisler, Steffen Mieske, Dante Minniti, Christian Moni-Bidin and Ricardo Muñoz) for stimulating a good scientific environment for discussions and collaboration. Last but not least, financial support from ESO, El Instituto Milenio de Astrofísica (MAS) and the Center for Excellence in Astrophysics and associated Technologies (CATA) is warmly acknowledged.

References

Bechtol, K. et al. 2015, ApJ, 807, 50
Bekki, K., Couch, W. J. & Drinkwater, M. J. 2001, ApJL, 552, 105
Besla, G. et al. 2007, ApJ, 668, 949
Brodie, J. P. & Strader, J. 2006, ARA&A, 44, 193
Dias, B. et al. 2016a, A&A, 590, 9
Dias, B. et al. 2016b, The Messenger, 165, 19
Dias, B. et al. 2016c, A&A, 591, 11
Diaz, J. & Bekki, K. 2011, MNRAS, 413, 2015
Fellhauer, M. & Kroupa, P. 2002, MNRAS, 330, 642
Geisler, D. et al. 2012, ApJL, 756, 40
Gratton, R. G., Carretta, E. & Bragaglia, A. 2012, A&ARv, 20, 50
Ivanov, V. D. et al. 2017, A&A, 600, 112
Koposov, S. E. et al. 2015, ApJ, 805, 130
Niederhofer, F. et al. 2017, MNRAS, 465, 4159
Salinas, R. et al. 2016, ApJL, 832, 14
Saviane, I. et al. 2012, A&A, 540, 27
Scannapieco, C. et al. 2011, MNRAS, 417, 154

Links

[1] Variables in the *Via Lactea* survey: https://vvvsurvey.org/
[2] Gaia-ESO survey: https://www.gaia-eso.eu/
[3] SDSS APOGEE survey: http://www.sdss3.org/surveys/apogee.php
[4] Workshop web pages: http://www.eso.org/CG2017

Engineering and Technical Research Fellowship Programme

Research and development is at the core of ESO's activities. Following the framework of the prestigious science Fellowship Programme, ESO is opening an engineering and technical research fellowship programme. Post-doctoral fellowships will be awarded to outstanding early-career young researchers in an engineering or technical discipline to begin in 2018. They will share their time between one of the ESO-defined projects and a personal research topic.
Full details and the call for candidates will be issued in July on the ESO Recruitment page (https://recruitment.eso.org/).

Inside one of the ESO laser labs.

DOI: 10.18727/0722-6691/5028

In Memoriam Giovanni Bignami

Tim de Zeeuw[1]
Roberto Gilmozzi[1]

[1] ESO

Giovanni Bignami, still very active at age 73 and a member of ESO Council from 2013 to 2015, has sadly passed away. He chaired the Tripartite Group, served on Council's Strategy Working Group, and was instrumental in convincing the Italian government to participate in ESO's Extremely Large Telescope (ELT) programme.

Giovanni (Nanni to everyone who knew him) graduated from the University of Milan and started work on detection of cosmic gamma-ray sources. From 1988 to 1997 he was Principal Investigator of the X-ray Multi-Mirror Mission (XMM-Newton) and a professor at the University of Pavia. He directed the Centre d'Etude Spatiale des Rayonnements in Toulouse (2003–2006). He chaired ESA's Space Science Advisory Committee and in this role was the main architect of *Cosmic Vision 2015–2025* which laid out the ambitious series of missions that ESA is currently implementing. Nanni was scientific director of the Italian Space Agency from 2007 to 2008 and served as its president from 2010 to 2012. In the same period he was the first Italian president of the Committee on Space Research (COSPAR). From 2011 to 2015 he was president of the National Institute of Astrophysics (INAF). At the time of his death Nanni was chair of the Board of the Square Kilometer Array (SKA) and vice chair of the Scientific and Technical Committee of the Cherenkov Telescope Array (CTA).

Nanni was well known for the discovery of Geminga. This peculiar object was first detected as a gamma ray source in the constellation of Gemini by the NASA Second Small Astronomy Satellite (SAS-2), hence its nickname as the Gemini gamma ray source (with an additional meaning in Milanese dialect for 'not there', alluding to the difficulty of its identification) and later confirmed, although not localised to better than a few degrees, by the COS-B satellite. It was detected by the Einstein satellite (as 1E 0630+178; Bignami et al. 1983) and then found to be X-ray bright, optically faint and with very weak radio emission: this demonstrated that it is an isolated neutron star which is relatively close to the Sun and hence has a large proper motion (178 mas yr^{-1}). Nanni continued to study Geminga in collaboration with his wife, Patrizia Caraveo, and together they contributed an authoritative review (Bignami & Caraveo, 1996)

Nanni was an enthusiastic and avid promoter of science and its role in our culture, with many appearances on television and articles in newspapers. He authored popular books on science (e.g., Bignami, 2012; 2014) and was a strong promoter of the exploration of the Solar System (Bignami & Sommariva, 2013), convinced that man would walk on Mars

Cirone-Musi

within our lifetime. He was awarded many honours and prizes, and asteroid 6852 was named after him ("Nannibignami").

Nanni's energetic and proactive approach to anything he turned his attention to was a shining example for all he worked with.

References

Bignami, G. F. et al. 1983, ApJ, 272, L9
Bignami, G. F. & Caraveo, P. A. 1996, ARAA, 34, 331
Bignami, G. F. 2012, *We are the Martians: Connecting Cosmology with Biology*, (Milan: Springer Verlag Italia Srl)
Bignami, G. F. & Sommariva, A. 2013, *A Scenario for Interstellar Exploration and Its Financing*, Springer Briefs in Space Development, (Milan: Springer Verlag Italia Srl)
Bignami, G. F. 2014, *Imminent Science: What Remains to be Discovered*, (Milan: Springer Verlag Italia Srl)

ESO/Juan Pablo Astorga

Giovanni Bignami (fourth from the right) at Paranal, during the visit by the Italian Prime Minister Matteo Renzi (third from the right) in October 2015.

DOI: 10.18727/0722-6691/5029

Fellows at ESO

Gergö Popping

Growing up in Groningen, the Netherlands, I was mostly passionate about classical ballet. Like many I enjoyed looking at the night sky, but never really saw myself pursuing a career as an astronomer. I imagined myself performing in theatres all over the world, becoming a star in dance, not studying them. It was only during the last year of high school that I realised a career in dance would also mean missing out on the intellectual challenge that mathematics and physics offered me. So I changed my plan and enrolled as a student in physics and astronomy at the University of Groningen. I had become acquainted with astronomy as a science through my family and thought it would be an interesting topic to study for me as well.

During my third year of university we went on an observing run with the Isaac Newton Telescope on La Palma as a part of the observational astronomy course. I observed the Hα emission line in two barred spirals (NGC 1530 and NGC 2903, the latter still being my favourite galaxy to date). The dark night sky was magical and it was during this run that, for the first time, it struck me how much fun a career in astronomy could actually be. Back in Groningen I used the observations for my first real science project, a multi-wavelength study of star formation within the bars of spiral galaxies.

By the end of my studies I applied for a PhD position within my home university and was lucky enough to get it. The project I applied for was supposed to be a little bit of theory with a lot of interferometric observational work, but it ended up being a lot of theory with no observational work at all. I developed galaxy formation models for the HI and H_2 content and the sub-mm line emission of galaxies. These models are geared towards the newest generation of interferometric observatories such as the Atacama Large Millimeter/submillimeter Array (ALMA) and the Square Kilometre Array (SKA) and its pathfinders. Galaxy formation theory was a completely new field for me, but one with a lot of exciting challenges and a field that I truly enjoy. The practical approach — I have an idea, I implement it in my model, I see what the result is — suits me well.

Joining ESO as a theorist may seem a little bit odd, but actually made a lot of sense. I felt that, after spending four years in the theory world, it would be wise to understand a bit more about the observational side of astronomy. On the more practical side, I had ALMA data sitting on a hard drive and had no clue what to do with it. Within ESO I mostly continued working on theory. Focusing more on sub-mm emission lines, but also changing fields towards the formation and destruction of dust in galaxies and dust absorption. ESO has been an ideal place to receive observational input for my own work, but also for me to provide theoretical insights for the observational projects of colleagues. Through my functional work in the ALMA Regional Centre (ARC), I have also learned what to do with the ALMA data sitting on my hard drive. I recently finished my first PI observational ALMA paper to study the gas properties of compact star-forming galaxies in the early Universe, something I could not have done without my experiences in the ARC.

Spending time at ESO to learn new things, like how observations are carried out, how different types of instruments at the La Silla Paranal enable different kinds of science, what the wide capabilities of ALMA and the Atacama Pathfinder EXplorer (APEX) are, how surveys are designed and how data handling works, have all provided me with the understanding I was hoping for when I started as a Fellow. Multiple surgeries in the Calama hospital because of appendicitis during an ALMA observing run gave me a memorably different look at what the life of an observational astronomer can be like. Recovering for two weeks in the Santiago guest house and being approached every day by different ESO colleagues saying “Oh, you are the appendicitis guy!” and “Oouw, Calama, that’s rough...”, will strangely enough always be one of my fondest memories of my time at ESO.

I will soon move on to a new position in Heidelberg with new adventures, challenges, and opportunities. I am still not always sure if choosing a career in astronomy over ballet was the right decision, but my time in astronomy has been great so far. The three years at ESO have been a scientific and social highlight with tremendous opportunities to develop as a scientist within an incredibly friendly and fun environment. Thank you all for enabling that!

Adriano Agnello

When I was four, my mum took me with her to the school where she was teaching. As she was demonstrating an experiment, heating samples of sugar into charcoal, I was amazed by this kind of magic that anyone could understand and that my mum would master so confidently (and explain so patiently). So I decided that I would be a scientist one day.

Encouraging my curiosity was easy for my parents, thanks to their scientific education, and I had the luck of attending nearby State schools with excellent teachers. There is a peculiar atmosphere where I grew up; about half of my science and maths teachers were women (a common occurrence in Italy), and half of the girls in my hometown would pursue STEM studies (science, technology, engineering and mathematics), but on the other hand volleyball or ballet were "girly things" that males were not supposed to do. Things changed somewhat when I moved to Pisa to attend University, in a town mostly populated by students and academics.

Adriano Agnello (on the left).

Despite my early enthusiasm, the path to science was not immediate. While at high-school, I often changed my mind, deciding that I would be an architect, a choreographer, an interpreter, ... before settling on physics, then astrophysics for my Masters, with a short hiatus when I briefly considered changing to mathematics. Still at "Scuola Normale", in my University years, I used to spend most of my spare time with my colleagues in the Humanities. The PhD itself was a bit of a drift: I started with paper-and-pen Bogoliubov–Born–Green–Kirkwood–Yvon (BBGKY) hierarchy computations, then did some dynamical modeling of discrete tracers in Milky Way dwarf spheroidals and nearby ellipticals, then changed to strong lensing. This happened also thanks to my supervisor, who wisely avoided giving me a single project that would stick with me for my whole career. In my first postdoc, while mining large databases to discover "new" lensed quasars, I was often sent observing at Keck, which spurred new interest in how telescopes and observatories work.

After Keck, the Nordic Optical Telescope (NOT), Paranal and La Silla, telescopes are strangely becoming a familiar environment, something I would have not foreseen a few years ago. On account of my job and age, I am used to moving to a new place every two or three years, crossing borders and oceans, so in this constant feeling of uncertainty, telescopes instill a sense of return to a "home away from home". La Silla, in particular, has gained a special place in my heart. Talking with other astronomers, I discovered that many of them share my love for its intimate atmosphere, the variety of telescopes all within a short walk, and the quiet days and nights (observing with music!) in the middle of some beautiful nature. Walking among its many domes, it is saddening to see some of them now with decommissioned instruments inside.

ESO is a demanding organisation to be managed, and Fellows are encouraged to help with small tasks. My little tasks include helping with the Visitor Selection Committee, where prospective visits are reviewed, feedback by previous visitors is discussed and recommendations are sent to the Office for Science. It has opened an interesting window onto how different people review the same application, and the expectations that visitors have towards ESO. As part of my ESO Fellowship duties, I opted for training and operations on Unit Telescopes (UT) 4 and 1 instruments. Timing was lucky, as I arrived when UT4 was being upgraded with four powerful lasers and new adaptive optics technology.

In the photo, I am standing with an old friend in front of UT4 during a laser demonstration at twilight. The view of the southern sky from Paranal is breathtaking, and somehow soothing during the long winter nights. When I sneak out onto the platform, the four UTs make an impressive presence; with their sizes, silently rotating and staring, they resemble temples high on sacred mountains where a few initiated interrogate the heavens. I wonder what some archeologists may think of us in a few thousand years.

ESO, and especially Paranal, is a truly multi-cultural environment, with enriching human experiences every day. Students, fellows and young staff are particularly active on diversity, inclusiveness and equal opportunities, despite the slow changes in rules (and sometimes mindsets) that unfortunately are physiological within a large inter-governmental organisation. There are, however, improvements that I hope will be considered in the near future; as in the motto proudly worn on our t-shirts at Paranal, "People are the Stars". The friendly and informal atmosphere is a precious asset; even though senior staff are very busy with their duties, they always have time for instructive chats and advice; and with two other Fellows, I am having fun organising a workshop on "Cosmic Beacons". As the "job hunting" season approaches, I can hardly realise that two years have already gone by; the clocks tick so quickly here!

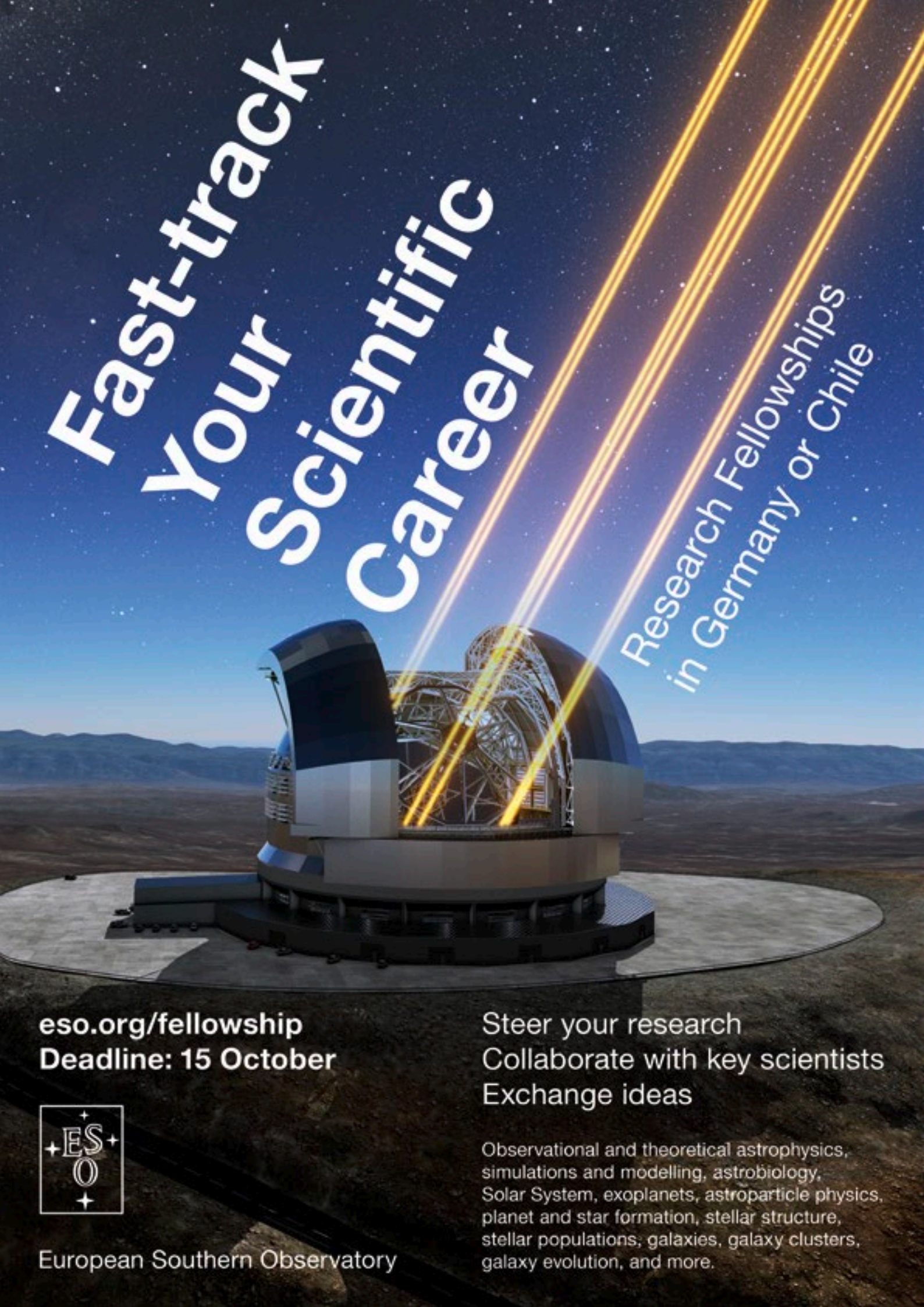
Fast-track
Your
Scientific
Career
Research Fellowships
in Germany or Chile
eso.org/fellowship
Deadline: 15 October
Steer your research
Collaborate with key scientists
Exchange ideas
Observational and theoretical astrophysics, simulations and modelling, astrobiology, Solar System, exoplanets, astroparticle physics, planet and star formation, stellar structure, stellar populations, galaxies, galaxy clusters, galaxy evolution, and more.
ESO
European Southern Observatory

ESO Fellowship Programme 2017/2018

Fast-track your scientific career at Europe's leading astronomy organisation

Each year, several outstanding early-career scientists have the opportunity to further develop their independent research programmes at the European Organisation for Astronomical Research in the Southern Hemisphere. The highly dynamic scientific environment supports ESO Fellows in steering their careers by gaining new skills, unique insights and valuable experience.

ESO's approximately 110 staff astronomers, 40 fellows and 40 PhD students conduct front-line research in fields ranging from exoplanets to cosmology. Observational, theoretical and fundamental astrophysics are all areas where fellows can benefit from one of the most vibrant and stimulating scientific settings anywhere in the world.

Fellowships are available both at ESO's Headquarters in Garching near Munich, Germany, and at ESO's astronomy centre in Santiago, Chile.

ESO Headquarters is situated in one of the most active research centres in Europe, boasting one of the highest concentrations of astronomers. High-calibre scientists, instrument experts, and other professionals within easy reach provide fellows with valuable opportunities for starting collaborations and learning new skills. ESO's offices are adjacent to the Max Planck Institutes for Astrophysics and for Extraterrestrial Physics and close to the observatory of Munich's Ludwig-Maximilian University. Additionally, ESO participates in the Excellence Cluster Universe at the Garching campus, which brings together nearly 200 scientists.

In Chile, fellows interact with visiting astronomers from a broad area of research and have the opportunity to collaborate with the rapidly growing Chilean astronomical community and with astronomers at other international observatories located in Chile. The ALMA building next to ESO's Santiago offices with its many astronomers and fellows further enhances the stimulating scientific environment available to ESO Chile Fellows.

At both sites, ESO Fellows are expected to actively participate in ESO's scientific life by proposing and getting involved in the organisation of scientific workshops, co-supervising PhD students, coordinating thematic research groups, joining scientific committees, organising seminars, etc.

The fellowship positions in Garching are three years in duration. In addition to developing their independent research programmes, ESO Garching Fellows are expected to engage in functional work for up to 25 % of their time. Previous fellows have rated functional work as much more positively influential in their career than previously thought as it had equipped them with essential professional skills. Duties are varied and can relate to instrumentation, the VLT/I, ALMA, APEX, ELT, science operations support either in Garching or at one of the ESO Observatories in Chile, software development, or public outreach and education via the unique on-site ESO Supernova Planetarium & Visitor Centre. The opportunity to gather experience from ESO's frontline projects and operations brings fellows a privileged vantage point, no matter where their career path takes them next.

Fellowships in Chile are granted for four years. During the first three years, the fellows are assigned to one of the science operation groups of Paranal, ALMA or APEX, where they will contribute at a level of 80 nights per year. For ALMA Fellows, a fraction of their duties can alternatively be spent on data processing, participation in the ALMA review process as technical experts, software testing, optimisation and extension of the array capabilities. At Paranal, fellows have the opportunity to join an Instrument Operations Team (IOT). In the role of Instrument Fellow, they gain an in-depth knowledge of different aspects of a given instrument, such as engineering and technological characteristics, operations and data reduction. They further develop useful skills in the basics of project management, team coordination, and communicating in a multidisciplinary environment. This exquisite mix of technical knowledge and close contact with the science carried out at the Observatories, allows ESO Chile Fellows to build a solid science programme that can boost their future careers.

During the fourth year, a Chile Fellow may choose to spend the fourth year either at ESO's astronomy centre in Santiago, or at ESO Headquarters in Garching, or at any astronomy/astrophysics institute in an ESO Member State. There are no functional duties during the fourth year, except in the case that the fourth year is spent at ESO Chile, where fellows are expected to carry out functional work for up to 25 % of their time. Under certain conditions, the fellow may also be hosted by a Chilean institution where she/he will be eligible to apply for time on all telescopes in Chile through competition for Chilean observing time.

The programme is open to applicants who will have achieved their PhD in astronomy, physics or a related discipline before 1 November 2018. Early-career scientists from all astrophysical fields are welcome to apply. While scientific excellence is the primary selection criterion for all fellowships, candidates should also explain (in their motivation letter) how ESO's facilities and environment and their work at ESO would facilitate their scientific development.

We offer an attractive remuneration package including a competitive salary and allowances (tax-free), comprehensive social benefits, and financial support for relocating families.

Application procedure

If you are interested in enhancing your early career through an ESO Fellowship at the most advanced ground-based observatory in the world, then please apply by completing the web application form available at http://recruitment.eso.org.

Please include in your application:

- a cover/motivation letter;
- a curriculum vitae with a list of publications, and a brief summary of relevant experience (e.g., observing/technical/programming/modelling);
- a proposed research plan (maximum of two pages);
- the names and contact details of three persons familiar with your scientific work and willing to provide a recommendation letter. Referees will be automatically invited to submit a recommendation letter. However, applicants are strongly advised to trigger these invitations (using the web application form) well in advance of the application deadline.

The closing date for applications is 15 October 2017. Review of the application documents, including the recommendation letters, will begin immediately. Incomplete or late applications will not be considered.

Candidates will be notified of the results of the selection process between December 2017 and February 2018. Fellowships will begin in the second half of 2018.

Further information
For more information about the fellowship programme and ESO's astronomical research activities, please see: http://www.eso.org/fellowship.

For a list of current ESO staff and fellows, and their research interests please see: http://www.eso.org/sci/activities/personnel.html.

Details of the Terms of Service for fellows including details of remuneration are available at: http://www.eso.org/public/jobs/conditions/fellows/.

For any additional questions please contact:
For Garching: Eric Emsellem, email: eric.emsellem@eso.org.
For Chile: Claudio De Figueiredo Melo, email: cmelo@eso.org.

Although recruitment preference will be given to nationals of ESO Member States (members are: Austria, Belgium, Brazil, the Czech Republic, Denmark, Finland, France, Germany, Italy, the Netherlands, Poland, Portugal, Spain, Sweden, Switzerland and the United Kingdom) and Chile, no nationality is in principle excluded.

The post is equally open to suitably qualified female and male applicants.

ESO/M. Kommesser

ESO's facilities in Chile merged into an imaginary landscape.

Personnel Movements

Arrivals (1 March–30 June 2017)

Europe

Dembet, Roderick (FR)	Software Engineer
Guerlet, Thibaut (FR)	Optical Laboratory Technician
Heijmans, Jeroen (NL)	Instrumentation Engineer/Physicist
Lyubenova, Mariya (BG)	Outreach Astronomer
Ubeira Gabellini, Maria Giulia (IT)	Student

Chile

Alarcon, Patricio (CL)	Mechanical Workshop Leader
André, Mylène (FR)	Outreach Officer
Faez, Robinson (CL)	Telescope Instruments Operator
Friedli, Ivanna (CL)	Bilingual Secretary
Jofré, Felipe (CL)	Procurement Officer
Palominos, Rodrigo (CL)	Telescope Instruments Operator

Departures (1 March–30 June 2017)

Europe

Laing, Robert (UK)	Instrument Scientist
Ménardi, Serge (FR)	Opto-Mechanical Engineer
Puglisi, Annagrazia (IT)	Student

Chile

Bugueno, Erich (CL)	Mechanical Engineer
Garcia, Diego Alex (ES)	Operations Astronomer
Glaves, Percy (CL)	Head, Central Services Desk
Iglesias, Daniela (CL)	Student
Mardones, Pedro (CL)	Instrumentation Engineer

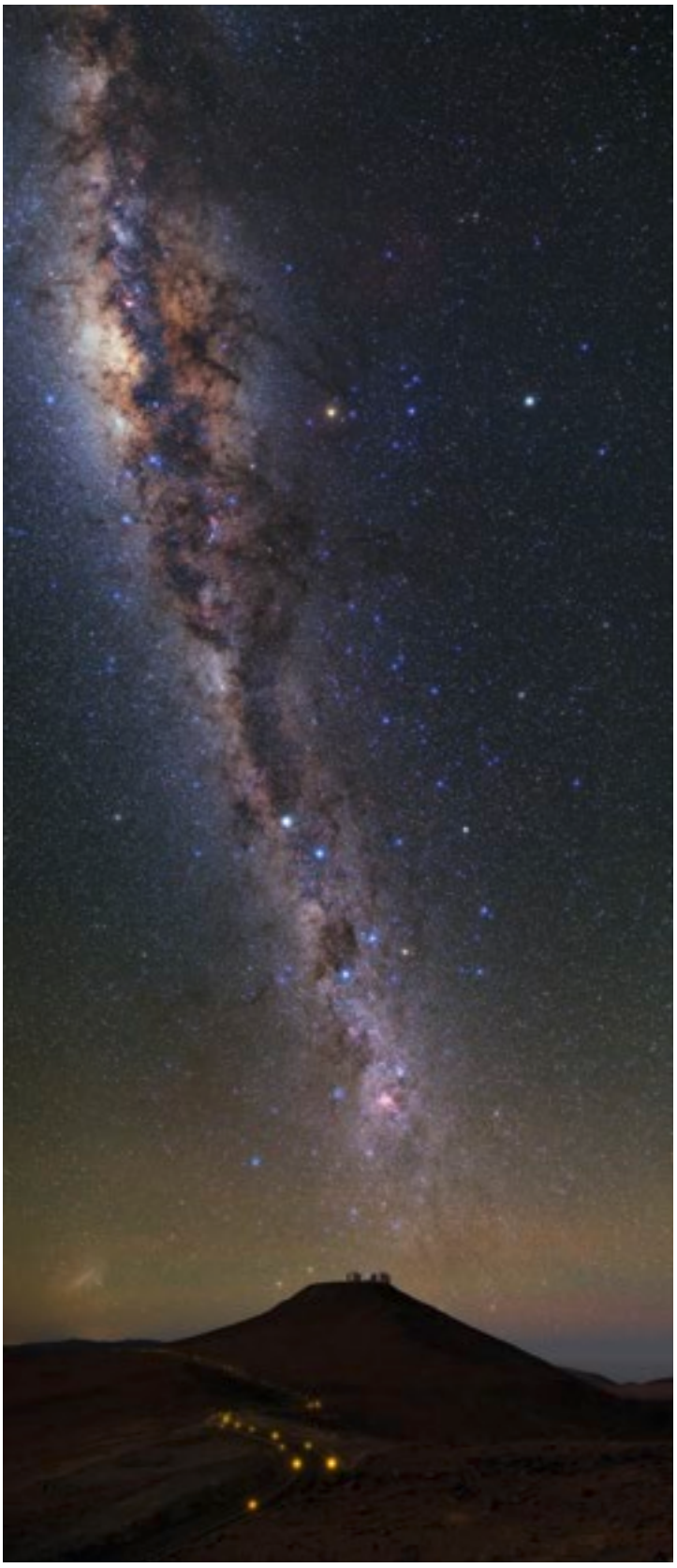

ESO/B. Tafreshi (twanight.org)

The Bulge and Plane of the Milky Way stretching above the Paranal Observatory.

ESO, the European Southern Observatory, is the foremost intergovernmental astronomy organisation in Europe. It is supported by 16 countries: Austria, Belgium, Brazil, the Czech Republic, Denmark, France, Finland, Germany, Italy, the Netherlands, Poland, Portugal, Spain, Sweden, Switzerland and the United Kingdom. ESO's programme is focused on the design, construction and operation of powerful ground-based observing facilities. ESO operates three observatories in Chile: at La Silla, at Paranal, site of the Very Large Telescope, and at Llano de Chajnantor. ESO is the European partner in the Atacama Large Millimeter/submillimeter Array (ALMA). Currently ESO is engaged in the construction of the Extremely Large Telescope.

The Messenger is published, in hard-copy and electronic form, four times a year: in March, June, September and December. ESO produces and distributes a wide variety of media connected to its activities. For further information, including postal subscription to The Messenger, contact the ESO education and Public Outreach Department at:

ESO Headquarters
Karl-Schwarzschild-Straße 2
85748 Garching bei München, Germany
Phone +49 89 320 06-0
information@eso.org

The Messenger:
Editors: Jeremy R. Walsh and Gaitee A. J. Hussain; Graphics: Ed Janssen; Design, Production: Jutta Boxheimer; Layout, Typesetting: Mafalda Martins.
www.eso.org/messenger/

Printed by G. Peschke Druckerei GmbH
Taxetstraße 4,
85599 Parsdorf, Germany

ISSN 0722-6691

Contents

Front cover: Artist's rendering of the Extremely Large Telescope (ELT) in night-time operation on Cerro Armazones. The ceremony for the First Stone of the ELT dome was held on 26 May 2017 and is described in de Zeeuw et al., p. 2. Credit: ESO/L. Calçada